

AD _____

Award Number: W81XWH-07-1-0532

TITLE: FoxP3 Functions as a Novel Breast Cancer Suppressor Gene Through Cooperation with NFAT

PRINCIPAL INVESTIGATOR: Weiquan Li, Ph.D.

CONTRACTING ORGANIZATION: University of Michigan, Ann Arbor, MI48105

REPORT DATE: Dec. 2008

TYPE OF REPORT: Final

PREPARED FOR: U.S. Army Medical Research and Materiel Command Fort Detrick,
Maryland 21702-5012

DISTRIBUTION STATEMENT:

X Approved for public release; distribution unlimited

~

The views, opinions and/or findings contained in this report are those of the author(s) and should not be construed as an official Department of the Army position, policy or decision unless so designated by other documentation.

REPORT DOCUMENTATION PAGE

Form Approved
OMB No. 0704-0188

Public reporting burden for this collection of information is estimated to average 1 hour per response, including the time for reviewing instructions, searching existing data sources, gathering and maintaining the data needed, and completing and reviewing this collection of information. Send comments regarding this burden estimate or any other aspect of this collection of information, including suggestions for reducing this burden to Department of Defense, Washington Headquarters Services, Directorate for Information Operations and Reports (0704-0188), 1215 Jefferson Davis Highway, Suite 1204, Arlington, VA 22202-4302. Respondents should be aware that notwithstanding any other provision of law, no person shall be subject to any penalty for failing to comply with a collection of information if it does not display a currently valid OMB control number. **PLEASE DO NOT RETURN YOUR FORM TO THE ABOVE ADDRESS.**

1. REPORT DATE (DD-MM-YYYY) 01-09-2008		2. REPORT TYPE Final		3. DATES COVERED (From - To) 1 Sep 2007-30 Aug 2008	
4. TITLE AND SUBTITLE FoxP3 Functions as a Novel Breast Cancer Suppressor Gene Through Cooperation with NFAT				5a. CONTRACT NUMBER	
				5b. GRANT NUMBER W81XWH-07-1-0532	
				5c. PROGRAM ELEMENT NUMBER	
6. AUTHOR(S) Weiquan Li, Ph.D. E-Mail: wqli@umich.edu				5d. PROJECT NUMBER	
				5e. TASK NUMBER	
				5f. WORK UNIT NUMBER	
7. PERFORMING ORGANIZATION NAME(S) AND ADDRESS(ES) AND ADDRESS(ES) University Of Michigan Ann arbor, MI48109				8. PERFORMING ORGANIZATION REPORT NUMBER	
9. SPONSORING / MONITORING AGENCY NAME(S) AND ADDRESS(ES) U.S. Army Medical Research and Materiel Command Fort Detrick, Maryland 21702-5012				10. SPONSOR/MONITOR'S ACRONYM(S)	
				11. SPONSOR/MONITOR'S REPORT NUMBER(S)	
12. DISTRIBUTION / AVAILABILITY STATEMENT Approved for Public Release; Distribution Unlimited					
13. SUPPLEMENTARY NOTES					
14. ABSTRACT TFoxP3 is among the newest members of the forkhead winged helix family and a gene responsible for X-linked autoimmune diseases IPEX (Immune dysregulation, polyendopathy, enteropathy, X-linked) in mice and humans (7-8). In our analysis of the immune functions of mice heterozygous for the FoxP3 mutation, we observed a high rate of spontaneous mammary cancer. Meanwhile, a recent study indicated that mice with a targeted mutation of NFAT also developed spontaneous mammary cancers. In our study, we found the FoxP3 gene was down-regulated in the mammary cancer tissues. Meantime, over-expression of FoxP3 in a variety of breast cancer cells resulted in a substantial inhibition of their growth. Furthermore, FoxP3 inhibited the transcription of ErbB2, the major oncogene for breast cancer, by targeting and repressing the ErbB2 promoter and the growth inhibition was completely reversed by constitutive expression of the ErbB2 gene. Our data revealed that FoxP3 is an important breast cancer suppressor gene in mice and humans and NFAT4 also repressed Erb2 transcription by measuring ErbB2 reporter activity, suggesting NFAT4 may serve as a repressor for ErbB2/Her-2 promoter. NFAT4 was found in a complex with FoxP3, indicating they may functionally play important roles together. Our further analysis also found decrease of NFAT4 expression in some of mice breast cancer samples. In summary, our data suggest FoxP3 and NFAT are important breast cancer suppressor genes in the mouse model.					
15. SUBJECT TERMS FoxP3, Breast cancer, NFAT, Tumor suppressor gene					
16. SECURITY CLASSIFICATION OF:			17. LIMITATION OF ABSTRACT	18. NUMBER OF PAGES	19a. NAME OF RESPONSIBLE PERSON
a. REPORT U	b. ABSTRACT U	c. THIS PAGE U			USAMRMC
			UU	44	19b. TELEPHONE NUMBER (include area code)

Table of Contents

Body	3 -10
Key Research Accomplishments.....	10
Reportable Outcomes.....	10-11
Conclusion.....	11
References.....	11-12
Appendices.....	13

We have identified FoxP3 as a novel tumor suppressor for breast and prostate cancer recently(1-3). Several other genes, such as Brca1/Brca2, TP53 and PTEN, have also been implicated in familial and sporadic cancer(4). However, the genetic basis for a major portion of breast cancer, including familial and sporadic, is yet to be elucidated. Surprisingly, in our analysis of the immune functions of mice heterozygous for the FoxP3 mutation, we observed a high rate of spontaneous mammary cancer. The heterozygous female mice are also substantially more susceptible to carcinogen DMBA. The involvement of FoxP3 is supported by several lines of evidence. First, the *FoxP3* gene is expressed in breast epithelial cells but down-regulated in the mammary cancer tissues. Second, transfection of FoxP3 cDNA into a variety of breast cancer cells resulted in a substantial inhibition of their growth. Thirdly, FoxP3 inhibits the transcription of ErbB2, the major oncogene for breast cancer, by repressing the ErbB2 promoter(3). Further studies demonstrate that the growth inhibition is completely reversed by constitutive expression of the ErbB2 gene. Furthermore we also found FoxP3 down-regulate c-Myc in prostate cancer development(1). Nuclear factor of activated T cell(NFAT) was firstly identified as a regulator of IL-2 transcription in activated T cells in response to TCR-mediated signals. Now there are at least five members in NFAT family transcription factors being identified. All NFAT proteins have a highly conserved DNA-binding domain which resembles to the DNA binding domain of REL-Family transcription factors to regulate variety of gene transcriptions. Among them, NFAT1-4 is functionally response to signal from calcium channel. In T cells, NFAT1 formed in a complex with FoxP3 and AP-1 to target the promoter region of regulated genes in Treg(5). Evidences from many research groups suggest NFAT may involve cell cycle regulation and tumor development. NFAT4 is one of members in NFAT family transcription factors and has been recently reported that mice with targeted mutation of NFAT4 developed spontaneous mammary cancer(6) , implying NFAT4 may function as a novel tumor suppressor gene in the breast cancer development. Therefore, it will be very interesting to explore the possibility if NFAT4 plays an important role as a partner with FoxP3 in repression of cell growth as we found FoxP3 functions as a tumor suppressor in breast cancer in mice.

Therefore, we set up the first task as below:

Task 1: Test if NFAT4 is inactivated in mammary tumors in NFAT4^{+/-} mice (month 1-12).

- We have obtained NFAT4/NFAT1 heterozygous mice from Harvard Medical School. We will breed these mice to accumulate 30 WT female mice, 30 female NFAT4 heterozygous (+/-) mice and 30 NFAT4 (-/-) mice and to record the tumor incidence. (month 1-9).
- When the mammary tumor is developed in female NFAT +/- mouse as reported, we will perform pathology examination. (Month 4-12).
- Immunohistochemical analysis on tumor tissue will be performed using anti-NFAT4 antibody. Tumor tissue RNA will be isolated and RT-PCR will be performed to examine the gene expression. (Month 4-12).
- We will treat the mice with carcinogen, 7,12-dimethylbenz [a] anthracene (DMBA), in conjunction with progesterone to speed up breast tumor formation in wild type and NFAT4 deficient mice (Month 4-12).

A published report demonstrated that both NFAT4^{-/-} and NFAT4^{+/-} mice developed mammary tumors at the age of 12-16 months, although the study involved too small numbers of mice to allow a comparison of the onset and incidence of the mammary tumors. We will take three approaches to determine whether NFAT4 works as a cell intrinsic tumor suppressor.

We have obtained the same BALB/c founder mice from Dr. Glimcher at Harvard Medical School (the same source as the one that reported mammary tumor). Published studies demonstrated that 2/3 NFAT4^{-/-} mice developed mammary tumors at 12.5 months, while 2/4 of the NFAT4^{+/-} mice developed cancer in 16.5 months, which is notable as none of 10 WT littermates developed cancer in their study. Since this is a time-consuming experiment, we have treated the mice with a carcinogen, 7,12-dimethylbenz [a] anthracene (DMBA), in conjunction with progesterone. In case of FoxP3 mutation, some mammary tumor became palpable within 3 weeks after the 7 week-treatment. We expanded the study to include 20 mice for each group as well as 20 WT littermates. First, we compared the incidence and onset of mammary tumors in NFAT4^{+/+}, and ^{-/-} mice. The development of palpable mammary tumors has been determined by physical examination

and confirmed by histology. The mice were sacrificed when the tumor reaches 5% body weight or when the mice reach 2 years of age. At the end of one year, all mice were sacrificed and examined by histology for the existence of hyperplasia or malignancies in mammary glands and metastasis into bone, lung, liver and lymph nodes Kaplan-Meier survival analysis has been carried out to determine whether there is NFAT4 gene dose will affect the risk of mammary tumors.

Here we showed tumor incidence results below from our animal model:

Figure 1. Tumor incidence in NFAT1 and NFAT4 mice

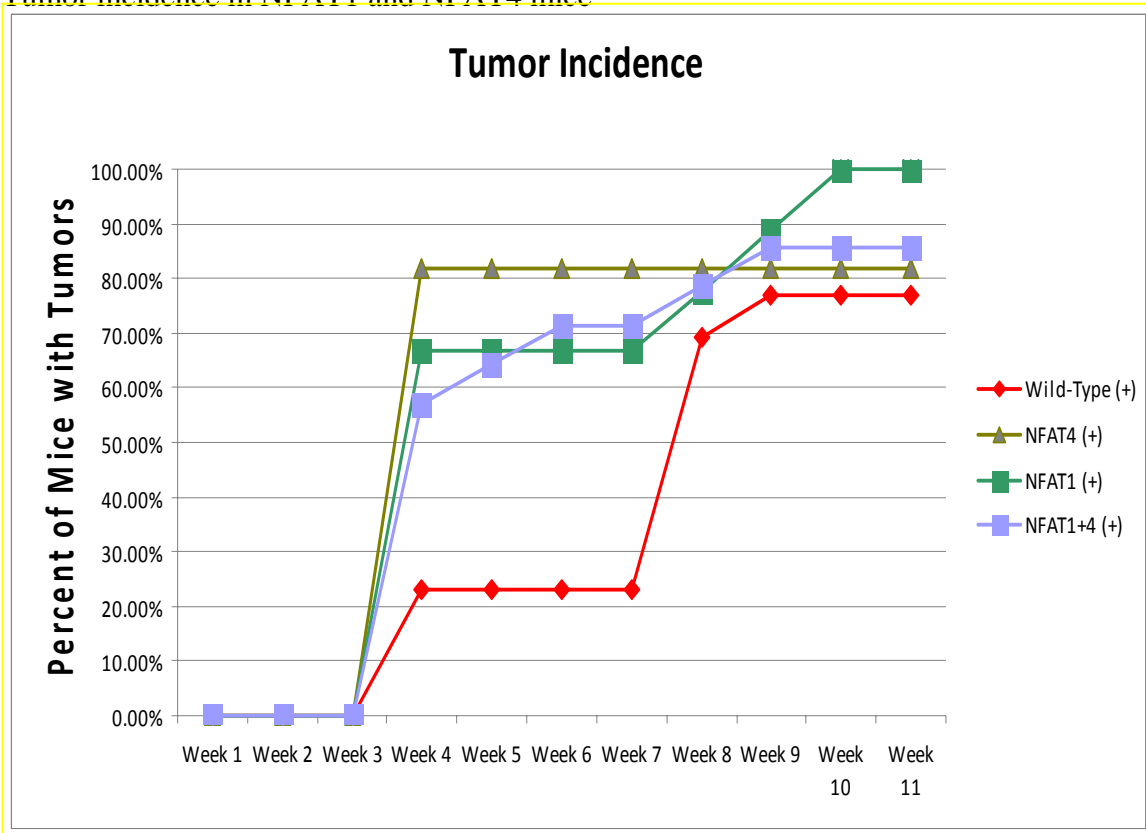
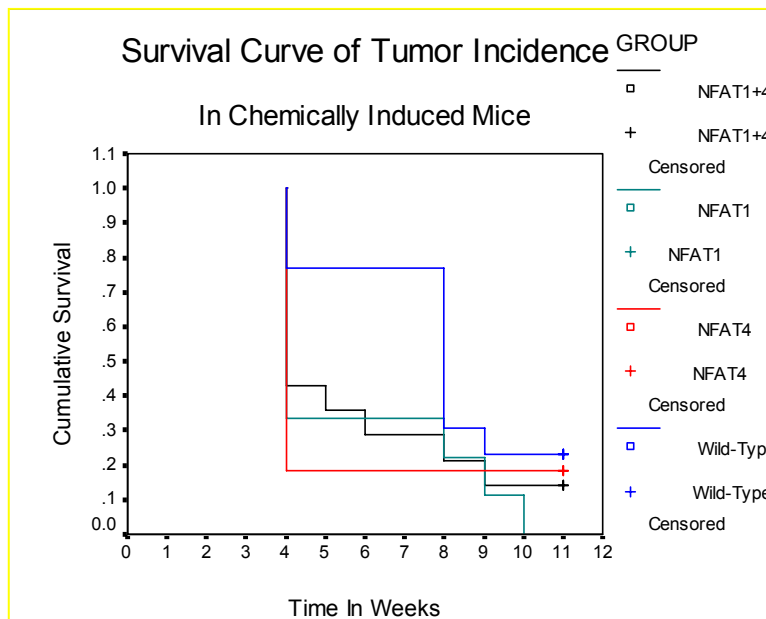


Figure 2. Survival Curve in NFAT1 and NFAT4 Mice.



The figure 1 showed that tumor incidence at earlier stage of stage happed induced by DMBA was significantly higher in NFAT4 or NFA1 mice than the wild type mice, suggesting NFAT4 or NFAT1 may function as tumor suppressor. The survival curve in the figure 2 also show wild type mice survived longer than mutant mice which are consistent with results from tumor incidence.

Second, we do pathological examination on the internal organs from studied mice to confirm the tumor formation and tumor metastasis. We used the anti-NFAT4 antibody (NFATc3-F1, Santa Cruz Biotechnology), a monoclonal antibody against the C-terminal peptide that cross-react with has been shown to work in the immunohistochemistry of paraffin sections. The availability of the NFAF4-deficient tissue allows us to obtain an optimal condition under which the signal can be completely removed in NFAT4^{-/-} cells. A selective absence of the protein in the tumor cells is consistent with the notion that NFAT4 is a tumor suppressor gene. A substantial reduction can be observed in the cancer samples, which may explain e that the WT allele in the cancer cells was inactivated by epigenetic mechanisms.

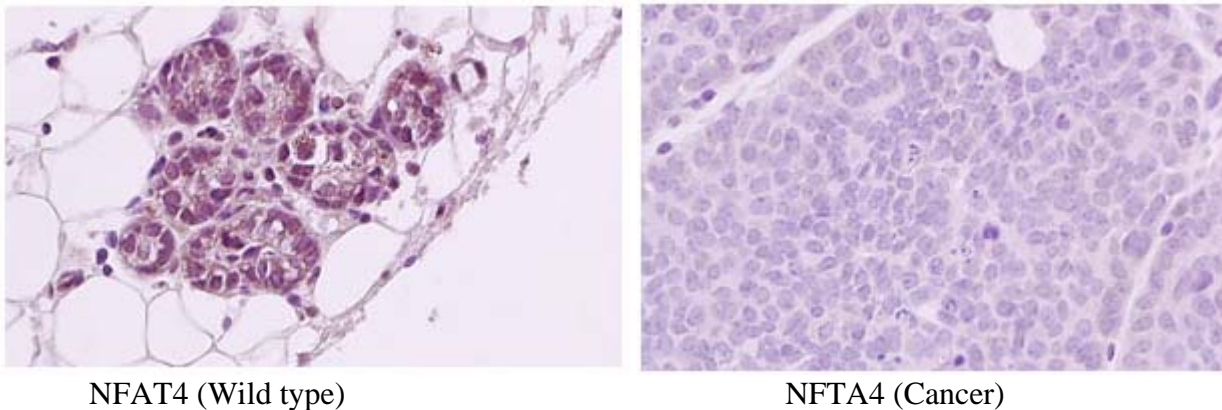


Figure 3. NFAT4 expression in wild and cancer mice breast tissues.

In figure 4. NFAT4 expression in tumor was reduced significantly, suggesting NFAT4 may play a role in the tutorigenesis.

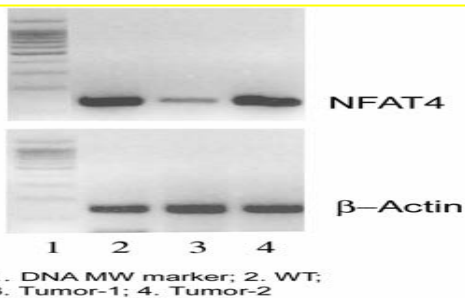


Fig. 4 NFAT4 expression in mammary tissues. Samples from normal and cancerous tissues of the scurfy FoxP3^{sf+/-} mice were cDNA from RT. Lane 1, DNA molecular weight; lane 2, normal mammary glands; lane 3, mammary cancer sample1; lane 4, mammary cancer sample

Next We ask if NFAT4 a partner of FoxP3 in ErbB2/Her-2 promoter repression? So we set up the second task below:

Task 2: Determine whether NFAT4 associates with FoxP3 in vivo and in vitro (Month 1-6).

- We will use co-transfection in vitro expression system to test if NFAT4 and FOXP3 forms a complex and map the required regions for their association.(Month 1-2)
- At meantime, we also will examine if they associate each other under physiological condition such as in normal breast epithelial cell lines.(Month 2-3)
- In the next phase, we will attempt to establish the interaction in living cells using bimolecular fluorescence complementation (BiFC). Once the constructs are optimized, we will transfect the mammary tumor cell line TSA in order to visualize the interaction in a model relevant to breast cancer.(Month 4-6)

To answer if NFAT4 interacts with FoxP3, we co-expressed NFAT4 and FoxP3 in 293 cells and did co-immunoprecipitation. The results showed that NFAT4 binds to FoxP3. As shown in Fig.4, when the 293T cells were transfected with Myc-tagged FoxP3 and HA-tagged NFAT4, anti-HA precipitated both NFAT4 and FoxP3. The specificity of the co-IP is confirmed as the WWRR mutation that inactivates the FoxP3-NFAT4 association, eliminated the co-IP. Thus, at least in the 293T cell lysates, the two molecules bind each other. We mapped c-terminal part of NFAT4 is required for their interaction. At same time, we tested their interaction under physiological condition by isolating breast epithelial cells from mice. We only saw very weak interacting bands from COIP due to antibody(results not showed here).

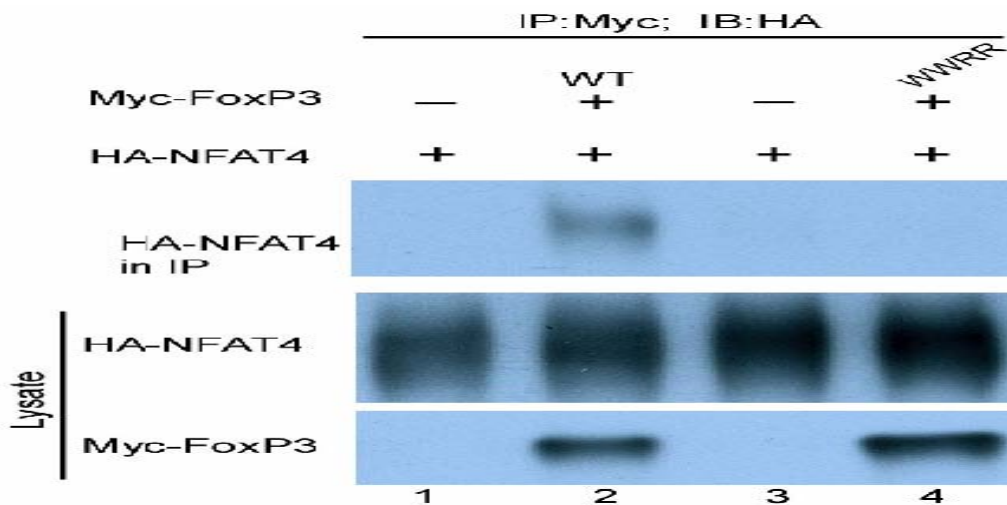


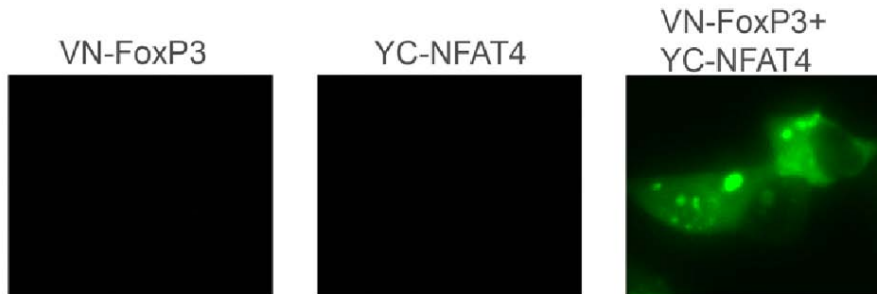
Fig. 5. FoxP3 interacts with NFAT4. Myc-FoxP3 and its mutant WWRR (T359W, N361W, E399R, E401R) were co-transfected with HA-NFAT4 (aa1-699) into HEK 293 cells. After 48 hours, transfected cells were lysed in lysis buffer and precleared lysates were incubated with anti-Myc for one hour and then extended for an additional hour with protein G beads. Immunoprecipitates were dissolved in SDS loading buffer for SDS PAGE gel to determine the NFAT4 protein associated with FoxP3 by anti-H A Western blot. The results showed NFAT4 was associated with wild type FoxP3 but not binding defect mutant WWRR.

Next , we have set up a system to test the interaction in living cells using bimolecular fluorescence complementation (BiFC) by collaborating with Dr. Tom Kerppola, an HHMI investigator and Professor of Biochemistry at University of Michigan, who invented the BiFc method(9). In principle, BiFC is based on the notion that fluorescent proteins can be divided into two non-fluorescent fragments, which can fold together to produce fluorescence if brought to proximity by interacting molecules. Since its invention, this method has been successfully used to visualize the molecular interaction in live cells. Furthermore, by using different fluorescent proteins, this method can be expanded to visualize interaction of multiple proteins. For the purpose of this study, we will use fragments of yellow fluorescent protein (YFP), truncated at residue 155, as it has been shown to exhibit relatively high efficiency of complementation and strict requirement for interaction of the fusion partners .

In order to test the interaction of FoxP3 and NFAT, we constructed YC-NFAT4 by linking YFP to C-terminus of NFAT4 and VN-FOXP 3 by tagging FoxP3 at N-terminal fragment of Venus GFP, respectively. When both VN-FoxP3 and YCNFAT4 co-expressed in 293 cells, a strong intensity of green fluorescence was observed, indicated FoxP3

strongly interacts with NFAT4 (Fig.6). We also tested the interaction between FoxP3 and other members such as NFAT1, NFAT2 and NFAT3 in NFAT family, the signal conveyed by NFAT4 is strongest (data not shown). Similar GFP signal were observed when we co-expressed both VN-FoxP3 and YCNFAT4 in breast cancer cell line TSA and 4T1 (picture not showed here).

Fig 6. Interaction of FOXP3 and NFAT4 in 293 cells. 293 cells was transfected with VN-FOXP3 (FOXP3 tagged at N-terminal fragment of Venus GFP) and YC-NFAT4 (NFAT4 tagged with C-terminal fragment of YFP). Images were captured using fluorescent microscope 24 hrs post-transfection.



To investigate if NFAT4 is a partner with FoxP3 functionally, we set up the below task to address:

Task 3: Establish the functional relevance of the interaction of NFAT4 and FoxP3 (Month 4-12)

- Is NFAT4 a partner in ErbB2/Her-2 promoter repression? By using Her-2 promoter luciferase assay system, we can monitor Her2 transcription level. We co-express NFAT4 and Her2 luciferase reporter in the HEK 293 cells and some breast cancer lines such as MCF7, MCF10A etc. Then we can assess the effects of NFAT4 on Her2 transcription through assaying luciferase activity. (month 4-6)
- Once we see the effects of NFAT4 on Her2 reporter activity, we will determine whether NFAT4 interacts with the *ErbB2* promoter by using ChIP assay. Our research of the 2 Kb promoter region that is susceptible to NFAT4 repression revealed two potential NFAT binding sites. Using immunohistochemistry and real time PCR, Her2 expression level in normal epithelial and mammary cancer cells will be compared and evaluated. (month 6-9)
- We also want to address if FoxP3-mediated repression of Her2 required endogenous NFAT4 protein. To test this possibility, we will use siRNA to silence NFAT4 and other 4 NFAT family members one by one, or all together, and evaluate whether FoxP3-mediated suppression is ablated. A careful titration of FoxP3 plasmids will be carried out to reveal a possible synergic function between FoxP3 and endogenous NFAT. (Month 10-12)

To assess if NFAT4 regulate ErbB2, we use ErbB2 promoter luciferase reporter assay system to assay. We co-expressed NFAT4 or Foxp3 and ErbB2 reporter in the 293 cells, then assay the luciferase activity. The results showed NFAT4 or Foxp3 reduced Her promoter luciferase activity, suggesting NFAT4 repressed Her2 promoter activity and negative regulated ErbB2. In the figure 7 left panel, NFAT4 and FoxP3 showed comparable inhibition on ErbB2 promoter. In figure 7 right panel, we show FoxP3 synergistically repress the ErbB2 promoter and CSA, a NFAT dephosphorylation inhibitor partially reverse FoxP3 and NFAT repressive activity on ErbB2 promoter in a reporter assay. Our data suggest FoxP3 and NFAT may functionally cooperate to repress ErbB2. Similar experiments have been conducted in the other cell lines such as MCF7 and MCF10A cells, which showed similar trends of results (detailed data not showed here).

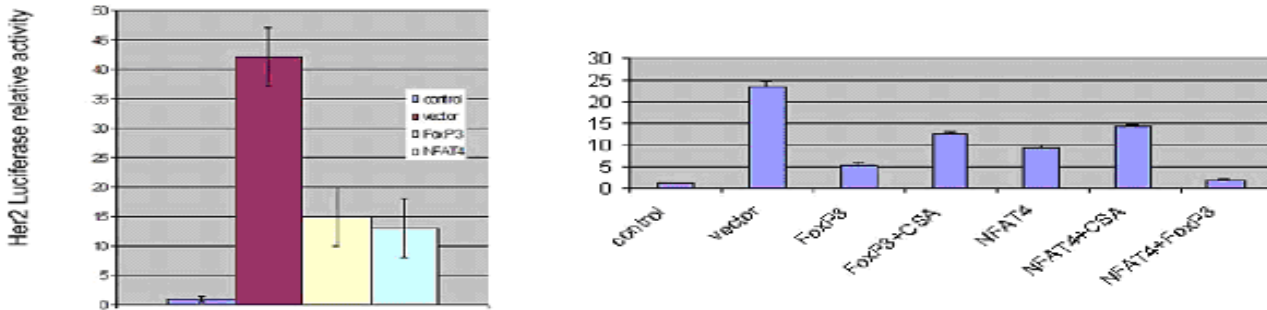


Fig. 7. NFAT4 and FoxP3 repress the ErbB22 promoter with comparable efficiency. FoxP 3 and NFAT4 synergistically repress ErbB22 promoter activity and their repressive function on ErbB22 promoter can be partially reversed by NFAT inhibitor CSA(Right Panel).The results showed here were means and SD from three independent experiments. The activity of the promoter luciferase construct is defined as 1.0.

Next, we determined whether NFAT4 interacts with the ErbB2 promoter. Our search of the 2 Kb promoter region that is susceptible to NFAT4 repression revealed only two potential NFAT-binding sites(potential NFAT binding site GGAAA). Remarkably, the two sites are adjacent to the multiple FoxP3 binding sites that we have identified.

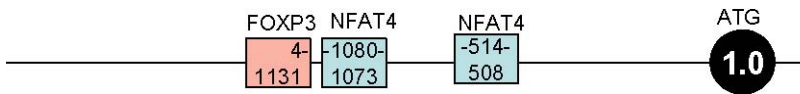
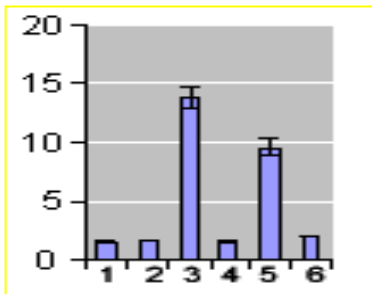


Fig.8. Diagram of the *HER-2* promoter. The functional FoxP3-binding site identified is marked in the pink box, while the two potential NFAT binding sites across the 2.1 Kb region searched were highlighted in two blue boxes. The primers for CHIP assay are indicated as brown bars underneath.



By using ChIP assay, we used the anti-NFAT4 antibody or control IgG to detect the amount of HER-2 promoter associated with the NFAT, using the total input DNA as control to normalize the amplification efficiency of different primers. Our preliminary data indicated that NFAT indeed binds to the promoter region of Her2. The data shown in figure 8 demonstrated which NFAT sites are associated with the NFAT4 protein at 1080-1073 and 515-508(Sample3 and 5 in Fig. 9)

Figure 9. Her promoter CHIP assay by NFAT4. Anti-NFAT4 was used for immuno-precipitation. IgG was used as a control .

To confirm the NFAT4 binding motif in ErbB2 promoter, we mutated the two binding motifs(GGAAA to GCCAA). Then co-expressing NFAT4 and ErbB2 promoter luciferase reporter . Mutating the NFAT4 binding motif in ErbB2 promoter is no longer repressed by NFAT4, suggesting the repressing activity by NFAT4 is specific.

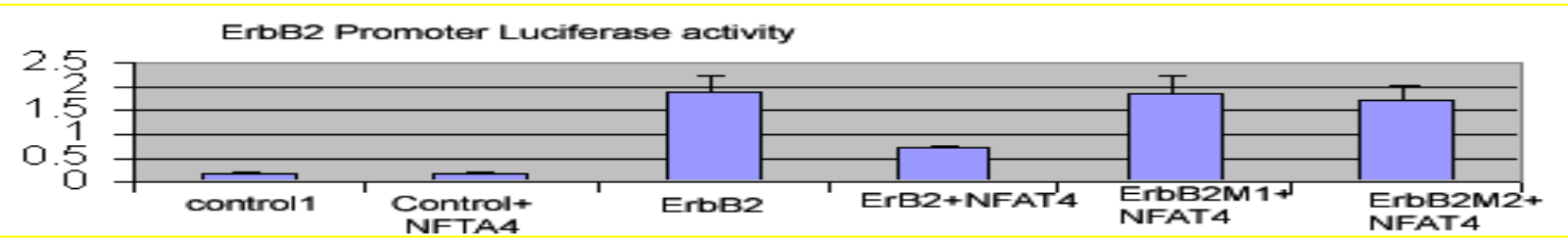


Figure 10. NFAT4 Binding sites in ErbB2 is required for its repressing activity.

The significance of NFAT-4 mediated repression has been assessed by comparing the ErbB2 levels in the normal and malignant mammary epithelial cells from WT and NFAT-4 deficient mice. Using immunohistochemistry, we have found that normal epithelial and mammary cancer cells in the WT mice have minimal levels of ErbB2. While the ErbB2 level is significantly higher in the NFAT4-deficient mammary epithelial cells, may suggest that NFAT4 deletion can cause elevation of ErbB2 before cancer development. However, we have met some difficulty to knockdown all four different isoforms of NFAT proteins. Since NFAT1, NFAT2, or NFAT3 may contribute to repressor activity of Foxp3 in the tumor development, it is hard to conclude FoxP3 collaborated with endogenous NFAT4 for its repressor function. (data not shown here)

Task 4: Determine whether NFAT4 is somatically mutated in human breast cancer (Month 1-12).

- Map NFAT4 mutations in human breast cancer cell lines. We have ten human breast cancer cell lines including MCF-7, SKBr3, BT474, MDA-MB-231, ZR75-1, T47D, BT549, BT20, MDA-MB468, and MDA-MB453, and several mouse breast cancer cell lines such as TSA, 4T1, etc. We also collected the non-malignant breast epithelial cell line MCF-10A, human mammary epithelial cells (HMEC-1, Cat# CC-2551) and mammary epithelial cell growth medium (MEGM Cat# CC-3051)(month1-4)
- Sequence the human NFAT4 gene from 65 cases of paired cancer and normal tissues of the same individual to determine whether somatic mutation of NFAT4 may occur in the cancer cells.(Month 5-8)
- We have a database of over 600 cases of human breast cancer samples, in which the HER-2 score and FoxP3 expression have been documented. We will use an anti-NFAT4 antibody to determine its expression among these samples by dividing them into NFAT+FoxP3+, NFAT+FoxP3-, NFAT-FoxP3+, NFAT-FoxP3-.(month 9-12)

We have sequenced NFAT4 from 6 human cell lines including MCF7, SKBR3, BT474, MDA-MB-231, T47D, MDA-MB468, and 293, and 2 mouse breast cancer cell lines such as TSA, 4T1.

Summaries of mutations in the NFAT4 genes in MCF7 and MDA-MB468 cells are listed below:

MCF7:

845- C or A*	1524 A or G*	1737 A to G*
877-G to T*	1529 A or C*	1811-12 G*
	1541 G or C*	
	1552 G or C*	
	1560 A or C*	
	1577 T or A*	

MDA-MB468 :

1308 A or G*	1625 A or T*	1818 T or G*	2139-40 C* weak
1319 A or G*	1629 A to G*	1824 A or T*	
1369 T or C*	1635 A or T*	1828 A to G*	
1393-1394 A weak	1640 A to C*	1831 T to G*	
1428 T or C*	1665 A or G*	1843 A or T*	
1430 G or C*	1688 A to G*	1844 A or T*	
	1692 A to C*	1856 A or G*	
	1710 A or G*	1863 A or G*	

In order to analyze mutations in human breast cancer samples, we have tried hard to get new patients cancer samples from clinical lab through collaboration. However, so far we have not obtained enough patient samples to be able to carry out this part of research.

Key Research Accomplishments

1. FoxP3 is an intrinsic tumor suppressive gene

In our analysis of the immune functions of mice heterozygous for the FoxP3 mutation, we observed a high rate of spontaneous mammary cancer. These data indicated that Foxp3 may play an important role as a tumor suppressor gene in breast cancer. In our study, we found the FoxP3 gene was expressed in breast epithelial cells but down-regulated in the mammary cancer tissues. Meantime, over-expression of FoxP3 in a variety of breast cancer cells resulted in a substantial inhibition of their growth. Furthermore, FoxP3 inhibited the transcription of ErbB2, the major oncogene for breast cancer, by targeting and repressing the ErbB2 promoter. Our further analysis demonstrated that the growth inhibition was completely reversed by constitutive expression of the ErbB2 gene.

2. NFAT is inactivated in mammary tumors in NFAT +/- mice

We have obtained NFAT4/NFAT1 heterozygous mice from Harvard Medical School. We bred these mice to accumulate 30 WT female mice, 30 female NFAT4 heterozygous (+/-) mice and 30 NFAT4 (-/-) mice and to record the tumor incidence. The results showed that NFAT4 deficiency is associated with high rate of breast tumor formation in mice based on their expression in the tumor at earlier stage.

3. NFAT associates with FoxP3 in vivo and in vitro. We use co-transfection in vitro expression system and found that NFAT4 and FOXP3 formed a complex and have mapped the required regions for their association. The results showed NFAT4 is a partner associated with FoxP3, implying their interaction is important for their functions in tumor repressing activity.

4. Establishing the functional relevance of the interaction of NFAT and FoxP3. By using Her-2 promoter luciferase assay system, NFAT4 was found to repress Her2 promoter activity as good as FoxP3. At same time, we found NFAT4 and Foxp3 have the synergic relationship on repressing Her2 transcription activity, suggesting their role as tumor co-suppressor in breast cancer development.

5. NFAT4 is somatically mutated in human breast cancer. To Map NFAT4 mutations in human breast cancer cell lines, we have sequenced 6 human breast cancer cell lines including MCF-7, SKBr3, BT474, MDA-MB-231, T47D, and MDA-MB468, and two mouse breast cancer cell lines such as TSA, 4T1. We have found many mutations in NFAT4 gene in these cell lines. Some mutations of NFAT4 have been found in these cell lines indicating the possibility of their contribution to tumorigenesis.

Reportable Outcomes:

1, Lizhong Wang(Runhua Liu), **Weiquan Li**, Chong Chen, Hiroto Katoh, Guo-Yun Chen, Beth McNally, Lin Lin Penghui Zhou, Tao Zuo, Kathleen A. Cooney, Yang Liu, Pan Zheng. Somatic Single Hits Inactivate the X-Linked Tumor Suppressor *FOXP3* in the Prostate. **Cancer Cell**. Vol 16, Issue 4, 6 October 2009, Pages 336-346.

2. Yan Liu, Yin Wang, **Weiquan Li**, Pan Zheng, Yang Liu. ATF2 and c-Jun-Mediated Induction of FoxP3 for Experimental Therapy of Mammary Tumor in the Mouse, **Cancer Research**. 69(14)5954-5960. 2009

3. Abstracts: Weiquan Li, et. al. FoxP3 is an X-link tumor suppressor gene in breast cancer. Era of Hope, Department of Defense, Breast cancer research Program Meeting, P66-12

4. Tao Zuo, Lizhong Wang, Carl Morrison, Xing Chang, Huiming Zhang, **Weiquan Li**, Yan Liu, Yin Wang, Xingluo Liu, Michael W.Y. Chan⁴, Jin-Qing Liu, Richard Love⁶, Chang-gong Liu, Virginia Godfrey, Rulong Shen, Tim H-M. Huang, Tianyu Yang, Bae Keun Park⁸, Cun-Yu Wang, Pan Zheng and Yang Liu. FOXP3 Is an X-Linked Breast Cancer Suppressor Gene and an Important Repressor of the HER-2/ErbB2 Oncogene. *Cell*. 2007 Jun 29;129(7):1275-86

5. Manuscript: Weiquan Li, et. al. FoxP3 functions as a novel breast cancer suppressor gene through cooperation with NFAT .

6. Training: Two graduate students and one undergraduate

Conclusion:

Our project was built on our discovery that mice with one defective copy of the FoxP3 gene developed spontaneous mammary tumor at a high rate. Meanwhile, another group of scientists found that a similar defect in the NFAT4 gene also leads to breast cancer. The impacts of our findings can be discerned from three different perspectives. First, FoxP3 and NFAT4 mutations resulting in breast tumor in the mouse model suggested that they are likely important breast cancer suppressor genes. Since known tumor suppressor genes can only explain a small portion of the genetic changes responsible for cancer, our work may substantially increase the understanding of the molecular pathobiology of breast cancer. Secondly, our work helps establishing a mechanism for antagonism between tumor suppressor genes and oncogenes at the transcriptional level. The demonstration that NFAT4 and FoxP3 suppressed ErbB2 expression also revealed a major mystery in the field of breast cancer, namely, what is the genetic basis for oncogenic ErbB2-2/NEU gene over-expression in human cancer patients? Understanding this issue may suggest a novel approach to regulate HER-2 expression and therefore breast cancer progression, which may provide some guidance for breast cancer patients treatment .

Since down-regulation of FoxP3 is observed breast cancer samples and similar down-regulation of NFAT4 was observed in mouse breast cancer samples, our study may help design and develop anti-cancer therapy of large section of breast cancer patients. FoxP3 is an X-link gene which is considerably more susceptible to genetic damages resulting in X-chromosomal inactivation and loss of heterozygosity (LOH). Thus, reactivating the silenced FoxP3 by pharmacologic drug may resume its suppressive function. Similarly, if NFAT4 is a required element for FoxP3 function, the drug targeting NFAT4 will have relevant effects on the FoxP3 function. For instance, immunosuppressant cyclosporine A is a known inhibitor of NFAT4. If our data is correct, one must monitor the risk of breast cancer for patients using this drug. Another important issue is that by showing the interaction of two tumor suppressors, drugs that may benefit patients with FOXP3 mutant tumors may also benefit those with NFAT mutation.

References:

1. Lizhong Wang(Runhua Liu), **Weiquan Li**, Chong Chen, Hiroto Katoh, Guo-Yun Chen, Beth McNally, Lin Lin, Penghui Zhou, Tao Zuo, Kathleen A. Cooney, Yang Liu, Pan Zheng. Somatic Single Hits Inactivate the X-Linked

Tumor Suppressor *FOXP3* in the Prostate. **Cancer** 336-34

Cell. Vol 16, Issue 4, 6 October 2009, Pages

2. Yan Liu(Yin Wang), **Weiquan Li**, Pan Zheng, Yang Liu. ATF2 and c-Jun-Mediated Induction of FoxP3 for Experimental Therapy of Mammary Tumor in the Mouse, **Cancer Research.** 69(14)5954-5960. 2009
3. Tao Zuo, Lizhong Wang, Carl Morrison, Xing Chang, Huiming Zhang, **Weiquan Li**, Yan Liu, Yin Wang, Xingluo Liu, Michael W.Y. Chan⁴, Jin-Qing Liu, Richard Love⁶, Chang-gong Liu, Virginia Godfrey, Rulong Shen, Tim H-M. Huang, Tianyu Yang, Bae Keun Park⁸, Cun-Yu Wang, Pan Zheng and Yang Liu. FOXP3 Is an X- Linked Breast Cancer Suppressor Gene and an Important Repressor of the HER-2/ErbB2 Oncogene. **Cell.** 2007 Jun 29;129(7):1275-86.
4. Wooster RaW, B.L. Breast and Ovarian Cancer. 2003. The New England Journal of Medicine. 348:2339-2347.
5. Wu Y, Borde M, Heissmeyer V, et al. 2006. FOXP3 controls regulatory T cell function through cooperation with NFAT. **Cell.** 126:375-387.
6. Lee H, Chouinard L, Bonin M, Michel RN. 2005. NFATc3 deficiency may contribute to the development of mammary gland adenocarcinoma in aging female mice. **Mol Ca rcinog.** 44:219-222.
7. Wildin RS, Ramsdell, F., Peake, J., Faravelli, F., Casanova, J.L., Buist, N., Levy-Lahad, E., Mazzella, M., Goulet, O., Perroni, L., Bricarelli, F.D., et al.. 2001. X-linked neonatal diabetes mellitus, enteropathy and endocrinopathy syndrome is the human equivalent of mouse scurfy. **Nat Genet.** 27:18-20.
8. Bennett CL, Christie, J., Ramsdell, F., Brunkow, M.E., Ferguson, P.J., Whitesell, L., Kelly, T.E., Saulsbury, F.T., Chance, P.F., Ochs, H.D.. 2001. The immune dysregulation, polyendocrin oopathy, enteropathy, X-linked syndrome (IPEX) is caused by mutations of FOXP3. **Nat Genet.** 27:20-21.
9. Hu CD, Chinenov Y, Kerppola TK. 2002. Visualization of interactions among bZIP and Rel family proteins in living cells using bimolecu lar fluorescence complementation. **Mol Cell.**9:789-798.

Appendices:

1. Lizhong Wang(Runhua Liu), **Weiquan Li**, Chong Chen, Hiroto Katoh, Guo-Yun Chen, Beth McNally, Lin Lin, Penghui Zhou, Tao Zuo, Kathleen A. Cooney, Yang Liu, Pan Zheng. Somatic Single Hits Inactivate the X-Linked Tumor Suppressor *FOXP3* in the Prostate. **Cancer Cell.** Vol 16, Issue 4, 6 October 2009, Pages 336-34
2. Yan Liu, Yin Wang, **Weiquan Li**, Pan Zheng, Yang Liu. ATF2 and c-Jun-Mediated Induction of FoxP3 for Experimental Therapy of Mammary Tumor in the Mouse, **Cancer Research.** 69(14)5954-5960. 2009
3. Tao Zuo, Lizhong Wang, Carl Morrison, Xing Chang, Huiming Zhang, **Weiquan Li**, Yan Liu, Yin Wang, Xingluo Liu, Michael W.Y. Chan⁴, Jin-Qing Liu, Richard Love⁶, Chang-gong Liu, Virginia Godfrey, Rulong Shen, Tim H-M. Huang, Tianyu Yang, Bae Keun Park⁸, Cun-Yu Wang, Pan Zheng and Yang Liu. FOXP3 Is an X- Linked Breast Cancer Suppressor Gene and an Important Repressor of the HER-2/ErbB2 Oncogene. **Cell.** 2007 Jun 29;129(7):1275-86.
4. Abstracts: Weiquan Li, et. al. FoxP3 is an X-link tumor suppressor gene in breast cancer. Era of Hope, Department of Defense, Breast cancer research Program Meeting, P66-12

Somatic Single Hits Inactivate the X-Linked Tumor Suppressor *FOXP3* in the Prostate

Lizhong Wang,^{1,5} Runhua Liu,^{1,5} Weiquan Li,¹ Chong Chen,¹ Hiroto Katoh,¹ Guo-Yun Chen,¹ Beth McNally,¹ Lin Lin,¹ Penghui Zhou,¹ Tao Zuo,⁴ Kathleen A. Cooney,² Yang Liu,^{1,2,*} and Pan Zheng^{1,3,*}

¹Division of Immunotherapy, Department of Surgery

²Department of Internal Medicine

³Department of Pathology

University of Michigan School of Medicine and Cancer Center, Ann Arbor, MI 48109, USA

⁴Department of Molecular Virology, Immunology, and Medical Genetics, The Ohio State University Medical Center, Columbus, OH 43210, USA

⁵These authors contributed equally to this work

*Correspondence: yangl@umich.edu (Y.L.), panz@umich.edu (P.Z.)

DOI 10.1016/j.ccr.2009.08.016

SUMMARY

Despite clear epidemiological and genetic evidence for X-linked prostate cancer risk, all prostate cancer genes identified are autosomal. Here, we report somatic inactivating mutations and deletion of the X-linked *FOXP3* gene residing at Xp11.23 in human prostate cancer. Lineage-specific ablation of *FoxP3* in the mouse prostate epithelial cells leads to prostate hyperplasia and prostate intraepithelial neoplasia. In both normal and malignant prostate tissues, *FOXP3* is both necessary and sufficient to transcriptionally repress *cMYC*, the most commonly overexpressed oncogene in prostate cancer as well as among the aggregates of other cancers. *FOXP3* is an X-linked prostate tumor suppressor in the male. Because the male has only one X chromosome, our data represent a paradigm of “single genetic hit” inactivation-mediated carcinogenesis.

INTRODUCTION

Genetic lesions of several autosomal tumor suppressor genes, including *PTEN* (Sansal and Sellers, 2004; Suzuki et al., 1998), *NKX3.1* (Emmert-Buck et al., 1995; Vocke et al., 1996), and *KLF6* (Bar-Shira et al., 2006; Narla et al., 2005; Narla et al., 2001), have been implicated in the molecular pathogenesis of prostate cancer. In addition, epidemiological studies have suggested a role for X-linked genes that control the susceptibility to prostate cancer (Monroe et al., 1995). Although two loci, one in Xp11.22 (Gudmundsson et al., 2008) and one in Xq27-28 (Xu et al., 1998), have been implicated, the genes in these regions have not been identified. X-linked tumor suppressor genes are of particular interest because the majority of X-linked genes are dose compensated, making a single hit sufficient to inactivate their functions (Spatz et al., 2004). Although we and others have reported X-linked tumor suppressor genes, *WTX1* (Rivera et al., 2007) and *FOXP3* (residing at Xp11.23) (Zuo et al., 2007b) in female cancer patients, none have been identified for cancer in male patients.

In addition to inactivation of tumor suppressors, activation of proto-oncogenes also play a critical role in carcinogenesis. Among them, *c-MYC* (hereby called *MYC*) is known as one of the most commonly overexpressed oncogenes. *MYC* overexpression occurs in more than 30% of all human cancer cases studied (Grandori et al., 2000). However, the mechanism by which *MYC* transcription is increased in the prostate cancer remains unclear. In Burkitt's lymphoma, the *MYC* locus is translocated into a constitutively active Ig locus (Dalla-Favera et al., 1982; Taub et al., 1982), which was found to lead to its transcriptional activation (Erikson et al., 1983). In lung cancer, high levels of gene amplification of the *MYC* locus have been documented (Wong et al., 1986), although such amplification occurred considerably less frequently than overexpression of *MYC* mRNA (Takahashi et al., 1989). Likewise, in breast and prostate cancer, upregulation of *MYC* mRNA was substantially more frequent than amplification of the *MYC* gene (Bieche et al., 1999; Jenkins et al., 1997; Latil et al., 2000). Because *MYC* has been shown to be a target of β -catenin activation (He et al., 1998; Sansom et al., 2007), an appealing hypothesis is that *MYC* upregulation may be a manifestation of aberrant Wnt

SIGNIFICANCE

The study describes two significant advances. First, we demonstrate *FOXP3* as an X-linked tumor suppressor gene in the male in both human and mice. Because the male has only one X chromosome, our work represents a compelling exception to the widely accepted “two hit” theory for inactivation of tumor suppressor genes. Second, our work demonstrates that *FOXP3* is a major transcriptional repressor of *c-MYC* oncogene in the prostate. *FOXP3* inactivation is necessary and sufficient for *c-MYC* overexpression, which is critical for molecular pathogenesis of prostate cancer.

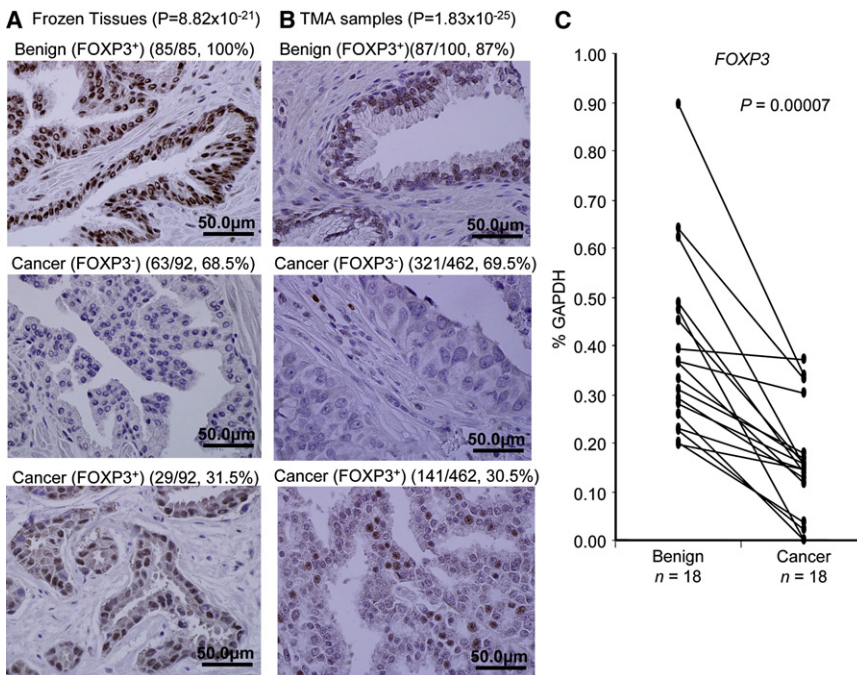


Figure 1. Downregulation of FOXP3 in Prostate Cancer

(A and B) Loss of FOXP3 expression in prostate cancer samples. Data show IHC data for FOXP3 expression in benign versus cancerous tissue in either thawed frozen tissues after short-term formalin fixation (A) or TMA samples after an extended antigen retrieval (B), using monoclonal anti-FOXP3 mAb (236A/E7, 1:100). Statistical significance was analyzed by chi-square tests.

(C) Downregulation of *FOXP3* transcripts in primary cancer tissue in comparison to normal prostate tissue from the same patients (p value by a Wilcoxon two-sample test). Data show real-time PCR quantitation of microdissection samples from 18 cases. The relative amounts are expressed as a percentage of *GAPDH*.

signaling, which occurs frequently in a variety of cancers (Fearon and Dang, 1999). However, a general significance of β -catenin-mediated *MYC* upregulation remains to be demonstrated (Kolligs et al., 1999; Bommer and Fearon, 2007). Therefore, for the majority of cancer types, the genetic change involved in the aberrant *MYC* expression remained to be defined.

MYC overexpression in benign prostate hyperplasia and prostate cancer was documented over 20 years ago (Fleming et al., 1986). Ectopic expression of *MYC* causes hyperplasia of prostate tissue (Thompson et al., 1989). Further studies demonstrated that *Myc* and *Ras* in combination could induce prostate cancer in mice (Lu et al., 1992). More recently, gene expression profiling of a mouse prostate cancer model induced by *Myc* transgene indicated similarity with human prostate cancer (Ellwood-Yen et al., 2003). Consistent with a role for *MYC* in the pathogenesis of prostate cancer, several whole genome scanning studies have strongly implicated a region 260 kb telomeric to the *MYC* gene in susceptibility to prostate cancer (Amundadottir et al., 2006; Gudmundsson et al., 2007; Haiman et al., 2007a; Haiman et al., 2007b; Witte, 2007; Yeager et al., 2007).

Here, we investigated whether the *FOXP3* gene is frequently inactivated in prostate cancer samples by deletion and somatic mutation. Moreover, we determined the significance of such inactivation by growth inhibition of normal and cancerous prostate cell lines and by identification of *FOXP3* targets. The impact of prostate-specific ablation of the *FoxP3* gene in the mouse was also tested.

RESULTS

Somatic Inactivation of the *FOXP3* Locus in Human Prostate Cancer Samples

We first evaluated the expression of *FOXP3* in both normal and malignant prostate tissues by immunohistochemistry. Although

our previous studies have demonstrated the expression of FoxP3 in the mouse prostate using an affinity-purified anti-FoxP3 peptide antibody (Chen et al., 2008), the *FOXP3* expression was not reported in either normal or malignant human prostate tissues by immunohistochemistry (IHC), even though *FOXP3* expression on infiltrating regulatory T cells was clearly detectable (Fox et al., 2007; Roncador et al., 2005). As the master regulator of regulatory T cells, *FoxP3* is expressed there at levels comparable to those of housekeeping genes, such as *GAPDH* and *HPRT* (Fontenot et al., 2003; Hori et al., 2003). Because *FoxP3* expression in prostate tissue is approximately 100-fold lower than what was found in regulatory T cells (Chen et al., 2008), we reasoned that the lack of detectable *FOXP3* in normal prostate tissue may be caused by low sensitivity of staining and/or tissue processing conditions. Therefore, we first fixed the frozen tissues in 10% formalin for 8–12 hr and screened a large panel of commercially available anti-*FOXP3* antibodies for their reactivity to endogenous *FOXP3* in epithelial tissues. A shown in Figure S1 (available with this article online), anti-*FOXP3* mAb stained prostate epithelial uniformly. However, compared with infiltrating lymphocytes, the level of *FOXP3* is considerably lower (Figure S2).

As summarized in Table S1, four commercially available mAbs gave uniform staining of *FOXP3* in normal prostate epithelia. The fact that multiple anti-*FOXP3* mAbs reacted to *FOXP3* demonstrated that *FOXP3* is expressed at significant levels in normal prostate tissue. Among them, two (hFOXY and 236A/E7) were also tested and found to react specifically with *FOXP3* protein in western blot of lysates made from immortalized mammary epithelial cell line MCF-10A. The specificity of the reactivity to human *FOXP3* was further confirmed by comparing reactivity of scrambled and *FOXP3* ShRNA-transduced normal epithelial cell line MCF10A by western blot and by IHC (Figure S3).

Using the uniform fixation and processing conditions, we evaluated the expression of *FOXP3* in 85 cases of normal and 92 cases of cancer tissues. As shown in Figure 1A, immunohistochemistry with anti-*FOXP3* mAb detected nuclear *FOXP3* staining in 100% of the normal prostate tissues tested. In contrast, only 31.5% of the prostate cancer samples show nuclear

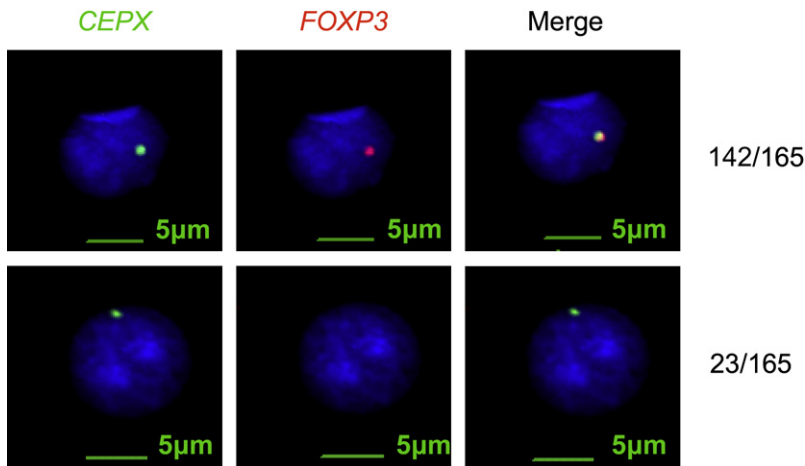


Figure 2. Deletion of a *FOXP3* Among Prostate Cancer Samples

TMA and frozen samples were hybridized to the *FOXP3* (red) or X chromosome probe (green). Of 165 cases with informative FISH data, a total of 23 cases showed *FOXP3* deletion.

FOXP3 staining ($p = 8.82 \times 10^{-21}$). Perhaps as a result of harsher fixation conditions in preparing samples for tissue microarrays, the *FOXP3* protein was generally difficult to detect by IHC, unless high concentrations of antibodies were used (data not shown). Using an extended antigen retrieval (37°C overnight following heating in microwave oven), we have obtained clear, albeit somewhat weaker, staining from tissue microarray samples using low concentrations of anti-*FOXP3* mAb. However, 13% of normal tissues were not stained, presumably because of harsher fixation conditions. As shown in Figure 1B, a significant reduction was observed among prostate cancer tissues. Furthermore, when the samples with prostate epithelial neoplasia (PIN) were compared with normal tissues, we observed a statistically significant reduction of *FOXP3* expression in PIN (Figures S4A and S4B). Taken together, our data demonstrated that *FOXP3* downregulation is widespread in prostate cancer and that such downregulation may have occurred at an early stage of prostate cancer.

We then used microdissection to obtain benign prostate tissue and cancer tissues from the same patients and compared the *FOXP3* mRNA levels. Because inflammatory T cells are a major source of *FOXP3* expression, we carefully avoided areas of inflammation for dissection. After normalizing against the house-keeping gene, 14 of 18 cases showed 2–10-fold reduction of *FOXP3* mRNA in comparison to the benign tissues (Figure 1C). Six of the 18 samples contain clearly identifiable PIN lesions. We therefore microdissected the PIN lesions and compared the levels of *FOXP3* mRNA transcript with normal and cancerous tissues. As shown in Figure S4C, *FOXP3* transcript is downregulated in PIN lesion. Thus, reduced *FOXP3* expression is widespread among prostate cancer samples, perhaps starting at early stage of carcinogenesis.

We used fluorescence in situ hybridization (FISH) to determine *FOXP3* gene deletion in the prostate cancer tissue. As shown in Figure 2 and Table S2, 23 (13.9%) of 165 samples tested showed a deletion of the *FOXP3* gene. Among them, 18 of the 23 cases had a single copy of the X chromosome. However, 5 of the 23 cases showed an increase in the number of X chromosomes. Interestingly, in cells with X polysomy and *FOXP3* deletion, the deletion was complete in all X chromosomes. Thus, X chromosome duplications in cancer tissues likely occurred after deletion of *FOXP3*.

To determine whether *FOXP3* was somatically mutated in primary prostate cancer samples, we isolated cancerous and normal prostate tissues from the same patients and compared the DNA from exons and some exon-intron junctions. A summary of the data is shown in Figure 3A and a representative chromatogram is shown in Figure 3B, with other chromatograms provided in Figure S5. Our sequencing analyses demonstrate single base-pair changes in 5 of 20 samples tested (Table S3). Among them, four were missense mutations, whereas one caused a change in intron 6. One of the missense mutation (K227R) was also reported in the breast cancer (Zuo et al., 2007b). The tumors with the intron 6 mutation showed reduced expression of *FOXP3* (Figure 3C). Among the five samples that contain *FOXP3* mutation in cancer tissue, two contained identifiable PIN lesions. We therefore microdissected the PIN lesion to determine whether the same mutation can be found. As shown in Figure S5, both samples had the same mutations in PIN and cancerous tissues.

To substantiate tumor suppressor activity of *FOXP3*, we transfected *FOXP3* cDNA into prostate cancer cell lines PC3, LNCaP, and Du145. Our data demonstrated strong growth inhibition by *FOXP3* (Figures S6 and S7). Importantly, although vector-transfected LNCaP responds to hormone 5 α -dihydrotestosterone (5 α -DHT), *FOXP3* expression abrogated its stimulation by the hormone (Figure S7). The growth inhibition by wild-type (WT) *FOXP3* provided an important functional test for the somatic mutants uncovered from the clinical samples. As shown in Figure 3D, only WT *FOXP3*, but none of the missense mutants, abrogated growth of prostate cancer cell line Du145. Similar data were obtained with another cell line PC3 (data not shown). Therefore, the somatic mutations of the *FOXP3* are functionally inactivated.

FOXP3 is a transcriptional regulator that functions by interacting with DNA in the nuclei (Zuo et al., 2007b). As the first step to understand the mechanism by which the mutations in *FOXP3* affect its function, we tagged the *FOXP3* protein with the green fluorescence protein (GFP) at the N terminus and visualized its intracellular localization by confocal microscopy. As shown in Figure 3E, three of four somatic mutants disrupted its translocation into nuclei. To substantiate these observations, we isolated cytoplasm, nucleoplasm, and chromatin from PC3 transfected with vector control and from WT and somatic *FOXP3* mutant cDNA and determined distribution of *FOXP3* by western blot. As shown in Figure 3F, although WT *FOXP3* and the V79A mutant reside in both the nucleoplasm and the chromatin, the overwhelming majority of the proteins encoded by other three missense mutants are excluded from the nucleus. Because these three mutations had a more severe impact on the growth

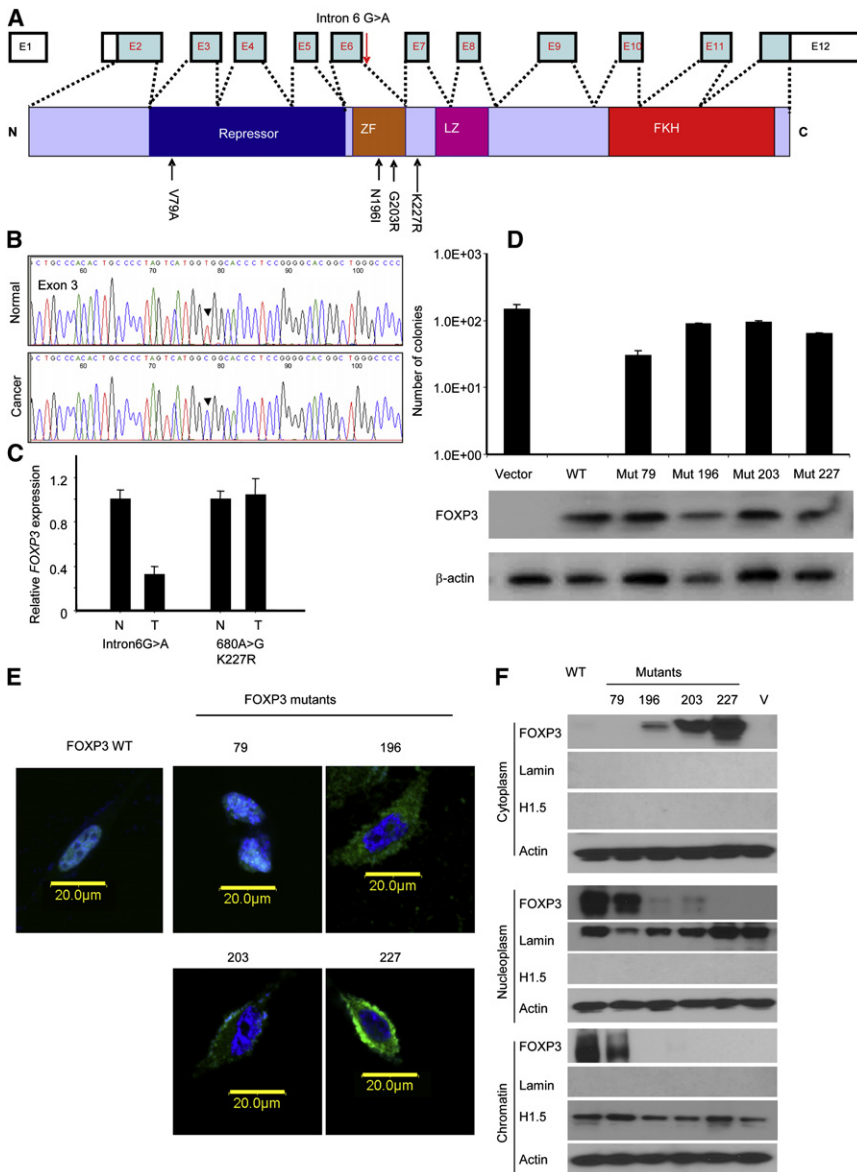


Figure 3. Somatic Mutation of *FOXP3* Gene in Prostate Cancer Samples

DNA samples from cancerous and benign tissues dissected from 20 cases of frozen prostate cancer tissues were amplified by PCR and sequenced. The somatic mutants were identified by comparing the DNA sequence of normal and cancerous tissues from the same patients.

(A) Diagram of the *FOXP3* gene showing the position of the somatic mutations identified.

(B) A representative chromatogram showing mutation of *FOXP3* in exon 3.

(C) Partial inactivation of the *FOXP3* locus in prostate cancer with an intronic mutation. Data shown are means and SD of relative levels of *FOXP3* transcripts, with the levels of normal tissues defined as 1.0. This experiment has been repeated once.

(D) Missense mutations of the *FOXP3* gene abrogated inhibition of the colony formation of the prostate cancer cell line Du145 by *FOXP3*. Data shown are means and SD of colony numbers in 10 cm dishes ($n = 3$). The expression of *FOXP3* is presented underneath the bar graph. This experiment has been repeated at least 3 times.

(E) Impact of missense mutations on nuclear translocation of *FOXP3*. WT and mutant *FOXP3* were tagged with GFP at the N termini and transfected into PC3 cell line. After drug selection to remove untransfected cells, the cells were stained with DAPI to visualize nuclei. Photos shown are merged DAPI and GFP images captured by confocal microscope.

(F) Cellular localization of WT and mutant *FOXP3* as measured by western blot after cellular fractionation. The cellular fractions were subject to western blot analysis with anti-*FOXP3* mAb (Abcam, ab450) and marker proteins.

inhibition by *FOXP3*, preventing nuclear localization of *FOXP3* appears to be the major mechanism to inactivate the tumor suppressor function. To confirm that disruption of nuclear localization is sufficient to abrogate growth inhibition by *FOXP3*, we used site-directed mutagenesis to inactivate the known nuclear localization sequence of *FOXP3*. As shown in Figure S8, mutation in nuclear localization sequence was sufficient to abrogate growth inhibition by *FOXP3*.

Prostate-Specific Deletion of *FoxP3* Caused Precancerous Lesions

To test the cell-intrinsic effect of *FoxP3* deletion, we crossed the mice with a floxed *FoxP3* locus (diagrammed in Figure 4A) (Fontenot et al., 2005) to a transgenic line that expresses Cre gene under the probasin promoter (PB-Cre4) (Wu et al., 2001). Previous studies have demonstrated that this promoter causes prostate-specific deletion of Floxed genes starting in new-born

less profound reduction in DNA levels likely reflected the fact that our microdissected samples also contained nonepithelial cells that do not express *FoxP3* (Chen et al., 2008). The reduction of *FoxP3* protein is confirmed by western blot using the lysates of total prostate (Figure 4D) and immunohistochemistry staining (Figure 4E). Consistent with the kinetics and levels of the *PB-Cre4* transgene expression (Wu et al., 2001), the deletion is more complete in the ventral and lateral prostate lobes than in the anterior and dorsal lobes.

We took several approaches to determine the effect of prostate-specific deletion in the *FoxP3* locus. First, we used magnetic resonance imaging (MRI) to monitor the prostate size in the live mice. As shown in Figure 5A, 12–15-week-old mice with prostate-specific deletion of the *FoxP3* locus had significant enlargement of the prostate. In comparison to WT, a 5-fold increase in the percentage of Ki67⁺ proliferating epithelial cells was observed in the mutant mice (Figure 5B). Histological

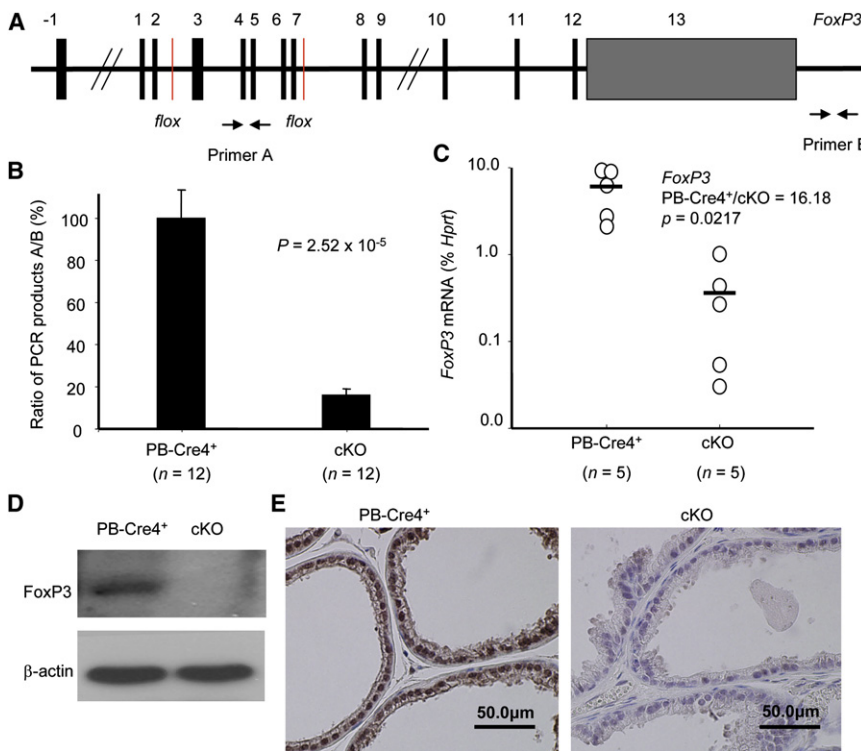


Figure 4. Targeted Deletion of *FoxP3* in the Prostate

(A) Diagram of the floxed *FoxP3* locus and the position of the primers used to measure the ratio of deleted versus undeleted alleles. (B) Efficient deletion of the *FoxP3* locus in the PB4-Cre4+*FoxP3*^{fllox/y} (cKO) but not the PB-Cre4+*FoxP3*^{+/y} transgenic mice (p value by an independent-samples t test). Data shown are means and SD of the ratio of product A/product B of DNA isolated from the microdissected prostate epithelium. (C) Targeted deletion of the *FoxP3* locus caused dramatic reduction of *FoxP3* transcripts in prostate tissue (p value by a Mann-Whitney U test). The RNA isolated from microdissected prostate epithelia were quantitated by real-time PCR. (D) Reduction in *FoxP3* expression, as determined by western blot with anti-FoxP3 mAb (hFOXY). Data shown are lysates of prostate tissues from PB-Cre4+*FoxP3*^{+/y} and PB-Cre4+*FoxP3*^{fllox/y} mice. (E) Reduction of *FoxP3* expression as determined by immunohistochemistry with a polyclonal rabbit anti-mouse *FoxP3* antibodies (Poly6238). Staining of ventral prostate lobes is presented. Similar reduction in *FoxP3* expression was also observed in lateral prostate. Significant, but less complete, reduction in anterior and dorsal lobes was also found. Data in (B–D) were obtained from tissues of 8–12-week-old mice, whereas those in (E) were obtained from 14–16-week-old mice.

examination of the prostate revealed signs of prostate hyperplasia as early as 14–16 weeks in five of six mutant mice. At 23–26 weeks old, 4 of 5 mutant mice, but none of the six age-matched WT mice, exhibited extensive hyperplasia (Figure 5C and Figure 6A). Early PIN was detectable at 23–26 weeks in a small fraction of ventral and dorsal prostate lobes with *FoxP3* deletion, characterized by increased layers of epithelial

cells and nuclear atypia (Figure 5C and data not shown). By 43–60 weeks, all cKO mice examined had hyperplasia. Moreover, all but 1 of 9 cKO mice exhibited early PIN, including multiple layers of epithelial cells (Figures 6B and 6C). The epithelial cells in this region had significantly enlarged nuclei, in comparison to either the single-layered epithelial cells in the same glandular structure (data not shown) or those in the control

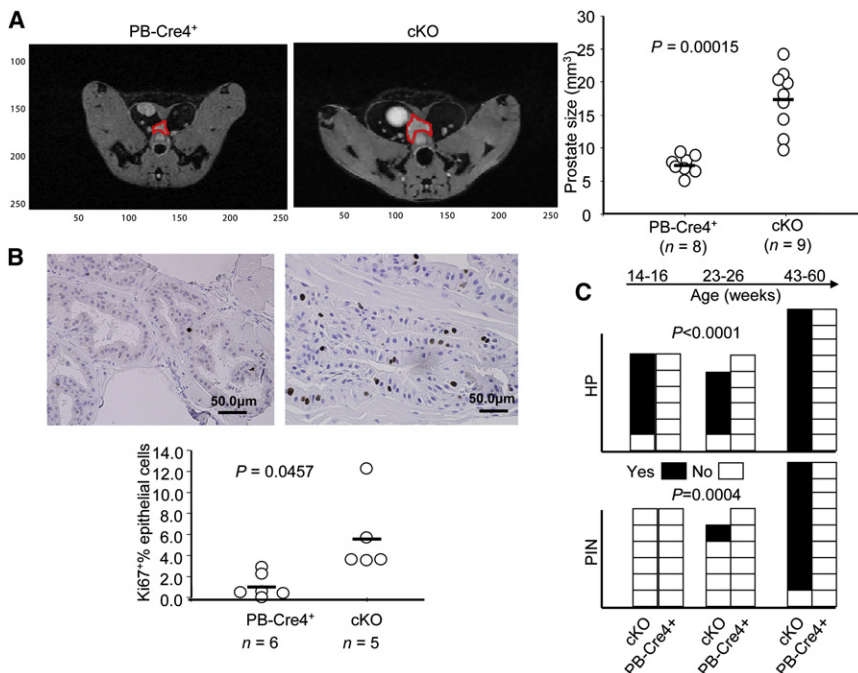


Figure 5. Prostate-Specific Deletion of *FoxP3* in the Prostate Induces Precancerous Lesions

(A) *FoxP3* deletion caused enlargement of prostates. The prostates of 12- to 15-week-old, age-matched WT and condition KO (cKO) mice were measured by magnetic resonance imaging (MRI) (p value by an independent-samples t test). The images of a representative prostate from each group are shown on the left, whereas the prostate volumes of individual mice are shown on the right. (B) *FoxP3* deletion led to increased proliferation of prostate epithelium, using expression of Ki67 as an indicator of proliferating cells (p value by a Mann-Whitney U test). Representative morphology and Ki67 staining are shown at the top, and the percentage of Ki67+ cells among the epithelial cells are shown at the bottom. At least five 40 \times fields for each mouse, at 14–16 weeks of age, were counted. (C) Incidence of prostate hyperplasia (HP) and prostatic intraepithelial neoplasia (PIN) in cKO (PB-Cre4+*FoxP3*^{fllox/y}) and in WT (combining both PB-Cre4+*FoxP3*^{+/y} and PB-Cre4+*FoxP3*^{fllox/y}). The statistical significance was determined by a log-rank test.

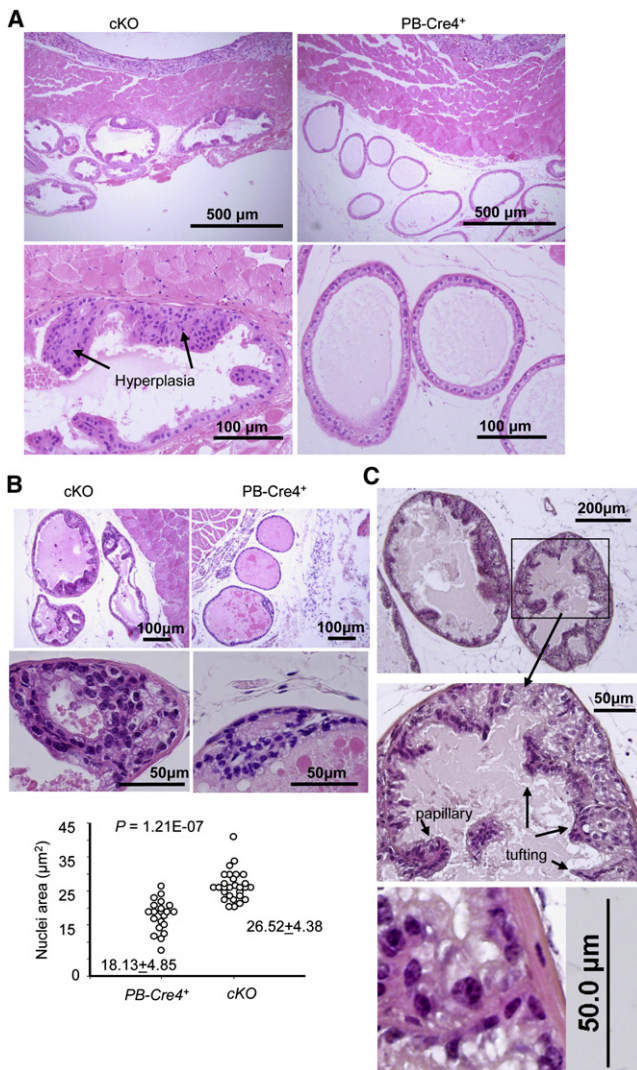


Figure 6. Histology Data of Hyperplasia and Early PIN

(A) Representative H&E staining of hyperplastic lesions in 24-week-old cKO ventral prostate sections. A 26-week-old WT (*PB-Cre4⁺FoxP3^{+/+}*) ventral prostate image is shown for comparison.

(B) A representative early PIN lesion in ventral prostate of a 43-week-old cKO mouse. The image of an age-matched (*PB-Cre4⁺FoxP3^{+/+}*) ventral prostate was included for comparison. Low (upper panels) and high (middle panels) power images are presented. The sizes of nuclei were determined by Scion Image software (Scion Corporation, Frederick, Maryland).

(C) A PIN lesion in ventral prostate of a 60-week-old cKO mouse, showing the papillary and tufting. A high-power image showing enlarged nuclei and active nucleoli is presented in the lower panel.

mice (Figure 6B, middle and lower panels). In most cases, the epithelia formed both papillary and tufting (Figure 6C) patterns. Under high power, the luminal epithelial cells in these areas appeared transformed, as demonstrated by enlargement of nuclei and more-active nucleoli (Figure 6C). In most mice, multiple PINs were found in the anterior, ventral, and lateral prostate lobes, although the lesions are all focal in nature. All WT prostates have normal morphology through the course of the study. Therefore, targeted mutation of the *FoxP3* gene in prostate

tissue is sufficient to initiate the process of prostate cancer development.

FOXP3 Is Necessary and Sufficient to Repress Expression of *MYC*

MYC is overexpressed in 80% of the prostate cancer samples starting as early as benign hyperplasia (Fleming et al., 1986). However, the mechanism by which *MYC* transcription is increased remains unclear. We tested whether *MYC* upregulation correlates with downregulation of the *FOXP3* transcripts. We measured the levels of the mRNA transcripts from microdissected cancerous and benign tissues from 18 patients by real-time PCR. We normalized the transcript levels in cancer tissue against the normal epithelia from the same patients in order to avoid differential RNA degradation under different sample procurement conditions. We observed an increased *MYC* expression in 15 of 18 cases. Importantly, a significant correlation was observed between *FOXP3* downregulation and *MYC* overexpression among malignant tumor samples (Figure 7A). When the levels of normal and cancer tissues were compared separately, a negative correlation between *FOXP3* and *MYC* levels was found in cancer but not normal samples (Figure S9). To test the relevance of this observation in human prostate cells, we tested the effect of the *FOXP3* shRNA on *MYC* expression in early passage primary human prostate epithelial cells. Normal prostate cell culture grew slowly and expressed low levels of *MYC*. ShRNA silencing increased the growth rate of the culture (Figure S10). As shown in Figure 7B, *FOXP3* shRNA caused a major reduction in the expression of *FOXP3* mRNA and protein. Correspondingly, the levels of *MYC* transcripts and protein were significantly elevated by *FOXP3* shRNA. To test whether the correlation could be causative and independent of cancer development in vivo, we microdissected normal WT and *FoxP3*-deleted prostate tissues and compared the *Myc* transcript levels. As shown in Figure 7C, prostate deletion of the *FOXP3* locus caused a more than 4-fold increase in *Myc* mRNA. Moreover, the increased transcript levels were also reflected in elevation of the *Myc* protein in the nuclei (Figure 7D). These data demonstrated that *FoxP3* is a necessary repressor for the *Myc* locus.

To test whether ectopic expression of *FOXP3* is sufficient to repress *MYC*, we transfected two prostate cancer cell lines with *FOXP3*. As shown in Figure 7E, *FOXP3* transfection almost completely abrogated the expression of *MYC* in both cell lines. To determine whether the growth inhibition was mediated by repression of *MYC*, we cotransfected *FOXP3* with *MYC* cDNA into Du145 cells. The cells were transfected with either pcDNA6-blasticidin vector or *MYC* cDNA (comprising the entire coding region but no untranslated regions) and either the pEF1-G418 vector or *FOXP3* cDNA. As shown in Figure 7F, ectopic expression of *MYC* overcame *FOXP3*-mediated tumor suppression. These data demonstrated that *MYC* repression explains the growth inhibition of *FOXP3*, at least for established prostate cancer cell line.

Molecular Mechanisms for *FOXP3*-Mediated *MYC* Repression and for Somatic Inactivation of *FOXP3*

To understand the mechanism by which *FOXP3* represses *MYC*, we used ChIP to identify the site of *FOXP3* binding in the *MYC* promoter. As shown in Figure 8A, quantitative PCR analysis indicated that, despite the abundance of forkhead binding sites,

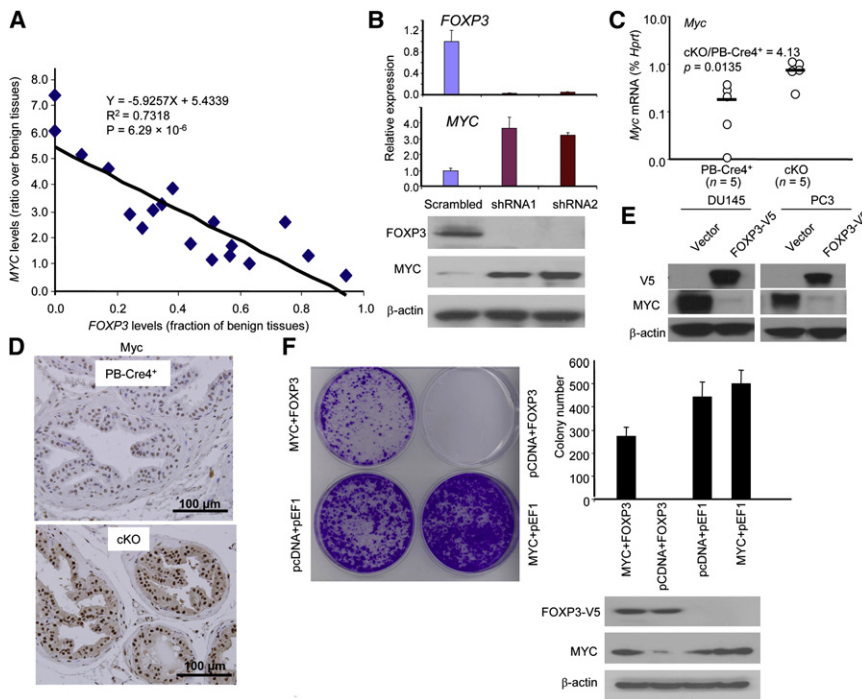


Figure 7. *FOXP3* Is Both Necessary and Sufficient to Repress the *MYC* Oncogene

(A) Inverse correlation between *FOXP3* and *MYC* expression in primary prostate cancer tissues. Statistical significance was observed by using a linear regression model. Data shown are ratio of transcript levels of tumor over benign prostate tissues from the same patients after they were normalized to housekeeping genes. Data from quantitative real-time PCR in 18 cases are presented.

(B) ShRNA silencing of *FOXP3* resulted in upregulation of *MYC* expression in primary HPEC. Early passage HPEC were infected with retroviral vector expressing either control or *FOXP3* shRNA. The uninfected cells were removed by drug selection. At 1 week after infection, the levels of *FOXP3* or *MYC* mRNA were quantitated by real-time PCR. The levels were normalized against *GAPDH*, and those in the control group were defined as 1.0. Data shown are the means and SD of triplicates and were repeated two times. The lower panel shows the levels of *FOXP3* and *MYC* proteins as revealed by western blot.

(C) Targeted deletion of the *FoxP3* locus caused elevation of the *Myc* transcripts in mouse prostate tissue (p value by a Mann-Whitney *U* test). The RNA isolated from microdissected prostate epithelia, from 8- to 12-week-old mice, was quantitated by real-time PCR. Data shown are relative levels of *Myc* mRNA, expressed as a percentage of *Hprt* mRNA.

(D) Immunohistochemistry analysis of *Myc* expression in PB-Cre4+ and cKO prostate. Data shown are images from dorsal lobes. A comparable elevation was observed in all four lobes.

(E) Ectopic expression of *FOXP3* into prostate cancer cell lines repressed *MYC* expression. PC3 and Du145 cell lines were transfected with V5-tagged *FOXP3*. After removal of uninfected cells by drug selection, the total cell lysates were analyzed for expression of *FOXP3*-V5, *MYC*, and β -actin as loading control.

(F) Transfection with *MYC* cDNA prevents *FOXP3*-mediated growth inhibition. In addition to either control or *FOXP3* cDNA, the tumor cell lines were infected with either control vector or *MYC* plasmid. A representative photograph of cell growth after crystal violet staining is shown on the left; representative data from one of four experiments using the Du145 cell line are presented in the right. Data shown are means and SD of colony numbers in 6 cm dishes (n = 3). The levels of *FOXP3* and *MYC* proteins are shown underneath the bar graph. Similar rescue was also found when the PC3 cell line was used (data not shown).

a strong binding of *FOXP3* centered around -0.2 kb 5' of the first transcription-starting site (TSS-P1). To test the significance of this site for the repression, we performed a deletional analysis to map the region that conveys susceptibility to *FOXP3* repression. As shown in Figure 8B, little repression by *FOXP3* can be observed when the reporter was truncated before the forked binding site at the -0.2 kb region (F1–F2). Strong inhibition was observed when the binding motif was included (F3–F5). Additional sequences did not increase the efficiency of repression. Sequence alignment revealed a conserved forkhead-binding site surrounding the promoter region with the highest ChIP signal (Figure 8C). When the site was either deleted or mutated, the repression was completely abrogated (Figure 8C). These data demonstrated that *FOXP3* represses *MYC* promoter activity by interacting with the forkhead motif at the -0.2 kb 5' of the *MYC* TSS.

To test whether somatic mutations of *FOXP3* affect *MYC* repression, we transfected WT and mutant *FOXP3* cDNA into the Du145 prostate cancer cell line in conjunction with the *MYC* promoter. Despite similar levels of *FOXP3* protein, somatic mutations substantially reduced *MYC* repression (Figure 8D). Because three of the four mutants failed to localize into the nuclei (Figures 8E and 8F), we tested the remaining mutant for its ability

to bind to the *MYC* promoter. As shown in Figure 8E, the V79A mutation significantly reduced the binding of *FOXP3* to the *MYC* promoter. Taken together, the data presented in this section demonstrate that *FOXP3* represses *MYC* expression by binding the forkhead-binding motif in the promoter. Somatic mutations uncovered in human prostate cancer abrogated the *MYC* repression by either preventing *FOXP3*'s nuclear localization or its binding to a *cis*-element in the *MYC* promoter.

DISCUSSION

Molecular pathogenesis of prostate cancer development includes both upregulation of oncogenes, such as *MYC*, and inactivation of tumor suppressor genes, such as autosomal genes *PTEN* and *NKX3.1*. Although X-linked genes have been implicated by genetic epidemiology and linkage analysis, no X-linked tumor suppressors have been identified for prostate cancer. Our study described herein fills a major gap by identifying the *FOXP3* gene as an X-linked tumor suppressor gene in males.

***FOXP3* Is a Tumor Suppressor in Prostate Cancer**

We and Rivera et al. have recently reported the involvement of X-linked tumor suppressor genes in female cancer patients, where

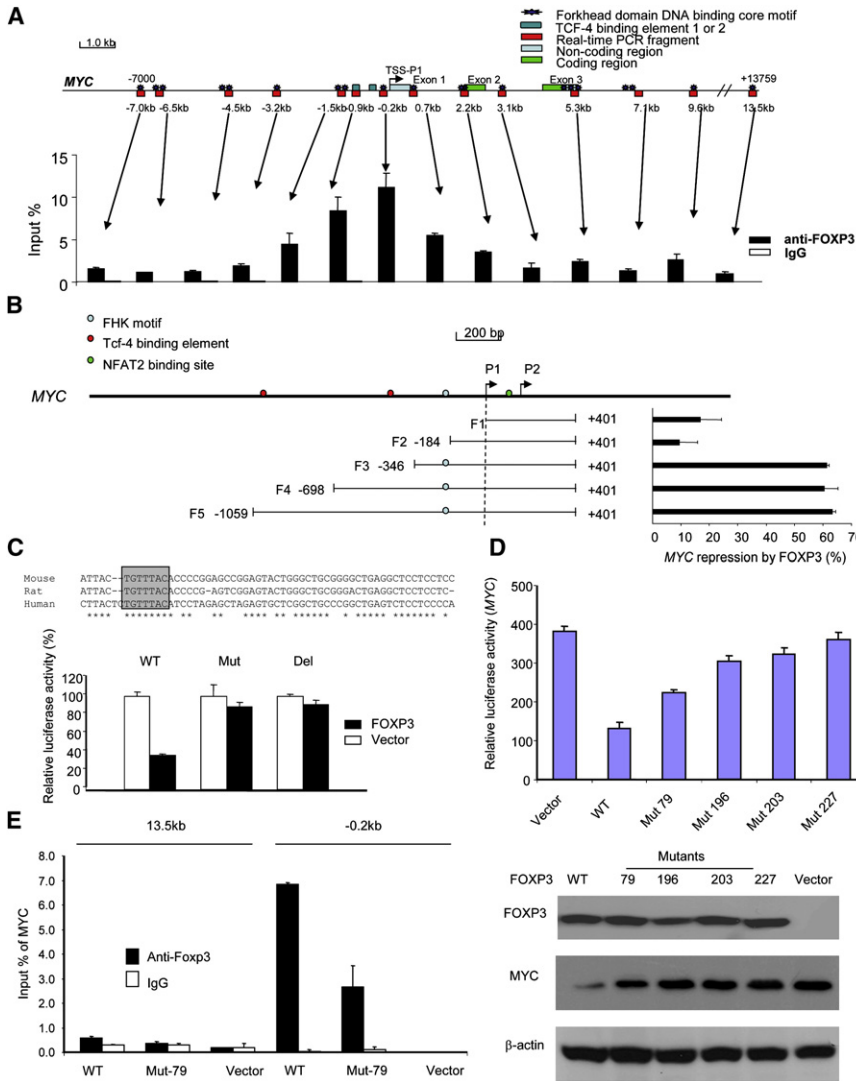


Figure 8. Molecular Mechanism for *MYC* Repression by *FOXP3* and Its Inactivation by Mutations in Cancer

(A) Identification of a *FOXP3*-binding site in the 5' region of the *MYC* gene. The top panel is a diagram of the *MYC* gene (Bossonne et al., 1992), with the Forkhead consensus motifs and the areas covered by PCR primers marked. The distances related to the transcriptional starting site (TSS) are shown. The lower panel shows the amounts of DNA precipitated, expressed as a percentage of input DNA. Data shown were repeated two times.

(B) *FOXP3* repressed the *MYC* promoter. The top panel shows a diagram of the *MYC* locus. The lower left panel shows the *MYC* regions included in the luciferase reporter, whereas the lower right panel shows the percentage of inhibition of the promoter activity, expressed as follows: (1 – luciferase activity in the presence of *FOXP3*/luciferase activity in the absence of *FOXP3*) × 100. Data shown are means of three independent experiments.

(C) Deletion or mutation of the *FOXP3*-binding sites abrogated *FOXP3*-mediated suppression of the *MYC* reporter. The top shows the alignment of human, mouse, and rat *MYC*, revealing that the identified *FOXP3*-binding motif in *MYC* is in conserved region. The *FOXP3*-binding motif is shown in the box. The F3 WT reporter or those with either deletion (–195 to –189: TGTTTAC) or mutation (–195 to –189: TGTTTAC to AAAAGGG) of the reporter were transfected into 293T cells in conjunction with either control or *FOXP3*-expressing vector. The mean luciferase activities in the absence of *FOXP3* cDNA were artificially defined as 100%.

(D) Somatic mutation of *FOXP3* reduced its repressor activity for the *MYC* promoter. In the upper panel, the F3 WT reporters were cotransfected with either vector control or cDNA encoding WT or mutant *FOXP3* into the 293T cell line. At 48 hr after transfection, the lysates were harvested to measure luciferase activity. Data shown have been reproduced three times. In the lower panel, WT or mutant *FOXP3* were transfected into the Du145 cells, and the *FOXP3* and *MYC* protein expression was analyzed by western blot.

(E) Despite normal nuclear translocation, V79A mutant show reduced binding to the critical *cis*-element at –0.2 kb region. Sonicated chromatins isolated from either WT or V79A mutant-transfected Du145 cells were precipitated with either control mouse IgG or mAb specific for *FOXP3* (Abcam, ab450). The amounts of specific DNA were quantitated by real-time PCR using primers corresponding to the –0.2 and +13.5 kb regions. Data shown are means percentage input DNA and have been reproduced three times. Error bars in this figure indicate SD.

the suppressor genes are functionally silenced by a programmed epigenetic event that occurred in all cells (X-inactivation) and another lesion such as gene deletion and/or mutation (Rivera et al., 2007; Zuo et al., 2007b). Here, we describe evidence that, in the male, the *FOXP3* locus is silenced by deletion and somatic mutation.

Immunohistochemical analysis demonstrated that the nuclear *FOXP3* protein is absent in 68.5% of prostate cancer cases tested. Thus, in addition to deletion and mutation identified herein, additional mechanisms, such as epigenetic silencing or mutations outside the areas analyzed, may also contribute to lack of *FOXP3* expression. In contrast, 100% of benign prostate samples exhibited clear epithelial expression of nuclear *FOXP3*.

The overwhelming difference strongly suggests a relationship between *FOXP3* downregulation and cancer development. This hypothesis has been confirmed by the impact of prostate-specific deletion of the *FoxP3* locus. These data, together with strong growth inhibition and *MYC* repression by *FOXP3*, demonstrate that the *FoxP3* gene plays a critical role in suppressing pathological transformation of the prostate. However, it should be pointed out that, similar to other tumor suppressors, including *Trp53* (Chen et al., 2005), *NKX3.1* (Abdulkadir et al., 2002; Kim et al., 2002), and *Pten* (Chen et al., 2005), we have not observed a full spectrum of prostate cancer during 60 weeks of observation. Because *FoxP3* regulates *Myc* and because the effect of transgenic *Myc* expression can be either hyperplasia (Zhang

et al., 2000) or carcinoma with gene profiles similar to human prostate cancer (Ellwood-Yen et al., 2003), it is unclear whether extended observation time or additional factors are needed to achieve the full spectrum of prostate cancer. The lack of full carcinogenesis over the observation period makes our model valuable for dissecting the contribution of other factors, such as inflammation and aging, in the pathogenesis of prostate cancer. Nevertheless, the development of prostate hyperplasia and intraepithelial neoplasia, a widely accepted precancerous lesion (Tomlins et al., 2006), demonstrates clearly that inactivation of *FOXP3* in prostate cancer patients contributes to prostate cancer development. It is of interest to note that statistically significant downregulation of *FOXP3* occurred in the PIN lesion of human samples. Moreover, somatic mutations of *FOXP3* were found in both PIN and cancerous lesions. Because deletion of *FoxP3* in the mouse caused early PIN but no cancerous lesions so far, it is likely that *FOXP3* inactivation is an early event in prostate carcinogenesis. Inactivation of *FOXP3* will likely work in concert with additional genetic hits to cause prostate cancer.

FOXP3 exhibits strong growth inhibition of prostate cancer cell lines, which is attenuated by somatic mutations in prostate cancer samples. Therefore, our genetic studies in mice and humans demonstrated a critical role for *FOXP3* as a tumor suppressor gene for prostate cancer. The presence of a X-linked tumor suppressor gene as demonstrated in this study revealed a major exception for the generally accepted two-hit theory of tumor suppressor genes in cancer development (Knudson, 1971).

Because the *FOXP3* resides near a region of a putative prostate cancer susceptibility locus (Gudmundsson et al., 2008), an interesting issue is whether identification of *FOXP3* may help to explain reported X-linked genetic susceptibility to prostate cancer (Monroe et al., 1995). In our analysis of more than 100 probands with familial prostate cancer, we have so far identified no germline mutation in the coding region of *FOXP3* (data not shown). Given the early onset of lethal autoimmune diseases associated with inactivating mutation of *FOXP3* (Bennett et al., 2001; Chatila et al., 2000; Wildin et al., 2001), it is unlikely that inactivating germline mutation of the *FOXP3* gene can be found in prostate cancer patients. Additional analyses are needed to determine whether the *FOXP3* polymorphisms affect susceptibility to prostate cancer.

FOXP3 as a Transcriptional Repressor of Oncogene *MYC*

MYC is arguably the most upregulated oncogene in human cancer, because overexpression has been observed in as many as 30% of all human cancer cases. Our results show frequent overexpression of *MYC* mRNA in prostate cancers, in comparison to adjacent normal epithelia. Although it is clear that a mutation of the *APC* gene resulted in upregulation of *MYC* and although *MYC* is essential for the development of colon cancer associated with *APC* mutation (He et al., 1998; Sansom et al., 2007), *APC* mutation is rare in prostate cancers thus cannot explain a *MYC* overexpression in prostate cancer. Likewise, although *MYC* overexpression has been observed in all stages of prostate cancer, a low level of gene amplification is observed only in late stages of prostate cancer (Jenkins et al., 1997; Latil et al., 2000). A similar disparity can be observed in

other tumor types, including breast and lung cancer (Takahashi et al., 1989; Bieche et al., 1999).

Our data presented here provide strong evidence that *FOXP3*-mediated repression of *MYC* is necessary to control *MYC* levels in normal prostate epithelial cells and explains much of the widespread overexpression of *MYC* in prostate cancer. Because transgenic expression of *Myc* resulted in the development of prostate cancer with genetic profiles similar to those in human prostate cancer (Ellwood-Yen et al., 2003), disruption of the *MYC* regulator *FOXP3*, as documented here, likely plays a critical role for molecular pathogenesis of human prostate cancer. Nevertheless, using expression array analysis, we have uncovered a large array of genes that are either up- or downregulated by ectopic expression of *FOXP3*. Notably, the genes involved in cancer are the most affected group (Figure S11). Therefore, much like what was observed in breast cancer, *FOXP3* will likely suppress development of prostate cancer by targeting multiple genes, including both tumor suppressor and oncogenes (Liu et al., 2009; Zuo et al., 2007a; Zuo et al., 2007b).

EXPERIMENTAL PROCEDURES

Prostate Cancer Samples

Three sources of prostate tissue samples were used for this study. Frozen tissues were obtained from the Prostate Cancer Tissue Bank of Ohio State University with no patient identification information. Tissue microarray samples came from the University of Michigan, Biomax (US Biomax, Inc., Rockville, MD), and Target Biotech (Target Biotech, Inc., Thurmont, MD). All human studies have been approved by the institutional review board of Ohio State University and University of Michigan.

Experimental Animals

Transgenic mice PB-Cre4 expressing the Cre cDNA under the control of the probasin promoter have been described elsewhere (Wu et al., 2001) and were obtained from the National Cancer Institute Mouse Model Deposit. Mice with floxed *FoxP3* locus (Fontenot et al., 2005) were provided by Dr. Alexander Rudensky. Male PB-Cre4^{+/+} mice were crossed to female *FoxP3*^{lox/lox} or *FoxP3*^{lox/+} mice. The male F1 mice of given genotypes were used in the study. The pathological evaluation was performed according to the Bar Harbor meeting guideline (Shappell et al., 2004). All animal studies have been approved by the University of Michigan Animal User and Carer Committee.

Cell Cultures and Antibodies

Human prostate epithelial cells (HPECs) were purchased from Lonza Group Ltd. (Switzerland) and cultured with medium from the same vendor. Early passage HPECs were infected with retrovirus expressing either control shRNA or *FOXP3* shRNA vector. Two *FOXP3* short hairpin RNA (shRNA) constructs are *FOXP3*-993-shRNA and *FOXP3*-1355-shRNA (GenBank accession number NM_014009). Oligonucleotides encoding small interfering RNA (siRNA) directed against *FOXP3* are 5'-GCTTCATCTGTGGCATCATCC-3' for *FOXP3*-993-shRNA (993-1013 nucleotides from TSS) and 5'-GAGTCTGCACAAGTGCTTTGT-3' for *FOXP3*-1355-shRNA (1355-1375 from TSS). The selected shRNA oligonucleotides were cloned into pSIREN-RetroQ vectors (Clontech, Mountain View, CA) to generate siRNA according to manufacturer's protocol. Prostate cancer cell lines Du145 and PC3 were obtained from the American Type Culture Collection (ATCC, Rockville, MD). Antibodies specific for the following targets were used for the study: cMyc (Santa Cruz Biotechnology, Santa Cruz, CA; catalog number sc-40), *FOXP3* (Abcam, ab20034 for IHC and ab450 for western blot, Cambridge, MA), hFOXY (eBioscience, catalog number 14-5779-82 for western blot in HPEC), anti-V5 (Invitrogen, SKU number R960-25), Ki67 (Dako Cytomation, code number M7249, Carpinteria, CA), β -actin (Sigma, catalog number A5441, St. Louis, MO), and anti-IgG (Santa Cruz Biotechnology, Santa Cruz, CA).

Immunohistochemistry

Because *FOXP3* is expressed at lower levels in epithelial cells than in the regulatory T cells, the conditions typically used for detecting Treg cells in tumor samples do not give reproducible staining in the epithelial cells. To facilitate replication of the current studies, we have screened commercially available anti-*FOXP3* antibodies and established staining conditions that give strong staining of *FOXP3* in human and mouse epithelial cells.

The normal and cancer prostate frozen samples were partially thawed at room temperature and then immersed in 10% formalin for 8–12 hr and embedded in paraffin. Antigens were retrieved by microwave in 1× target retrieval buffer (Dako) for 12 min. For TMA samples, antigens were retrieved at 37°C overnight after the microwave antigen retrieval treatment. ABC detection system was used for immunostaining according to the manufacturer's protocol (Vectastain Elite ABC, Burlingame, CA). The incubation time for primary antibody *FOXP3* (Abcam 236A/E7, 1:100), *FoxP3* (BioLegend Poly6238, 1:100), c-Myc (Santa Cruz Biotechnology 9E10, 1:200), c-Myc (Abcam ab39688, 1:100), and Ki67 (Dako TEC-3, 1:100) was overnight at 4°C. After incubation with primary antibody, staining was followed by ABC detection system using biotinylated anti-mouse/rabbit/rat IgG. AEC was used as chromogen. The slides were counterstained with hematoxylin and mounted in xylene mounting medium for examination.

Statistical Analysis

The distribution of samples for each group was evaluated using a one-sample Kolmogorov-Smirnov test. In the samples with normal distributions, we compared the means of the dependent variable using a paired-samples *t* test and means of the independent variable using an independent-samples *t* test between two groups. In the samples with nonnormal distribution, we compared the means of the independent variable between two groups using a Mann-Whitney *U* test. Chi-square test was used to compare the relationship between the expression of *FOXP3* and *MYC* among patients. The relationship between the levels of gene expression was estimated using a linear regression model. All data were entered into an access database and analyzed using the Excel 2000 and SPSS (version 10.0; SPSS, Inc.) software.

ACCESSION NUMBERS

The raw data for Figure S11 have been submitted to ArrayExpress under accession number E-MTAB-108.

SUPPLEMENTAL DATA

Supplemental data include four tables, 11 figures, and Supplemental Experimental Procedures and can be found with this article online at [http://www.cell.com/cancer-cell/supplemental/S1535-6108\(09\)00263-3](http://www.cell.com/cancer-cell/supplemental/S1535-6108(09)00263-3).

ACKNOWLEDGMENTS

We thank Dr. Alexander Rudensky for the *FoxP3^{fllox/fllox}* mice, Dr. Hong Wu, Jianting Huang from UCLA, and Dr. George V. Thomas from Institute of Cancer Research and Royal Marsden Hospital, UK, for pathological evaluation of mouse prostate; Drs. Eric Fearon, Steve Gruber, Michael Sabel, and Yuan Zhu for valuable discussion and critical reading of the manuscript; and Ms Darla Kroft for editorial assistance. This study is supported by grants from NIH, Department of Defense, Cancer Research Institute in New York, American Cancer Society, and by a gift made the University of Michigan Cancer Center.

Received: December 12, 2008

Revised: May 8, 2009

Accepted: August 17, 2009

Published: October 5, 2009

REFERENCES

Abdulkadir, S.A., Magee, J.A., Peters, T.J., Kaleem, Z., Naughton, C.K., Humphrey, P.A., and Milbrandt, J. (2002). Conditional loss of *Nkx3.1* in adult mice induces prostatic intraepithelial neoplasia. *Mol. Cell. Biol.* 22, 1495–1503.

Amundadottir, L.T., Sulem, P., Gudmundsson, J., Helgason, A., Baker, A., Agnarsson, B.A., Sigurdsson, A., Benediksdottir, K.R., Cazier, J.B., Sainz, J., et al. (2006). A common variant associated with prostate cancer in European and African populations. *Nat. Genet.* 38, 652–658.

Bar-Shira, A., Matarasso, N., Rosner, S., Bercovich, D., Matzkin, H., and Orr-Urtreger, A. (2006). Mutation screening and association study of the candidate prostate cancer susceptibility genes *MSR1*, *PTEN*, and *KLF6*. *Prostate* 66, 1052–1060.

Bennett, C.L., Christie, J., Ramsdell, F., Brunkow, M.E., Ferguson, P.J., Whitesell, L., Kelly, T.E., Saulsbury, F.T., Chance, P.F., and Ochs, H.D. (2001). The immune dysregulation, polyendocrinopathy, enteropathy, X-linked syndrome (IPEX) is caused by mutations of *FOXP3*. *Nat. Genet.* 27, 20–21.

Bieche, I., Laurendeau, I., Tozlu, S., Olivi, M., Vidaud, D., Lidereau, R., and Vidaud, M. (1999). Quantitation of *MYC* gene expression in sporadic breast tumors with a real-time reverse transcription-PCR assay. *Cancer Res.* 59, 2759–2765.

Bommer, G.T., and Fearon, E.R. (2007). Role of c-Myc in *Apc* mutant intestinal phenotype: case closed or time for a new beginning? *Cancer Cell* 11, 391–394.

Bossone, S.A., Asselin, C., Patel, A.J., and Marcu, K.B. (1992). MAZ, a zinc finger protein, binds to c-MYC and C2 gene sequences regulating transcriptional initiation and termination. *Proc. Natl. Acad. Sci. USA* 89, 7452–7456.

Chatila, T.A., Blaeser, F., Ho, N., Lederman, H.M., Voulgaropoulos, C., Helms, C., and Bowcock, A.M. (2000). JM2, encoding a fork head-related protein, is mutated in X-linked autoimmunity-allergic dysregulation syndrome. *J. Clin. Invest.* 106, R75–R81.

Chen, G.Y., Chen, C., Wang, L., Chang, X., Zheng, P., and Liu, Y. (2008). Cutting edge: broad expression of the *FoxP3* locus in epithelial cells: a caution against early interpretation of fatal inflammatory diseases following in vivo depletion of *FoxP3*-expressing cells. *J. Immunol.* 180, 5163–5166.

Chen, Z., Trotman, L.C., Shaffer, D., Lin, H.K., Dotan, Z.A., Niki, M., Koutcher, J.A., Scher, H.I., Ludwig, T., Gerald, W., et al. (2005). Crucial role of p53-dependent cellular senescence in suppression of *Pten*-deficient tumorigenesis. *Nature* 436, 725–730.

Dalla-Favera, R., Bregni, M., Erikson, J., Patterson, D., Gallo, R.C., and Croce, C.M. (1982). Human c-myc oncogene is located on the region of chromosome 8 that is translocated in Burkitt lymphoma cells. *Proc. Natl. Acad. Sci. USA* 79, 7824–7827.

Ellwood-Yen, K., Graeber, T.G., Wongvipat, J., Iruela-Arispe, M.L., Zhang, J., Matusik, R., Thomas, G.V., and Sawyers, C.L. (2003). Myc-driven murine prostate cancer shares molecular features with human prostate tumors. *Cancer Cell* 4, 223–238.

Emmert-Buck, M.R., Vocke, C.D., Pozzatti, R.O., Duray, P.H., Jennings, S.B., Florence, C.D., Zhuang, Z., Bostwick, D.G., Liotta, L.A., and Linehan, W.M. (1995). Allelic loss on chromosome 8p12–21 in microdissected prostatic intraepithelial neoplasia. *Cancer Res.* 55, 2959–2962.

Erikson, J., ar-Rushdi, A., Drwina, H.L., Nowell, P.C., and Croce, C.M. (1983). Transcriptional activation of the translocated c-myc oncogene in burkitt lymphoma. *Proc. Natl. Acad. Sci. USA* 80, 820–824.

Fearon, E.R., and Dang, C.V. (1999). Cancer genetics: tumor suppressor meets oncogene. *Curr. Biol.* 9, R62–R65.

Fleming, W.H., Hamel, A., MacDonald, R., Ramsey, E., Pettigrew, N.M., Johnston, B., Dodd, J.G., and Matusik, R.J. (1986). Expression of the c-myc proto-oncogene in human prostatic carcinoma and benign prostatic hyperplasia. *Cancer Res.* 46, 1535–1538.

Fontenot, J.D., Gavin, M.A., and Rudensky, A.Y. (2003). *Foxp3* programs the development and function of CD4⁺CD25⁺ regulatory T cells. *Nat. Immunol.* 4, 330–336.

Fontenot, J.D., Rasmussen, J.P., Williams, L.M., Dooley, J.L., Farr, A.G., and Rudensky, A.Y. (2005). Regulatory T cell lineage specification by the forkhead transcription factor *foxp3*. *Immunity* 22, 329–341.

Fox, S.B., Launchbury, R., Bates, G.J., Han, C., Shaiba, N., Malone, P.R., Harris, A.L., and Banham, A.H. (2007). The number of regulatory T cells in prostate cancer is associated with the androgen receptor and hypoxia-inducible factor (HIF)-2 α but not HIF-1 α . *Prostate* 67, 623–629.

- Grandori, C., Cowley, S.M., James, L.P., and Eisenman, R.N. (2000). The Myc/Max/Mad network and the transcriptional control of cell behavior. *Annu. Rev. Cell Dev. Biol.* 16, 653–699.
- Gudmundsson, J., Sulem, P., Manolescu, A., Amundadottir, L.T., Gudbjartsson, D., Helgason, A., Rafnar, T., Bergthorsson, J.T., Agnarsson, B.A., Baker, A., et al. (2007). Genome-wide association study identifies a second prostate cancer susceptibility variant at 8q24. *Nat. Genet.* 39, 631–637.
- Gudmundsson, J., Sulem, P., Rafnar, T., Bergthorsson, J.T., Manolescu, A., Gudbjartsson, D., Agnarsson, B.A., Sigurdsson, A., Benediksdottir, K.R., Blondal, T., et al. (2008). Common sequence variants on 2p15 and Xp11.22 confer susceptibility to prostate cancer. *Nat. Genet.* 40, 281–283.
- Haiman, C.A., Le Marchand, L., Yamamoto, J., Stram, D.O., Sheng, X., Kolonel, L.N., Wu, A.H., Reich, D., and Henderson, B.E. (2007a). A common genetic risk factor for colorectal and prostate cancer. *Nat. Genet.* 39, 954–956.
- Haiman, C.A., Patterson, N., Freedman, M.L., Myers, S.R., Pike, M.C., Waliszewska, A., Neubauer, J., Tandon, A., Schirmer, C., McDonald, G.J., et al. (2007b). Multiple regions within 8q24 independently affect risk for prostate cancer. *Nat. Genet.* 39, 638–644.
- He, T.C., Sparks, A.B., Rago, C., Hermeking, H., Zawel, L., da Costa, L.T., Morin, P.J., Vogelstein, B., and Kinzler, K.W. (1998). Identification of c-MYC as a target of the APC pathway. *Science* 281, 1509–1512.
- Hori, S., Nomura, T., and Sakaguchi, S. (2003). Control of regulatory T cell development by the transcription factor Foxp3. *Science* 299, 1057–1061.
- Jenkins, R.B., Qian, J., Lieber, M.M., and Bostwick, D.G. (1997). Detection of c-myc oncogene amplification and chromosomal anomalies in metastatic prostatic carcinoma by fluorescence in situ hybridization. *Cancer Res.* 57, 524–531.
- Kim, M.J., Cardiff, R.D., Desai, N., Banach-Petrosky, W.A., Parsons, R., Shen, M.M., and Abate-Shen, C. (2002). Cooperativity of Nkx3.1 and Pten loss of function in a mouse model of prostate carcinogenesis. *Proc. Natl. Acad. Sci. USA* 99, 2884–2889.
- Knudson, A.G., Jr. (1971). Mutation and cancer: statistical study of retinoblastoma. *Proc. Natl. Acad. Sci. USA* 68, 820–823.
- Kolligs, F.T., Hu, G., Dang, C.V., and Fearon, E.R. (1999). Neoplastic transformation of RK3E by mutant beta-catenin requires deregulation of Tcf/Lef transcription but not activation of c-myc expression. *Mol. Cell. Biol.* 19, 5696–5706.
- Latil, A., Vidaud, D., Valeri, A., Fournier, G., Vidaud, M., Lidereau, R., Cussenot, O., and Biache, I. (2000). htert expression correlates with MYC over-expression in human prostate cancer. *Int. J. Cancer* 89, 172–176.
- Liu, R., Wang, L., Chen, G., Katoh, H., Chen, C., Liu, Y., and Zheng, P. (2009). FOXP3 up-regulates p21 expression by site-specific inhibition of histone deacetylase 2/histone deacetylase 4 association to the locus. *Cancer Res.* 69, 2252–2259.
- Lu, X., Park, S.H., Thompson, T.C., and Lane, D.P. (1992). Ras-induced hyperplasia occurs with mutation of p53, but activated ras and myc together can induce carcinoma without p53 mutation. *Cell* 70, 153–161.
- Monroe, K.R., Yu, M.C., Kolonel, L.N., Coetzee, G.A., Wilkens, L.R., Ross, R.K., and Henderson, B.E. (1995). Evidence of an X-linked or recessive genetic component to prostate cancer risk. *Nat. Med.* 1, 827–829.
- Narla, G., Difeo, A., Reeves, H.L., Schaid, D.J., Hirshfeld, J., Hod, E., Katz, A., Isaacs, W.B., Hebbing, S., Komiya, A., et al. (2005). A germline DNA polymorphism enhances alternative splicing of the KLF6 tumor suppressor gene and is associated with increased prostate cancer risk. *Cancer Res.* 65, 1213–1222.
- Narla, G., Heath, K.E., Reeves, H.L., Li, D., Giono, L.E., Kimmelman, A.C., Glucksman, M.J., Narla, J., Eng, F.J., Chan, A.M., et al. (2001). KLF6, a candidate tumor suppressor gene mutated in prostate cancer. *Science* 294, 2563–2566.
- Rivera, M.N., Kim, W.J., Wells, J., Driscoll, D.R., Brannigan, B.W., Han, M., Kim, J.C., Feinberg, A.P., Gerald, W.L., Vargas, S.O., et al. (2007). An X chromosome gene, *WTX*, is commonly inactivated in Wilms tumor. *Science* 315, 642–645.
- Roncador, G., Brown, P.J., Maestre, L., Hue, S., Martinez-Torrecuadrada, J.L., Ling, K.L., Pratap, S., Toms, C., Fox, B.C., Cerundolo, V., et al. (2005). Analysis of FOXP3 protein expression in human CD4+CD25+ regulatory T cells at the single-cell level. *Eur. J. Immunol.* 35, 1681–1691.
- Sansal, I., and Sellers, W.R. (2004). The biology and clinical relevance of the PTEN tumor suppressor pathway. *J. Clin. Oncol.* 22, 2954–2963.
- Sansom, O.J., Meniel, V.S., Muncan, V., Pesse, T.J., Wilkins, J.A., Reed, K.R., Vass, J.K., Athineos, D., Clevers, H., and Clarke, A.R. (2007). Myc deletion rescues Apc deficiency in the small intestine. *Nature* 446, 676–679.
- Shappell, S.B., Thomas, G.V., Roberts, R.L., Herbert, R., Ittmann, M.M., Rubin, M.A., Humphrey, P.A., Sundberg, J.P., Rozenburg, N., Barrios, R., et al. (2004). Prostate pathology of genetically engineered mice: definitions and classification. The consensus report from the Bar Harbor meeting of the Mouse Models of Human Cancer Consortium Prostate Pathology Committee. *Cancer Res.* 64, 2270–2305.
- Spatz, A., Borg, C., and Feunteun, J. (2004). X-chromosome genetics and human cancer. *Nat. Rev. Cancer* 4, 617–629.
- Suzuki, H., Freije, D., Nusskern, D.R., Okami, K., Cairns, P., Sidransky, D., Isaacs, W.B., and Bova, G.S. (1998). Interfocal heterogeneity of PTEN/MMAC1 gene alterations in multiple metastatic prostate cancer tissues. *Cancer Res.* 58, 204–209.
- Takahashi, T., Obata, Y., Sekido, Y., Hida, T., Ueda, R., Watanabe, H., Ariyoshi, Y., Sugiura, T., and Takahashi, T. (1989). Expression and amplification of myc gene family in small cell lung cancer and its relation to biological characteristics. *Cancer Res.* 49, 2683–2688.
- Taub, R., Kirsch, I., Morton, C., Lenoir, G., Swan, D., Tronick, S., Aaronson, S., and Leder, P. (1982). Translocation of the c-myc gene into the immunoglobulin heavy chain locus in human Burkitt lymphoma and murine plasmacytoma cells. *Proc. Natl. Acad. Sci. USA* 79, 7837–7841.
- Thompson, T.C., Southgate, J., Kitchener, G., and Land, H. (1989). Multistage carcinogenesis induced by ras and myc oncogenes in a reconstituted organ. *Cell* 56, 917–930.
- Tomlins, S.A., Rubin, M.A., and Chinnaiyan, A.M. (2006). Integrative biology of prostate cancer progression. *Annu. Rev. Pathol.* 1, 243–271.
- Vocke, C.D., Pozzatti, R.O., Bostwick, D.G., Florence, C.D., Jennings, S.B., Strup, S.E., Duray, P.H., Liotta, L.A., Emmert-Buck, M.R., and Linehan, W.M. (1996). Analysis of 99 microdissected prostate carcinomas reveals a high frequency of allelic loss on chromosome 8p12–21. *Cancer Res.* 56, 2411–2416.
- Wildin, R.S., Ramsdell, F., Peake, J., Faravelli, F., Casanova, J.L., Buist, N., Levy-Lahad, E., Mazzella, M., Goulet, O., Perroni, L., et al. (2001). X-linked neonatal diabetes mellitus, enteropathy and endocrinopathy syndrome is the human equivalent of mouse scurfy. *Nat. Genet.* 27, 18–20.
- Witte, J.S. (2007). Multiple prostate cancer risk variants on 8q24. *Nat. Genet.* 39, 579–580.
- Wong, A.J., Ruppert, J.M., Eggleston, J., Hamilton, S.R., Baylin, S.B., and Vogelstein, B. (1986). Gene amplification of c-myc and N-myc in small cell carcinoma of the lung. *Science* 233, 461–464.
- Wu, X., Wu, J., Huang, J., Powell, W.C., Zhang, J., Matusik, R.J., Sangiorgi, F.O., Maxson, R.E., Sucov, H.M., and Roy-Burman, P. (2001). Generation of a prostate epithelial cell-specific Cre transgenic mouse model for tissue-specific gene ablation. *Mech. Dev.* 101, 61–69.
- Xu, J., Meyers, D., Freije, D., Isaacs, S., Wiley, K., Nusskern, D., Ewing, C., Wilkens, E., Bujnovszky, P., Bova, G.S., et al. (1998). Evidence for a prostate cancer susceptibility locus on the X chromosome. *Nat. Genet.* 20, 175–179.
- Yeager, M., Orr, N., Hayes, R.B., Jacobs, K.B., Kraft, P., Wacholder, S., Minichiello, M.J., Fearhead, P., Yu, K., Chatterjee, N., et al. (2007). Genome-wide association study of prostate cancer identifies a second risk locus at 8q24. *Nat. Genet.* 39, 645–649.
- Zhang, X., Lee, C., Ng, P.Y., Rubin, M., Shabsigh, A., and Buttyan, R. (2000). Prostatic neoplasia in transgenic mice with prostate-directed overexpression of the c-myc oncoprotein. *Prostate* 43, 278–285.
- Zuo, T., Liu, R., Zhang, H., Chang, X., Liu, Y., Wang, L., Zheng, P., and Liu, Y. (2007a). FOXP3 is a novel transcription repressor for the breast cancer oncogene SKP2. *J. Clin. Invest.* 117, 3765–3773.
- Zuo, T., Wang, L., Morrison, C., Chang, X., Zhang, H., Li, W., Liu, Y., Wang, Y., Liu, X., Chan, M.W.Y., et al. (2007b). FOXP3 is an X-linked breast cancer suppressor gene and an important repressor of HER-2/ErbB2 oncogene. *Cell* 129, 1275–1286.

Activating Transcription Factor 2 and c-Jun–Mediated Induction of FoxP3 for Experimental Therapy of Mammary Tumor in the Mouse

Yan Liu,¹ Yin Wang,¹ Weiquan Li,¹ Pan Zheng,^{1,2} and Yang Liu^{1,3}

¹Division of Immunotherapy, Department of Surgery, Section of General Surgery, and Comprehensive Cancer Center; ²Department of Pathology; and ³Division of Molecular Medicine and Genetics, Department of Medicine, University of Michigan, Ann Arbor, Michigan

Abstract

FOXP3 is inactivated in breast cancer cells by a number of mechanisms, including somatic mutations, deletion, and epigenetic silencing. Because the mutation and deletion are usually heterozygous in the cancer samples, it is of interest to determine whether the gene can be induced for the purpose of cancer therapy. Here, we report that anisomycin, a potent activator of activating transcription factor (ATF) 2, and c-Jun-NH₂-kinase, induces expression of FoxP3 in both normal and malignant mammary epithelial cells. The induction is mediated by ATF2 and c-Jun. Targeted mutation of ATF2 abrogates both constitutive and inducible expression of FoxP3 in normal epithelial cells. Both ATF2 and c-Jun interact with a novel enhancer in the intron 1 of the FoxP3 locus. Moreover, shRNA silencing of ATF2 and FoxP3 reveals an important role of ATF2-FoxP3 pathway in the anisomycin-induced apoptosis of breast cancer cells. A low dose of anisomycin was also remarkably effective in treating established mammary tumor in the mice. Our data showed that FoxP3 can be reactivated for cancer therapy. [Cancer Res 2009;69(14):5954–60]

Introduction

The overwhelming majority of tumor suppressor genes are autosomal, and their inactivations involve two genetic events (1–4). The best defined two hits of the tumor suppressors in cancer cells are usually irreversible, such as deletion or mutations (3, 4). More recently, however, it has become increasingly clear that epigenetic inactivation of tumor suppressors plays a critical role in inactivating tumor suppressor genes (5). On the other hand, due to X-inactivation, the X-linked tumor suppressor genes are operatively hemizygous, and can be inactivated by a single hit (6). This notion has been substantiated by the recent identification of two tumor suppressor genes, *FoxP3* for breast cancer (7) and *WTX* for Wilms' tumor (8). Because the majority of mutations and/or deletions associated with X-linked tumor suppressor genes are heterozygous (7, 8), most cancer cells have a wild-type (WT) allele that has not been irreversibly inactivated (7).

An important aspect of tumor therapy is how to restore the function of tumor suppressors. For those with two irreversible genetic changes, such as p53, this has been technically challenging, although a pharmaceutical restoration of mutant protein function has been reported (9). Because X-linked tumor suppressor genes are operationally hemizygous, only one allele is subject to genetic selection in cancer cells. The other allele is therefore genetically intact and can potentially be induced to suppress tumor growth. Based on this concept, we searched for a biochemical pathway that can be activated to induce FOXP3 expression in breast cancer cells. Here, we report that anisomycin, which is commonly used to induce stress responses of cells, induces expression of *FOXP3* in breast cancer cell lines. Our biochemical and genetic analyses revealed that activating transcription factor (ATF)2, which was recently shown to be a tumor suppressor gene in the mouse (10), is essential for the induction of FoxP3 and FoxP3-mediated apoptosis. Moreover, ATF-2 forms heterodimer with c-Jun to activate transcription of *FoxP3*. These data show a novel function of ATF2 in the expression of *FoxP3* in the epithelial cells and suggest a novel approach for the therapy of breast cancer.

Materials and Methods

Antibodies and reagents. Anti-ATF-2 (20F1), phospho-ATF2-(Thr71), and activated caspase-3 were purchased from Cell Signaling, Inc. Other vendors are as follows: anti-Foxp3 (eBioscience; #14-5779-82); and anti- β -actin (I-19), c-Jun (NX), and phosphor-c-Jun (KM-1; Santa Cruz Biotechnology, Inc.). Chemicals SP600125, SB203580, and PD98059 were purchased from CalBiochem, Inc., whereas anisomycin was purchased from Sigma, Inc.

Experimental animals. Mice heterozygous for *Atf2* null mutation (*Atf2^{tm1Glm}/Atf2⁺129S2/SvPas*; ref. 11) were revived from the frozen embryo bank in The Jackson Laboratory. Heterozygous mice were crossed to produce *Atf2^{+/+}* and *Atf2^{-/-}* littermates. BALB/c mice were purchased from Charles River through a National Cancer Institute Subcontract. All studies involving animal has been approved by University Committee on Use and Care of Animals at University of Michigan.

Preparation of mammary epithelial cell culture. Mouse mammary fat pads were removed from 6- to 8-wk-old virgin female mice and minced into small pieces. After collagenase digestion at 37°C in a shaking incubator in DMEM supplemented with 5% FCS, cells were sieved through a 70- μ m cell strainer (BD Falcon) to obtain a single-cell suspension. The cells were cultured in DMEM supplemented with 10% fetal bovine serum and 10 ng/mL epithelial growth factor. At day 3 of culture, fibroblast cells were removed by a short digestion with 0.05% trypsin-EDTA as less adherent cells.

Measurement of FOXP3 transcripts. Total cDNA were prepared from breast cancer cell lines or epithelial cultures. The levels of FOXP3 mRNA were measured by reverse transcription-PCR (RT-PCR) under two conditions. Full-length encoding regions were analyzed by agarose

Note: Supplementary data for this article are available at Cancer Research Online (<http://cancerres.aacrjournals.org/>).

Y. Liu and Y. Wang contributed equally to the study.

Requests for reprints: Yang Liu or Pan Zheng, University of Michigan, 109 Zina Pitcher Place, Ann Arbor, MI 48109. Phone: 734-615-3158; Fax: 734-763-2162; E-mail: yangl@umich.edu or panz@umich.edu.

©2009 American Association for Cancer Research.

doi:10.1158/0008-5472.CAN-09-0778

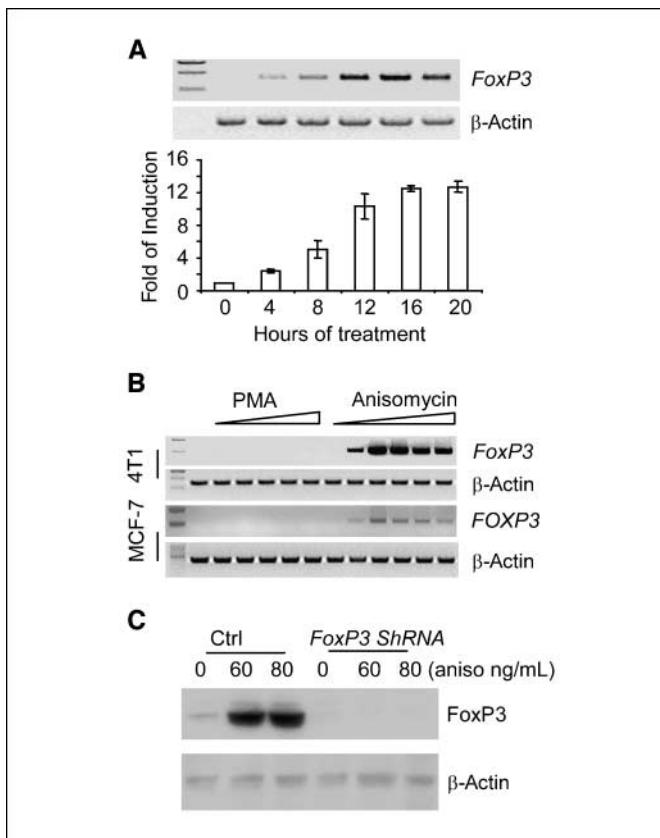


Figure 1. Anisomycin rapidly induces FoxP3 expression in mouse and human breast cancer cell lines. *A*, induction of FoxP3 transcripts by anisomycin (0.1 $\mu\text{g}/\text{mL}$). *Top*, kinetics of FoxP3 induction in mouse mammary tumor cell line TSA, as measured by RT-PCR for cDNA covering the entire coding region. *Bottom*, the induction of FoxP3 in TSA by real-time PCR. *Columns*, means of three independent experiments; *bars*, SD. The transcript level of 0 h is artificially defined as 1.0. *B*, induction of FoxP3 by anisomycin (0.01, 0.05, 0.1, 0.25, 0.5, 1.0 $\mu\text{g}/\text{mL}$), but not by PMA (0.01, 0.1, 0.5, 1.0, 2.5 $\mu\text{g}/\text{mL}$), in mouse mammary tumor cell line 4T1 or human breast cancer cell line MCF7 by RT-PCR, using primers spanning from start codon to stop codon. *C*, anisomycin induces FoxP3 protein, as revealed by Western blot. The specificity of analysis and dependence of FoxP3 transcript is confirmed by FoxP3 shRNA. All data are representative of at least three independent experiments.

gel electrophoresis, whereas shorter transcripts were quantitated using real-time PCR. All primers for PCR were listed in Supplementary Table S1.

ShRNA lentiviral vector. The lentivirus-based shRNA expressing vectors were created by introducing the murine U6 RNA polymerase III promoter and a murine phosphoglycerate kinase promoter (pGK)-driven enhanced green fluorescent protein expression cassette into a vector of pLenti6/V5-D-TOPO back bone without cytomegalovirus promoter. Hairpin shRNA sequence of FoxP3, JNK1, JNK2, and Atf2 (FoxP3: 5'-aagccatggcaatagttcctt-3'; FOXP3: 5'-gcagcggacactcaatgag-3'; JNK1/2: 5'-agaaggttaggacattcctt-3' and 5'-aagcctagtaatatagtagt-3'; Atf2: 5'-cttctgtttagaacaac-3' and 5'-agcactgaatgacagtgtca-3') were cloned into the lentiviral shRNA expressing vectors by restriction sites of *ApaI* and *EcoRI*.

Electrophoresis mobility shift assay. Anisomycin were added to 4T1 cells in conjunction with either vehicle control or kinase inhibitor SP600125 at a dose of 2 $\mu\text{g}/\text{mL}$ for 2 h before cells lysed. The nuclear extracts were mixed with either WT or mutant probes in the presence of either control anti-c-Jun (Santa Cruz; sc-45X) or anti-ATF2 (Cell Signaling, #9226) antibodies, as indicated and analyzed by electrophoresis, as described (12).

Western blot. Protein samples for Western blot were prepared by lysing cultured cells in SDS sample buffer, resolved on 10% SDS-PAGE, and

electroblotted onto nitrocellulose membranes. Membranes with transferred proteins were incubated with primary antibody followed by incubation with horseradish peroxidase conjugated to the secondary antibody. Chemiluminescence reaction using the enhanced chemiluminescence kit (Amersham Biosciences) was detected by film.

Chromatin immunoprecipitation (ChIP) was carried out according to a published procedure (13). Briefly, the vehicle or 2-h anisomycin-treated 4T1 cells were sonicated and fixed with 1% paraformaldehyde. The anti-phospho-c-Jun or anti-phosphor-ATF2 antibodies or control rabbit IgG were used to pull down chromatin associated with these proteins. The amounts of the specific DNA fragments were quantitated by real-time PCR and normalized against the genomic DNA preparation from the same cells.

Immunofluorescence staining. TSA cells were treated or left untreated with vehicle DMSO or 50 ng/mL of anisomycin for 24 h. After that, the cells were fixed by methanol, permeabilized with 0.3% Triton-X100, and stained with rabbit antibody against cleaved Caspase 3 (Cell signaling, #9661s) overnight. The stained cells were then visualized with Cy3-conjugated anti-rabbit IgG (Jackson ImmunoResearch Laboratory).

3-(4,5-Dimethylthiazol-2-yl)-2,5-diphenyltetrazolium bromide (MTT) cell viability assay has been described in details (14).

DNA contents Anisomycin-treated or control cells were stained by Propidium Iodide using "PI/RNase Staining Buffer" from BD Biosciences according to the manufacturer's manual.

Results

Induction of FoxP3 by anisomycin. We have recently shown that the expression of FoxP3 cDNA leads to rapid cell death of breast cancer cell lines (7, 15). These results raised the possibility that the induction of FoxP3 may represent a novel therapeutic approach for the treatment of breast cancer. When we screened for drugs that induce FoxP3 expression in mammary tumor cell lines, we observed a rapid induction of FoxP3 mRNA by anisomycin. As shown in Fig. 1A, significant levels of the FoxP3 transcripts were induced in a mouse mammary tumor cell line, TSA, as early as 4 hours after anisomycin treatment. Similar effects were observed in another mouse mammary tumor cell line 4T1 and human breast cancer cell line MCF-7 (Fig. 1B), which we showed to harbor the WT FOXP3 gene (7). In contrast, treatment of phorbol 12-myristate 13-acetate (PMA) did not result in any induction of FoxP3 (Fig. 1B). Because higher doses of anisomycin can inhibit translation, we tested induction of the FoxP3 protein by Western blot. As shown in Fig. 1C, low doses of anisomycin induced high levels of FoxP3 protein, which indicated that activation of FoxP3 locus can be achieved at doses that did not prevent translation of the FoxP3 protein. Importantly, the induction of FoxP3 protein can be prevented by FoxP3 shRNA. These data not only proved the specificity of Western blot but also confirmed that the accumulation of FoxP3 protein depends on induction of FoxP3 mRNA.

Involvement of ATF2, c-Jun-NH₂-kinase in FoxP3 induction. As a first step to identify the mechanism by which anisomycin induced FoxP3, we treated mammary tumor cell line with anisomycin in conjunction with inhibitors of overlapping specificity, including ATF-2/c-Jun-NH₂-kinase (JNK) inhibitor SP10096 (SP), p38 α inhibitor SB203580 (SB), and p41/42 MAP kinase inhibitor PD9786 (PD). As shown in Fig. 2A, SP completely prevented the induction of FoxP3. On the other hand, SB and PD had little effect. These data raised the possibility that ATF-2 and JNK pathways may be involved in the induction of FoxP3 by anisomycin.

To test this hypothesis, we generated lentiviral vectors expressing shRNA for JNK1/2 or ATF2. The efficacy of shRNA

silencing and the effect of the silencing on anisomycin-mediated induction of *FoxP3* is shown in Fig. 2B. These data showed that silencing either *JNK* or *ATF2* resulted in abrogation of the induction of the *FoxP3* transcripts and protein by anisomycin. These data provide important genetic evidence for the involvement of JNK and ATF2 in anisomycin-induced *FoxP3* expression.

Interestingly, a recent study showed that mice with heterozygous deletion of the *ATF2* gene developed spontaneous mammary tumors (10). Because *FoxP3* heterozygous mutants have the same phenotype, it is intriguing that ATF2 may be responsible

for constitutive and/or inducible expressions of *FoxP3* in mammary epithelial cells. To address this issue, we obtained *ATF2*^{+/-} mice from the frozen embryo bank of The Jackson Laboratory. The *ATF2*^{+/+} and the *ATF2*^{-/-} mice were obtained by F1 cross. A previous report indicated that the only a small fraction of the *ATF2*^{-/-} mice survive to adulthood (11). We obtained two *ATF2*^{-/-} females, from which we obtained two independent primary mammary epithelial cell cultures (Fig. 2D). The epithelial origin of the cultures was shown by the expression of CK19. Because T cells are the major source of *FoxP3* transcripts *in vivo*, we also confirmed that the primary culture has no T-cell

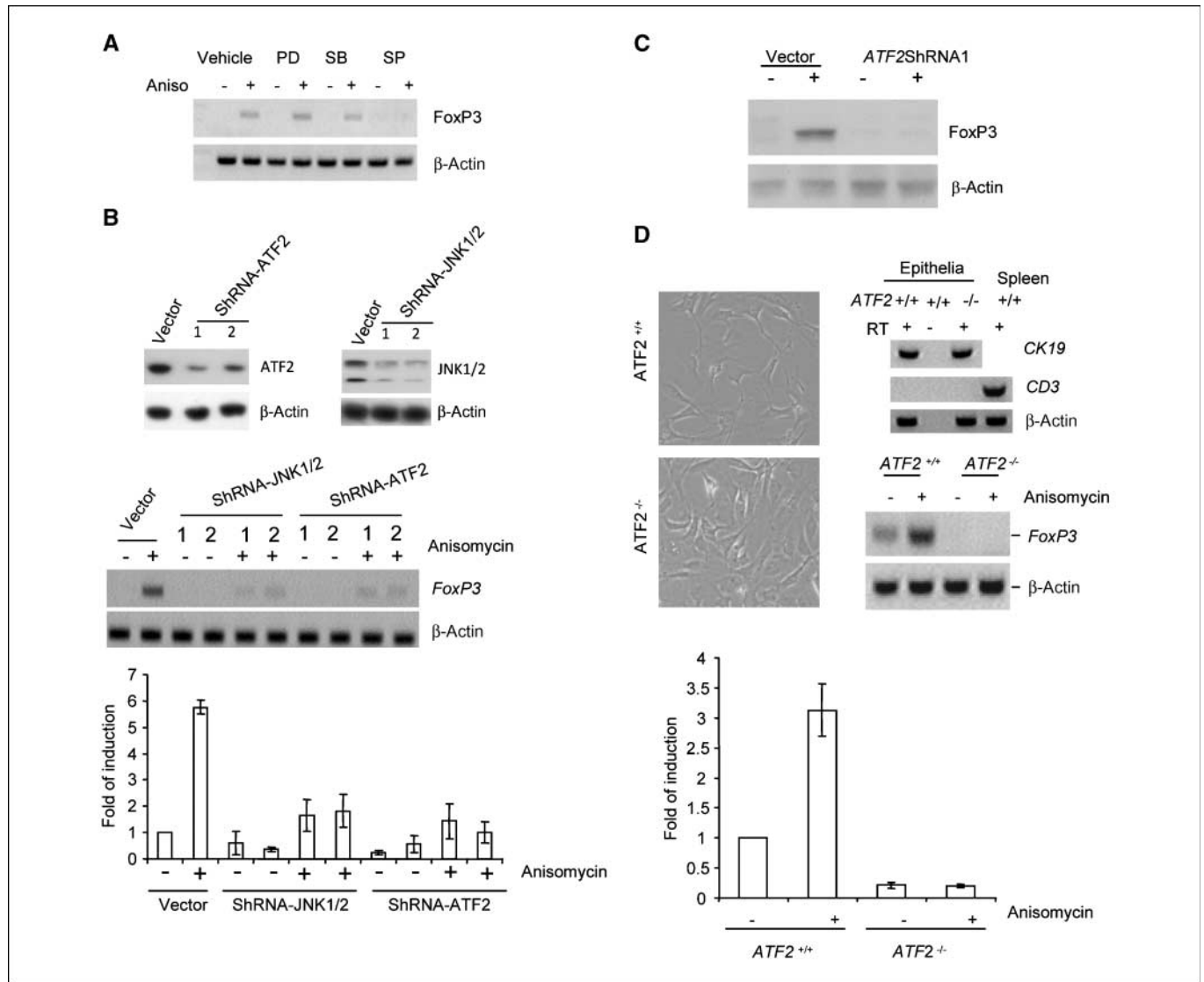


Figure 2 A critical role of ATF2 and JNK1/2 in *FoxP3* induction by anisomycin. **A**, inhibitor of JNK and ATF-2 prevented induction of *FoxP3*. 4T1 cells were stimulated with anisomycin (0.1 μg/mL) in presence or absence of inhibitors (2 μg/mL) for ATF-2 and JNK SP, SB, and PD. The induction of *FoxP3* was measured by RT-PCR 16 h after induction. **B**, effect of shRNA silencing of *ATF2* and *JNK1/2* on anisomycin-induced *FoxP3* expression. *Top*, efficacy of shRNA using lentiviral vector control or that with given shRNA, as measured by Western blot. Levels of β-actin are used as loading controls. *Middle*, RT-PCR results as determined by electrophoresis. Two independent shRNA (called 1 and 2) were used. 4T1 cells treated with either vehicle control (-) or 0.1 μg/mL of anisomycin for 16 h. *Bottom*, real-time PCR results. The *FoxP3* mRNA levels were determined by RT-PCR as detailed in Fig. 1 legends. **C**, shRNA for *ATF2* prevented induction of *FoxP3* protein, as measured by Western blot. **D**, targeted mutation of *ATF2* abrogated both constitutive and inducible expression of the *FoxP3* gene in mouse mammary epithelial culture. *Top and middle left*, morphology of epithelial culture. Note higher cellular density of the *ATF2*^{-/-} epithelial culture. *Top right*, the primary cell culture expressed epithelial cell marker (CK19) and had no T-cell contamination as judged by the lack of CD3 transcript. *RT*, reverse transcriptase. *Middle right*, constitutive and inducible expression of *FoxP3* in *ATF2*^{+/+} but not *ATF2*^{-/-} cultures. *Bottom*, real-time PCR quantitation of *FoxP3* induction. *Columns*, means of three independent experiments; *bars*, SD. All data have been repeated at least thrice.

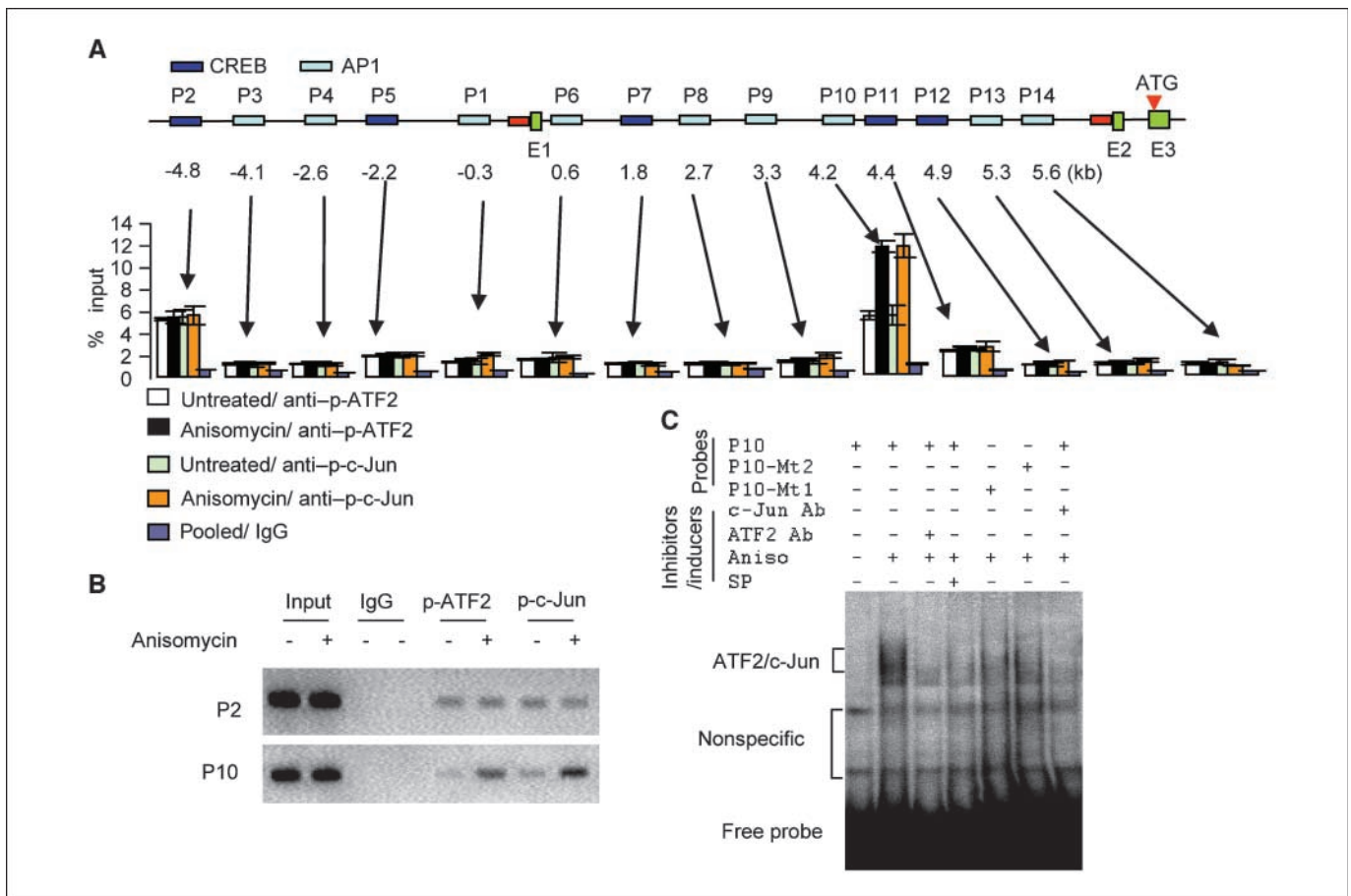


Figure 3. Identification of *cis*-elements that interact with ATF2/c-Jun heterodimer. **A** to **C**, ChIP scanning of potential c-Jun and ATF2 binding sites. The 4T1 cells were treated with either vehicle control or anisomycin for 2 h. The chromatin was cross-linked with paraformaldehyde and precipitated with either control IgG, anti-phospho-ATF2, or anti-phospho-c-Jun. The amounts of DNA were quantified by PCR. **A**, quantitative analysis of the ATF2 and c-Jun binding sites in the FoxP3 locus. *Top*, the genomic structure of the 5' of the FoxP3 locus. The DNA quantitation was shown in the bar graph (*bottom*). Data shown are means of triplicate samples and have been repeated thrice. **B**, PCR amplification of FoxP3 sequences P2 and P10 in ChIPs from anisomycin-treated and untreated cells. Note that although the binding of P10 to ATF2 and c-Jun are inducible, that of P2 was largely unaffected by anisomycin. **C**, the ATF2 and c-Jun bound to the AP1 site in P10. The sequence of WT probe (P10) is agatggagctc**ac**ctaccacatcacgg (bold letters for core AP1 sequence), that for P10-Mt1 is agatggagctc**tg**cgccacatcacgg (bold letters indicate mutations), whereas that for P10-Mt2 is agatggagctc**gac**gcccacatcacgg. The data have been repeated thrice.

contamination by the lack of CD3 transcripts (Fig. 2D). WT epithelial cultures expressed significant amounts of Foxp3 transcripts, which were further induced by the treatment of anisomycin. ATF2^{-/-} cells had no detectable Foxp3 transcripts and did not express Foxp3 after stimulation by anisomycin. These data revealed an essential role for ATF2 in both constitutive and inducible expressions of FoxP3 in normal epithelial cells. On the other hand, the thymocytes from the ATF2^{-/-} mice had normal number of CD4⁺FoxP3⁺ T cells (data not shown). Therefore, the function of ATF2 in FoxP3 expression seems to be epithelia specific.

Identification of the FoxP3 enhancer associated with ATF2 and c-Jun. To study the mechanism of ATF2/JNK-mediated induction of FoxP3, we carried out ChIP to identify an anisomycin-inducible binding site of the FoxP3 locus. To identify specific ATF2 binding sites, we treated the 4T1 cell line with or without anisomycin and carried out ChIP with either control IgG or anti-p-ATF2 antibodies. Because JNK regulate transcription by phosphorylation of c-Jun (16), we used anti-phospho-c-Jun antibodies in the ChIP. To identify the FoxP3 sequence associated

with p-ATF2 and p-c-Jun, we first analyzed the 5' sequence of the FoxP3 gene and identified 14 potential AP1 and cAMP-responsive element binding protein sites. PCR primers were designed across the 10.4 kb regions, and the amounts of each PCR product were normalized against that amplified from the input DNA. The quantitative real-time PCR results were shown in Fig. 3A, whereas the PCR products from two major peaks were shown in Fig. 3B. These data reveal two potential sites for ATF2/cJun interaction. The first is hereby called P2, which is 4.8 kb 5' of exon 1. The second and the stronger binding site P10 is 4.2 kb 3' of exon 1. Importantly, whereas the P2 ATF2/cJun association is not inducible by anisomycin, the P10 binding is enhanced by >2-fold by anisomycin. Moreover, comparison of mouse and human FoxP3 sequence revealed that the P10, but not the P2 site, is highly conserved (Supplementary Fig. S1). Therefore, we focused on the potential significance of P10 as the site for p-ATF2 and p-c-Jun interaction.

Sequencing comparison identified a typical AP1 site within the P10 (Supplementary Fig. S1). To directly show interactions of ATF2 and c-Jun to the FoxP3 promoter, we radiolabeled an

oligonucleotide probe containing conserved AP1 site as well as two control oligos with mutations in the AP1 site and tested their binding to nuclear extracts. As shown in Fig. 3C, the nuclear extracts from anisomycin-treated, but not those from the untreated, 4T1 cells showed strong interaction with the WT P10 probe. The specificity was confirmed as mutations in the AP1 site significantly reduced the binding. Furthermore, the involvement of ATF2 and c-Jun was shown as their specific antibodies abolished the binding of nuclear extracts to WT probe. Thus, both ChIP and electrophoresis mobility-shift assay identify a specific activator protein (AP1) site with 4.2 kb 3' of the TSS, which binds to both p-ATF2 and p-cJun by anisomycin-inducible fashion.

To test whether the P10 sequence was a functional *FoxP3* enhancer, we generated a series of constructs consisting of the basal promoter and putative enhancer elements. As shown in Supplementary Fig. S2, a 265 bp sequence 5' of TSS of the *FoxP3* locus plus 50 bp down-stream of TSS is sufficient to convey a significant basal promoter activity. This fragment is therefore chosen to measure the enhancer activity. As shown in Fig. 4, addition of three copies of P2 fragment increased the promoter activity by ~2-fold, which suggests that P2 is at best a weak enhancer. Inclusion of three copies of P10 sequences, however, increased the *Foxp3* promoter activity by 10-fold. Surprisingly, this seems unidirectional as the inversion of the P10 fragment eliminated its enhancer activity. Moreover, the involvement of AP1 site in P10 was confirmed as a mutation of the AP1 site significantly reduced the enhance activity. Moreover, addition of P2 to P10 failed to further enhance the promoter activity. Taken together, our data showed that anisomycin induced ATF2/c-Jun interaction with a specific enhancer within the intron 1 of the *FoxP3* gene.

A critical role for *ATF2-FoxP3* pathway in anisomycin-induced apoptosis and the therapy of breast cancer. Our recent

studies have shown that the induced expression of *FoxP3* caused apoptosis of breast cancer cell lines (7, 11, 15). To determine whether anisomycin treatment caused apoptosis of breast cancer cells, we measured the cytotoxic effect of anisomycin on several of breast cancer cell lines, by MTT assay. As shown in Fig. 5A, both mouse (TSA) and human breast cancer cell lines (BT474, MCF-7) were highly susceptible to anisomycin, with an IC₅₀ between 50 and 100 ng/mL. The reduced viability is due to apoptosis as revealed by the increased expression of active caspase 3 in TSA cells (Fig. 5B, top) with less than 2C DNA contents (Fig. 5B, bottom). Given the critical role for ATF2 in *FoxP3* induction, we tested the contribution of ATF2 to anisomycin-induced cell death by comparing the dose response to anisomycin in cells transfected with either vector alone or those with *ATF2* shRNA. As shown in Fig. 5C and D, *ATF2* and *FoxP3* shRNAs increased resistance to anisomycin by nearly 3-fold. These data show a critical role for the ATF2-*FoxP3* pathway in anisomycin-induced cell death of breast cancer cells.

To test whether induction of *FoxP3* by ATF2-*FoxP3* pathway can be explored for breast cancer therapy, we injected the TSA cell line into the mammary pad. Seventeen days later, when the cancer cells established locally, the mice were treated with either vehicle control or anisomycin. As shown in Fig. 6, the growth of the TSA tumor cells in syngeneic mammary pad is abrogated by anisomycin. These data show the potential of ATF2-*FoxP3* pathway in the therapeutic development for breast cancer.

Discussion

FOXP3 is an X-linked gene that is subject to X-inactivation (7, 17). Our inquiry into the high incidence of spontaneous mammary tumors in mice heterozygous for the *Scurfy* mutation led to the identification of it as the first X-linked tumor suppressor for

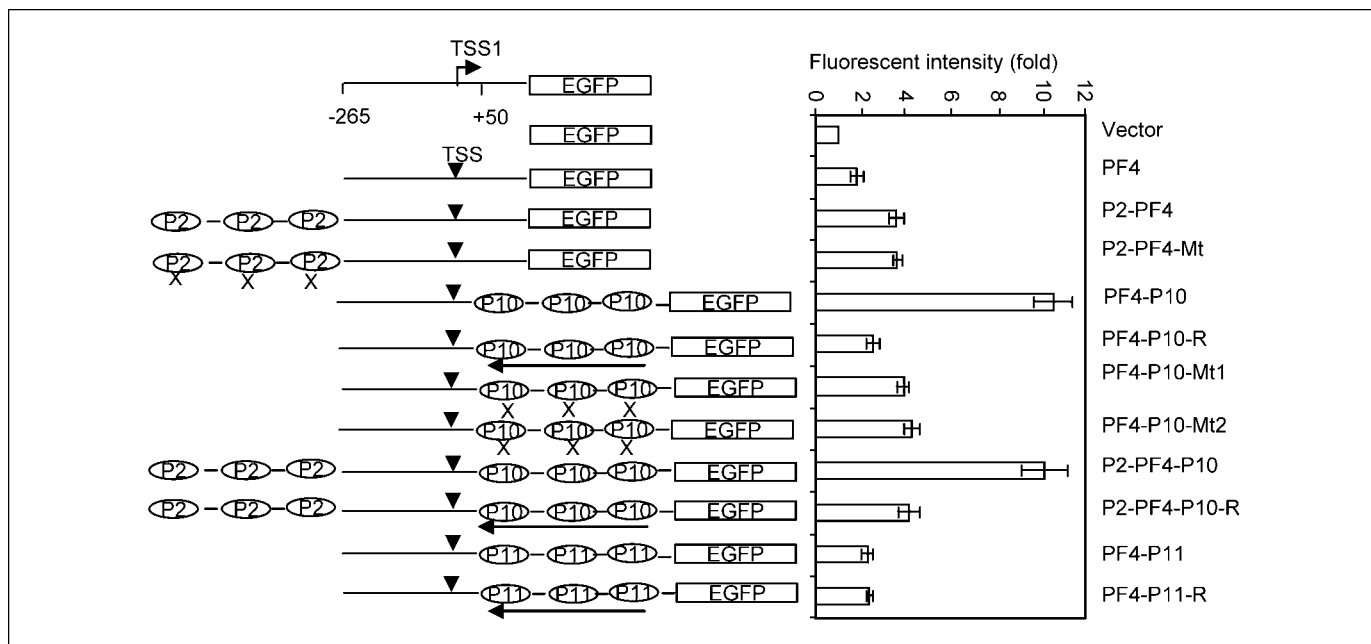


Figure 4. Enhancer activity of the ATF2/cJun binding sites in transcription of *FoxP3*. Quantitative analysis of enhancer activity. *Left*, configurations of the constructs used, including the basal promoter regions used (PF4); *right*, fluorescence intensity as measured by flow cytometry. The promoter activities were normalized by the following formula: (GFP fluorescence sample/GFP fluorescence control)/(renilla luciferase activity sample/renilla luciferase control). The promoter-less GFP construct is used as control. *Columns*, means of triplicates, repeated thrice; *bars*, SD.

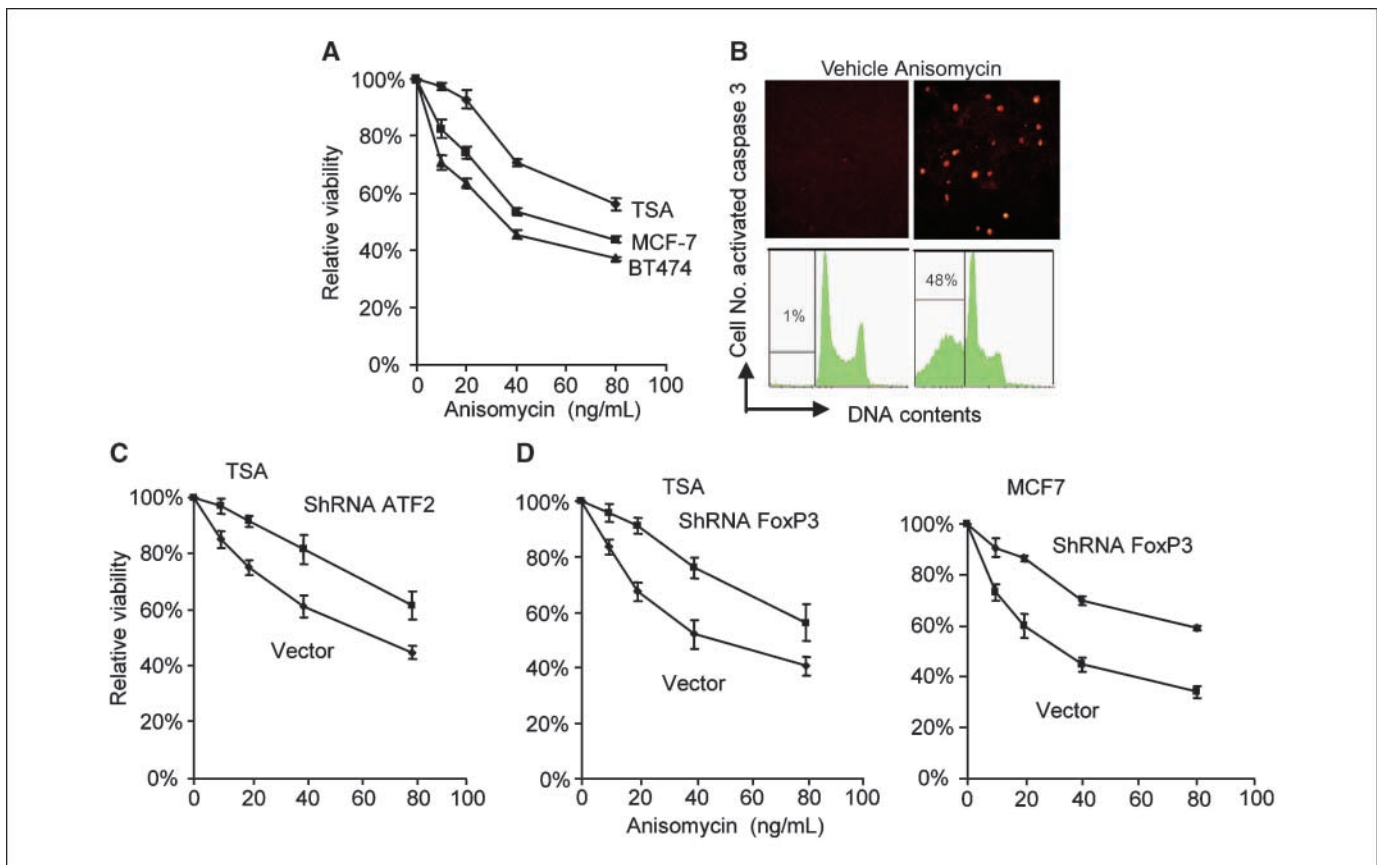


Figure 5. ATF2-FoxP3 pathway induces apoptosis of breast cancer cells. *A*, growth inhibition of mouse and human breast cancer cell lines by anisomycin, as determined by MTT assay. Mouse cell line (10^4 /well; TSA) or human breast cancer cell lines TB474 or MCF7 were cultured in the presence of given concentration of anisomycin for 48 h. The amounts of viable cells were determined by MTT assay, with viability of the untreated cells defined as 100%. Points, means of triplicate samples, repeated thrice; bars, SD. *B*, anisomycin induction of apoptosis in TSA cell line at 24 h after treatment. Top, staining of activated caspase 3; bottom, DNA contents. The % of gated cells was apoptotic based on their sub-2C DNA contents. Data shown have been repeated thrice. *C*, requirements for ATF2 in growth inhibition of TSA by anisomycin. *D*, requirement for FoxP3 in growth inhibition TSA (left) and MCF-7 cells (right) by anisomycin. The indicated cell lines were transduced with lentiviral vector encoding either scrambled shRNA or shRNA specific for ATF2 or FoxP3. The transfected cells were enriched by short-term treatment of blastocidin at a dose of 6.5 μ g/mL and subject to treatment of different doses of anisomycin. The viability was measured by MTT assay. Points, means of triplicates, repeated thrice; bars, SD.

breast cancer in mouse and in woman (7). FOXP3 acts as a transcriptional repressor of oncogenes such as *ErbB2* and *SKP2* (7, 15). Moreover, ectopic expression of FOXP3 cause an apoptosis of breast cancer cells (7). These data showed that the induction of FOXP3 in the tumor cells may prove valuable for the treatment of breast cancer.

Because the one WT allele was not irreversibly inactivated in the overwhelming majority of breast cancer samples analyzed (7), it is theoretically possible to reactivate the expression of *FOXP3* locus for the treatment of breast cancer. The data presented herein showed such reactivation by anisomycin.

We observed that anisomycin, a drug commonly used to activate MAP kinases, rapidly induced FOXP3 expression in multiple breast cancer cell lines tested. Using shRNA specific for *Jnk* and *Atf2*, we showed that the *Jnk* and *Atf2* genes are required for the induction of *FoxP3* expression. Moreover, biochemical analysis allowed us to identify critical *cis*-element involved in the induction of *FoxP3* and that this *cis*-element interacts with c-Jun and ATF2 to cause the activation of the *FoxP3* gene. It is worth considering whether the effect of anisomycin can be related to reactivation of X-inactivated *FoxP3*, given recent reports of chromatin modification-dependence of c-Jun-induced transcriptions (18, 19).

Using mammary epithelial culture isolated from WT and *ATF2*^{-/-} mice, we showed that the targeted mutation of *Atf2* not only reduced the basal levels of *FoxP3* transcripts in the mammary epithelial cells, but also eliminated its induction by anisomycin. Therefore, ATF2 plays an essential role in both constitutive and inducible expression of *FoxP3*. It is of great interest to note that mice heterozygous for *Atf2*-null allele spontaneously developed mammary tumors (10). The similarity in tumor onset suggests that the lack of *FoxP3* expression may be an underlying cause for the spontaneous mammary tumors, although the *Atf2*^{+/-} mice available to us is in 129/SV background, which is not suitable to address this issue.

FOXP3 is expressed in both T cells and epithelial cells (7, 20, 21). Because the majority of the *Atf2*^{-/-} mice die shortly after birth (11), a systemic analysis of the effect on expression of FOXP3 in the T-cell lineage remained to be determined. However, our preliminary analysis suggested that *Atf2* is not essential for FOXP3 expression in the thymocytes (data not shown). Therefore, ATF2 may play different roles in different lineages. Consistent with this notion, both *cis*-element and the *trans*-activating factors identified here differ from what were reported in *FoxP3* induction in T cells (22–25).

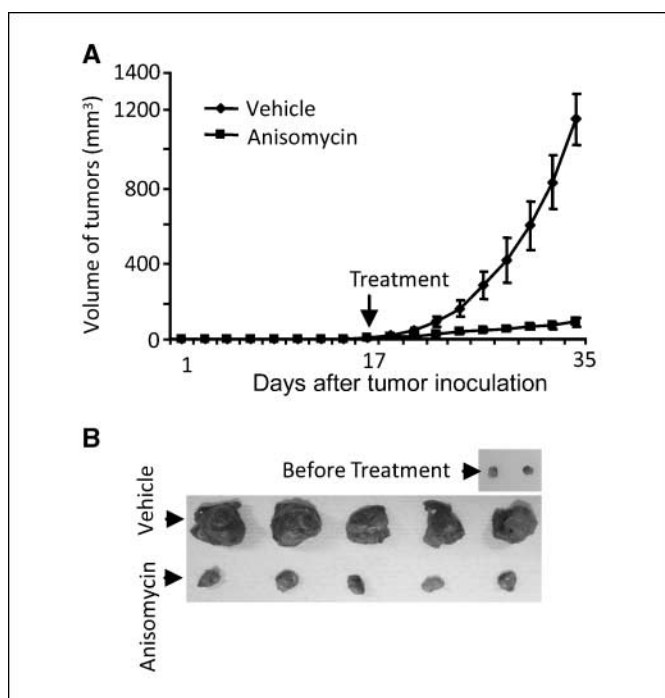


Figure 6. Anisomycin conferred significant therapeutic effect for established mammary tumor in mice. TSA cells (5×10^5) were injected into mammary fat pads of syngeneic BALB/c mice. After 17 d of injection, the mice with palpable tumors were randomly grouped and treated with anisomycin or vehicle control i.p., every 2 d for 8 times, at a dose of 0.5 mg per mouse. The dose used did not give obvious side effects and was $\sim 1/20$ of LD50 in the mice. The tumor diameters were derived from the average of largest diameters in two dimensions. The tumor volumes defined as $0.75\pi r^3$, where r is radius. **A**, the growth kinetics is shown; **B**, photographs of tumors before, and at the end of treatments were shown at the bottom. Similar therapeutic effects have been observed in three independent experiments.

Finally, an important but unresolved issue is how to reactivate tumor suppressor function in the tumor cells. Classic tumor suppressors are inactivated by two irreversible hits (2). Therefore, despite an elegant recent approach (9), restoring the function of classic tumor suppressors remains a major challenge for cancer therapy. On the other hand, recent data from our group and that of another indicated that X-linked tumor suppressor genes are subject to X-inactivation (7, 8). Because X-inactivated genes are not subject to selection during tumor growth and because deletion and mutation found in the majority of the cases are heterozygous (7, 8), it may be possible to reactivate *FOXP3* for the treatment of breast cancer. In this regard, we have shown that anisomycin cause apoptosis in an ATF2- and *FOXP3*-dependent manner. Moreover, the doses used here do not interfere with protein translation and cause no obvious side effect, yet the drug causes dramatic inhibition of growth of established mammary tumors in syngeneic hosts. Although more work is needed to evaluate the potential for anisomycin for breast cancer treatment, our data suggest that one may be able to reactivate X-linked tumor suppressor genes for cancer treatment.

Disclosure of Potential Conflicts of Interest

No potential conflicts of interest were disclosed.

Acknowledgments

Received 3/4/09; revised 4/22/09; accepted 5/6/09; published OnlineFirst 7/7/09.

Grant support: National Cancer Institute, Department of Defense, and American Cancer Society.

The costs of publication of this article were defrayed in part by the payment of page charges. This article must therefore be hereby marked *advertisement* in accordance with 18 U.S.C. Section 1734 solely to indicate this fact.

We thank Lynde Shaw and Todd Brown for assistance.

References

- Hanahan D, Weinberg RA. The hallmarks of cancer. *Cell* 2000;100:57–70.
- Knudson AG, Jr. Mutation and cancer: statistical study of retinoblastoma. *Proc Natl Acad Sci U S A* 1971;68:820–3.
- Fearon ER, Vogelstein B. A genetic model for colorectal tumorigenesis. *Cell* 1990;61:759–67.
- Hollstein M, Sidransky D, Vogelstein B, Harris CC. p53 mutations in human cancers. *Science* 1991;253:49–53.
- Herman JG, Baylin SB. Gene silencing in cancer in association with promoter hypermethylation. *N Engl J Med* 2003;349:2042–54.
- Spatz A, Borg C, Feunteun J. X-chromosome genetics and human cancer. *Nature reviews* 2004;4:617–29.
- Zuo T, Wang L, Morrison C, et al. *FOXP3* is an X-linked breast cancer suppressor gene and an important repressor of *HER-2/ErbB2* oncogene. *Cell* 2007;129:1275–86.
- Rivera MN, Kim WJ, Wells J, et al. An X chromosome gene, *WTX*, is commonly inactivated in Wilms tumor. *Science* 2007;315:642–5.
- Bykov VJ, Issaeva N, Shilov A, et al. Restoration of the tumor suppressor function to mutant p53 by a low-molecular-weight compound. *Nat Med* 2002;8:282–8.
- Maekawa T, Shinagawa T, Sano Y, et al. Reduced levels of ATF-2 predispose mice to mammary tumors. *Mol Cell Biol* 2007;27:1730–44.
- Reimold AM, Grusby MJ, Kosaras B, et al. Chondrodysplasia and neurological abnormalities in ATF-2-deficient mice. *Nature* 1996;379:262–5.
- Wang CY, Cusack JC, Jr., Liu R, Baldwin AS, Jr. Control of inducible chemoresistance: enhanced anti-tumor therapy through increased apoptosis by inhibition of NF- κ B. *Nat Med* 1999;5:412–7.
- Im H, Grass JA, Johnson KD, Boyer ME, Wu J, Bresnick EH. Measurement of protein-DNA interactions *in vivo* by chromatin immunoprecipitation. *Methods Mol Biol* 2004;284:129–46.
- Wang Y, Liu Y, Wu C, McNally B, Liu Y, Zheng P. Laforin confers cancer resistance to energy deprivation-induced apoptosis. *Cancer Res* 2008;68:4039–44.
- Zuo T, Liu R, Zhang H, et al. *FOXP3* is a novel transcription repressor for the breast cancer oncogene *SKP2*. *J Clin Invest* 2007;117:3765–73.
- Su B, Jacinto E, Hibi M, Kallunki T, Karin M, Ben-Neriah Y. JNK is involved in signal integration during costimulation of T lymphocytes. *Cell* 1994;77:727–36.
- Tommasini A, Ferrari S, Moratto D, et al. X-chromosome inactivation analysis in a female carrier of *FOXP3* mutation. *Clin Exp Immunol* 2002;130:127–30.
- Rahman I. Oxidative stress and gene transcription in asthma and chronic obstructive pulmonary disease: antioxidant therapeutic targets. *Curr Drug Targets* 2002;1:291–315.
- Tsai CL, Li HP, Lu YJ, et al. Activation of DNA methyltransferase 1 by EBV LMP1 involves c-Jun NH(2)-terminal kinase signaling. *Cancer Res* 2006;66:11668–76.
- Chen GY, Chen C, Wang L, Chang X, Zheng P, Liu Y. Cutting edge: Broad expression of the *Foxp3* locus in epithelial cells: a caution against early interpretation of fatal inflammatory diseases following *in vivo* depletion of *Foxp3*-expressing cells. *J Immunol* 2008;180:5163–6.
- Fontenot JD, Gavin MA, Rudensky AY. *Foxp3* programs the development and function of CD4+CD25+ regulatory T cells. *Nat Immunol* 2003;4:330–6.
- Floess S, Freyer J, Siewert C, et al. Epigenetic control of the *foxp3* locus in regulatory T cells. *PLoS Biol* 2007;5:e38.
- Kim HP, Leonard WJ. CREB/ATF-dependent T cell receptor-induced *Foxp3* gene expression: a role for DNA methylation. *J Exp Med* 2007;204:1543–51.
- Tone Y, Furuuchi K, Kojima Y, Tykocinski ML, Greene MI, Tone M. Smad3 and NFAT cooperate to induce *Foxp3* expression through its enhancer. *Nat Immunol* 2008;9:194–202.
- Venuprasad K, Huang H, Harada Y, et al. The E3 ubiquitin ligase Itch regulates expression of transcription factor *Foxp3* and airway inflammation by enhancing the function of transcription factor TIEG1. *Nat Immunol* 2008;9:245–53.

FOXP3 Is an X-Linked Breast Cancer Suppressor Gene and an Important Repressor of the *HER-2/ErbB2* Oncogene

Tao Zuo,² Lizhong Wang,¹ Carl Morrison,³ Xing Chang,¹ Huiming Zhang,¹ Weiyan Li,¹ Yan Liu,¹ Yin Wang,¹ Xingluo Liu,³ Michael W.Y. Chan,² Jin-Qing Liu,³ Richard Love,⁴ Chang-gong Liu,² Virginia Godfrey,⁵ Rulong Shen,³ Tim H.-M. Huang,² Tianyu Yang,³ Bae Keun Park,⁶ Cun-Yu Wang,⁶ Pan Zheng,^{1,*} and Yang Liu^{1,*}

¹Division of Immunotherapy, Section of General Surgery, Department of Surgery, Comprehensive Cancer Center, and Program of Molecular Mechanisms of Disease, University of Michigan, Ann Arbor, MI 48109, USA

²Program in Molecular, Cellular, and Developmental Biology and Department of Molecular Virology, Immunology, and Medical Genetics

³Department of Pathology

⁴Department of Internal Medicine

Ohio State University Medical Center and Comprehensive Cancer Center, Columbus, OH 43210, USA

⁵Department of Pathology, University of North Carolina, Chapel Hill, NC 27599, USA

⁶Laboratory of Molecular Signaling and Apoptosis, Department of Biologic and Materials Sciences, School of Dentistry, University of Michigan, Ann Arbor, MI 48109, USA

*Correspondence: yangl@umich.edu (Y.L.), panz@umich.edu (P.Z.)

DOI 10.1016/j.cell.2007.04.034

SUMMARY

The X-linked *Foxp3* is a member of the forkhead/winged helix transcription factor family. Germline mutations cause lethal autoimmune diseases in males. Serendipitously, we observed that female mice heterozygous for the “scurlin” mutation of the *Foxp3* gene (*Foxp3*^{scf/+}) developed cancer at a high rate. The majority of the cancers were mammary carcinomas in which the wild-type *Foxp3* allele was inactivated and *HER-2/ErbB2* was overexpressed. *Foxp3* bound and repressed the *HER-2/ErbB2* promoter. Deletion, functionally significant somatic mutations, and downregulation of the *FOXP3* gene were commonly found in human breast cancer samples and correlated significantly with *HER-2/ErbB2* overexpression, regardless of the status of *HER-2* amplification. Our data demonstrate that *FOXP3* is an X-linked breast cancer suppressor gene and an important regulator of the *HER-2/ErbB2* oncogene.

INTRODUCTION

Identification of *BRCA1* and *BRCA2* marks a key advance in understanding the genetic defects responsible for breast cancer (Miki et al., 1994; Wooster et al., 1995). Several other genes, such as *TP53*, *PIK3CA*, and *PTEN*, have also been implicated in familial and sporadic cancers (Samuels et al., 2004; Wooster and Weber, 2003). How-

ever, the genetic defects for breast cancer have yet to be fully elucidated. There is an important distinction between autosomal and X-linked genes, as many genes in the latter category are subject to X inactivation, making it easier to fulfill Knudson’s two-hit theory (Knudson, 1971). As such, X-linked tumor suppressor genes can potentially be more important, as LOH or mutation of a single allele can in effect functionally silence the gene (Spatz et al., 2004). However, essentially all tumor suppressor genes are autosomal (Spatz et al., 2004), although tantalizing evidence concerning abnormalities in the X chromosome, including LOH, skewed inactivation, and selective loss, has been reported in breast cancer samples (Kristiansen et al., 2005; Piao and Malkhosyan, 2002; Richardson et al., 2006; Roncuzzi et al., 2002).

HER-2/Neu/ErbB2 is one of the first oncogenes to be identified (Schechter et al., 1984) and has been demonstrated to be expressed in a large proportion of cancer cells (Garcia de Palazzo et al., 1993). The level of *HER-2/NEU* is an important prognostic marker (Slamon et al., 1987). Anti-*HER-2/NEU* antibody Herceptin has emerged as an important therapeutic for patients with overexpressed *HER-2/NEU* on cancer tissues (Slamon et al., 2001). Given the clinical and therapeutic significance of *Her-2/Neu/ErbB2* overexpression, it is important to identify the molecular mechanisms responsible for the overexpression. A well-established mechanism responsible for *HER-2* overexpression in human cancer is gene amplification (Slamon et al., 1987). However, it is unclear whether gene amplification alone is sufficient to cause *HER-2* overexpression. Moreover, a significant proportion of human cancers with moderate overexpression of *HER-2* does not show gene amplification (Bofin et al., 2004; Jimenez

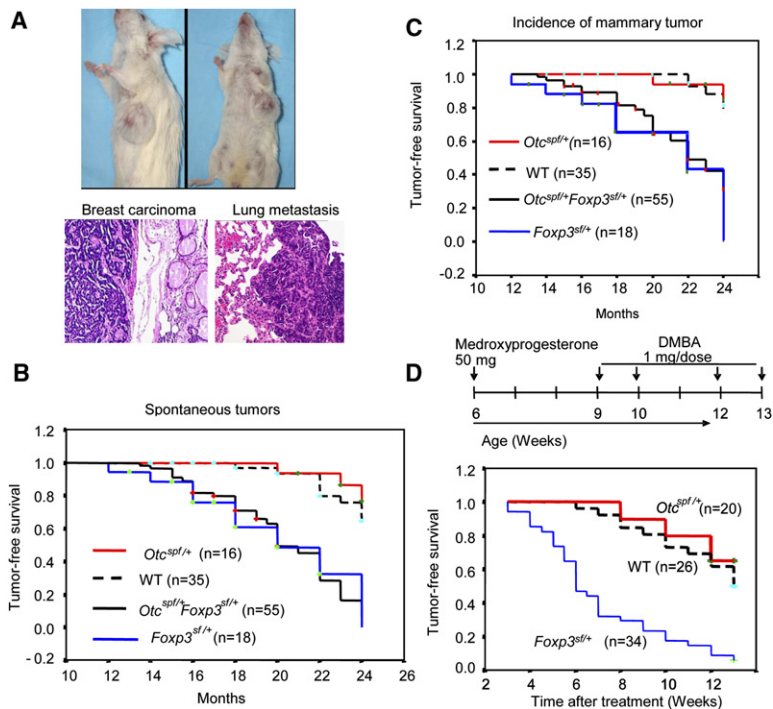


Figure 1. Increased Susceptibility to Breast Cancer in Mice Heterozygous for *Foxp3^{sf}*

(A) Representative breast cancers developed in female *Foxp3^{sf/+}Otc^{spfl/+}* mice. The top panel shows the gross anatomy, while the lower panel shows the histology of local and metastatic lesions of a breast cancer. (B) Cancer-free survival analysis of *Foxp3^{sf/+}*, *Foxp3^{sf/+}Otc^{spfl/+}*, *Otc^{spfl/+}*, and WT littermates. Mice were sacrificed when moribund to identify the tissue origins of cancers. *Foxp3^{sf/+}* versus WT, $p < 0.0001$; *Foxp3^{sf/+}* versus *Otc^{spfl/+}*, $p = 0.0003$; *Foxp3^{sf/+}* versus *Foxp3^{sf/+}Otc^{spfl/+}*, $p = 0.9526$; *Foxp3^{sf/+}Otc^{spfl/+}* versus WT, $p = 0.0001$; *Foxp3^{sf/+}Otc^{spfl/+}* versus *Otc^{spfl/+}*, $p = 0.0001$; *Otc^{spfl/+}* versus WT, $p = 0.4164$.

(C) As in (B), except that only incidences of mammary tumors were included. *Foxp3^{sf/+}* versus WT, $p = 0.00015$; *Foxp3^{sf/+}Otc^{spfl/+}* versus WT, $p = 0.00011$.

(D) Increased susceptibility of *Foxp3^{sf/+}* mice to carcinogen DMBA and progesterone. The diagram on top depicts experimental protocol, while survival analysis is shown in the bottom panel. *Foxp3^{sf/+}* versus WT, $p < 0.0001$; *Foxp3^{sf/+}Otc^{spfl/+}* versus *Otc^{spfl/+}*, $p = 0.0005$; *Otc^{spfl/+}* versus WT, $p = 0.8157$. In (B) and (C), those mice that were observed for only part of the duration were incorporated as censored samples and were marked with a cross in the Kaplan-Meier survival curves. The p values in (B) and (C) were derived from log-rank tests.

et al., 2000; Todorovic-Rakovic et al., 2005). It is therefore of great interest to identify regulators for *HER-2* expression in breast cancer. In this context, Xing et al. (2000) reported that DNA-binding protein PEA3 specifically targets a DNA sequence on the *HER-2/neu* promoter and downregulates the promoter activity. It is less clear, however, whether genetic lesions of PEA3 can cause *HER-2* overexpression.

Foxp3 was identified during position cloning of *Scurfin*, a gene responsible for X-linked autoimmune diseases in mice and humans (immune dysregulation, polyendopathy, enteropathy, X-linked, IPEX) (Bennett et al., 2001; Brun-kow et al., 2001; Chatila et al., 2000; Wildin et al., 2001). Serendipitously, we observed a high rate of spontaneous mammary cancer. Our systemic analyses reported herein demonstrate that the *Foxp3* gene is a mammary tumor suppressor in mice and humans. Moreover, *Foxp3* represses the transcription of the *HER-2/ErbB2* gene via interaction with forkhead DNA-binding motifs in the *ErbB2* promoter.

RESULTS

Spontaneous and Carcinogen-Induced Mammary Cancer in *Foxp3^{sf/+}* Female Mice

The mutant BALB/c mice we used for the initial study carried mutations in two closely linked X chromosome

genes, *Foxp3^{sf}* and *Otc^{spfl}*. During the course of the study, a spontaneous segregation of *Otc^{spfl}* allowed us to obtain a BALB/c *Otc^{spfl/+}* strain. Meanwhile, we obtained an independent line of Scurfy mice that had never been crossed to the *Spf* mutant mice and we backcrossed the *Scurfy* mutant allele (*Foxp3^{sf}*) for more than 12 generations into the BALB/c background (Chang et al., 2005). Female mice with only one copy of the *Foxp3* gene survived to adulthood and appeared normal within the first year of life (Godfrey et al., 1991) with normal T cell function (Fontenot et al., 2003, 2005; Godfrey et al., 1994). Our extended observations of the retired breeders for up to two years revealed that close to 90% of the *Foxp3^{sf/+}Otc^{spfl/+}* and *Foxp3^{sf/+}* mice spontaneously developed malignant tumors. Cancer incidences in the littermate controls and a line of congenic mice with a mutation in *Otc* but not *Foxp3* were comparable with each other (Figures 1A and 1B). About 60% of the tumors were mammary carcinomas (Figures 1A and 1C), although other tumors, such as lymphoma, hepatoma, and sarcoma were observed. Histological analyses revealed lung metastasis (Figure 1A; lower panels, based on expression of ER and/or PR, data not shown) in about 40% of the mice with mammary cancer. More than a third of the tumor-bearing mice had multiple lesions in the mammary glands. Most, although not all, mammary carcinomas expressed the estrogen receptor (ER^+ , 14/18) and progesterone receptor (PR^+ , 12/18).

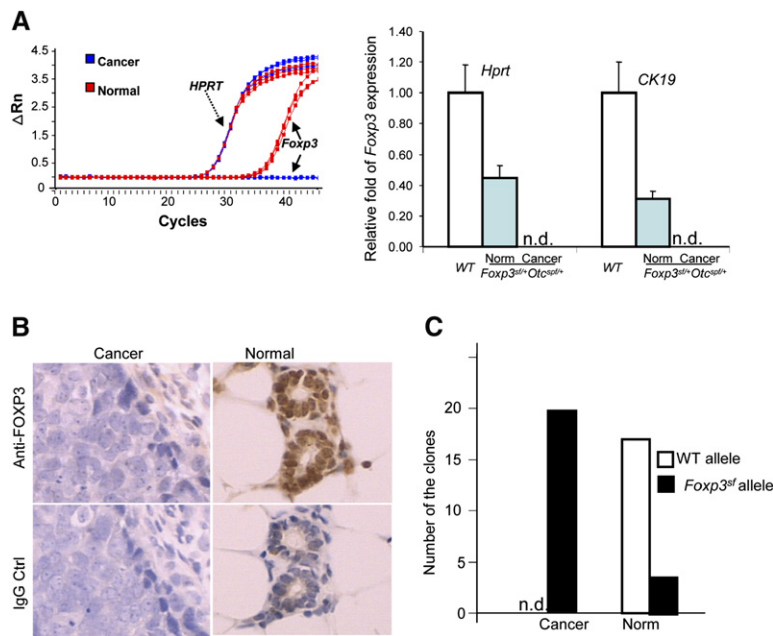


Figure 2. Inactivation of the WT *Foxp3* Allele in Mammary Cancer Cells

(A) Defective *Foxp3* expression in breast cancer. RNA extracted from the cells isolated by laser-capture microdissection was subjected to quantitative real-time RT-PCR using primers specific for *Foxp3*, *Hprt*, and *CK19*. In the left panel, fluorescence intensity (ΔRn) was plotted versus cycle number. Mean and standard deviation (SD) from three individual mice per group are presented in the right panel ($p < 0.0001$, one-way ANOVA test when either internal standard was used).

(B) Immunohistochemical staining of normal mammary glands and adenocarcinomas from a *Foxp3^{sf/+}Otc^{spfl/+}* mouse using rabbit anti-FOXP3 polyclonal antibody and normal rabbit IgG as the control.

(C) Specific silencing of the WT allele in breast cancer cells. *Foxp3* transcripts were amplified from microdissected breast cancers or normal breast epithelium by two rounds of anchored PCR and were cloned into the TOPO vector and sequenced. The number of clones with sequences of WT or mutant alleles in the breast cancer and normal epithelium is presented. A total of 20 clones were sequenced from each group. Data shown are from pooled samples that lack *CD3* transcripts. n.d., not detectable.

In order to focus on mammary cancer, we treated the mice with a carcinogen, 7,12-dimethylbenz [a] anthracene (DMBA), in conjunction with progesterone. Mice heterozygous for *Foxp3^{sf}*, but not those heterozygous for *Otc^{spfl}*, showed substantially increased susceptibility to mammary cancer, as revealed by earlier onset and increased incidence (Figure 1D) and multiplicity (data not shown) of the breast tumors. These data demonstrate that a mutation of *Foxp3*, but not *Otc*, results in a major increase in susceptibility to mammary carcinoma.

***Foxp3* Expression in Normal and Cancerous Mammary Tissues**

Since expression of *Foxp3* has not been reported in mammary tissue, we isolated normal and cancerous cells by laser-capture microdissection (Figure S1A) and compared expression of *Foxp3* and *Otc* by real-time RT-PCR and histochemistry. The complete absence of the *cd3* transcripts (Figure S1B) indicated that the microdissected samples were devoid of T cells, the main cell types known to express *Foxp3* (Fontenot et al., 2005). A representative profile and summarized data of *Foxp3* expression in *Foxp3^{sf/+}Otc^{spfl/+}* mice and age-matched wild-type (WT) control mice are shown in Figure 2A. *Foxp3* mRNA was detected in normal mammary epithelium from both the WT and *Foxp3^{sf/+}Otc^{spfl/+}* mice, but not in mammary cancer cells from the same *Foxp3^{sf/+}Otc^{spfl/+}* mice. Immunohistochemical staining (Figure 2B) confirmed the loss of expression of *Foxp3* in the mammary carcinoma generated from the *Foxp3^{sf/+}Otc^{spfl/+}* mice.

Foxp3 is an X-linked gene that is subject to X-chromosomal inactivation (Fontenot et al., 2005). We carried out

an anchored RT-PCR and cloned the low levels of *Foxp3* mRNA in the breast tissues. We sequenced the cDNA clones from pooled samples after ruling out potential T cell contamination (based on a lack of T cell specific *cd3* transcripts; Figure S1B). As shown in Figure 2C, 100% of the *Foxp3* transcripts in the cancerous tissues were from the mutant alleles, which indicate that the wild-type allele was silenced in the tumor cells. In contrast, the transcripts from the mutant allele constituted 15% of the transcripts in the normal mammary samples from the same mice. Thus, the expression pattern of *Foxp3* fulfills another criterion for a tumor suppressor gene.

***FOXP3* Is a Repressor of *ErbB2* Transcription**

Our characterization of the mammary tumors in the mutant mice revealed widespread upregulation of *ErbB2*, in contrast to those rare tumors from WT mice, as shown in Figure 3A and Table S1. Using real-time RT-PCR, 8- to 12-fold more *ErbB2* mRNA was found in the cancer cells than in normal epithelium (Figure 3A). There was also more *ErbB2* mRNA in the *Foxp3^{sf/+spfl/+}* epithelium than in that of the WT female mice (Figure 3A), which indicates a potential gene dosage effect of *Foxp3* on the regulation of *ErbB2* expression in vivo. Transfection of the TSA cell line with *Foxp3* cDNA repressed *ErbB2* levels on the TSA cell line (Figure 3B).

Analysis of the 5' sequence of the *ErbB2* gene revealed multiple binding motifs for the forkhead domain (Figure 3C). To test whether *Foxp3* interacts with the *ErbB2* promoter, we used anti-V5 antibody to precipitate sonicated chromatin from the TSA cells transfected with the *Foxp3*-V5 cDNA and used real-time PCR to quantitate

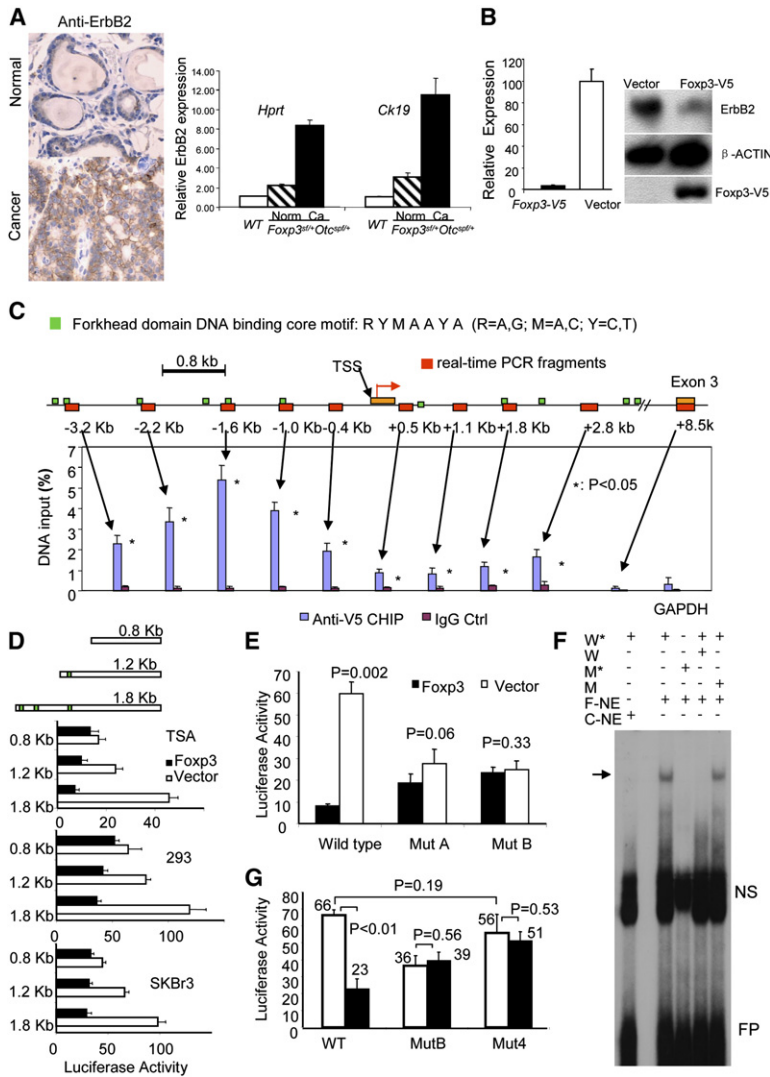


Figure 3. *Foxp3* Represses the Expression of *ErbB2*

(A) Overexpression of *ErbB2* in mouse mammary cancers. The left panels show immunohistochemical staining of a noncancerous mammary gland and an adjacent adenocarcinoma from a *Foxp3^{stfl/+}Otc^{stfl/+}* mouse using anti-ErbB2 antibody. The right panel shows relative expression levels of *ErbB2* in normal mammary epithelium of WT and *Foxp3^{stfl/+}Otc^{stfl/+}* mice and of cancer tissues from *Foxp3^{stfl/+}Otc^{stfl/+}* mice as revealed by real-time RT-PCR of LCM samples. Data shown are means and SD. The expression of *ErbB2* was normalized against either *Hprt* or *CK19*. Highly significant differences were observed between cancerous and normal tissue ($p < 0.001$, ANOVA test when either internal standards were used).

(B) Transfection of *Foxp3-V5* into TSA cells repressed expression of the *ErbB2* locus. The left panel shows mRNA levels as measured by real-time PCR. Data shown are means and SD of triplicates. The right panel shows the protein levels by western blot of the cell lysates using anti-ErbB2 antibody. The amount of actin- β was used as loading control, while the amount of transfected *Foxp3-V5* was measured by western blot using anti-V5 antibodies.

(C) Binding of the *Foxp3-V5* fusion protein to the promoter region of the *ErbB2* gene. Top panel is a diagram of the 5' region of the *ErbB2* gene, including the promoter, exon 1, intron 1, and exon 3. The forkhead-binding motifs are illustrated with small green bars, while the regions surveyed by real-time PCR are marked in red bars. The lower panel shows the amount of DNA precipitated by either control IgG or anti-V5 mAb expressed as percentage of the total input genomic DNA. Data shown are means and standard deviation (SD) of triplicates. This experiment has been repeated twice with similar results.

(D) *Foxp3*-mediated repression of the *ErbB2* promoter requires forkhead-binding motifs as evaluated by dual-luciferase reporter assay.

The promoter regions differed in the number of forkhead-binding motifs, as illustrated in the diagram on the left. Three different cell lines were transfected with either vector control or *Foxp3* (1 μ g/well) in conjunction with the luciferase reporter driven by different 5' promoter regions of the *ErbB2* gene (0.6 μ g/well). pRL-TK was used as internal control. The luciferase activity from the cells transfected with the pGL2-basic vector was arbitrarily defined as 1.0. Data shown are means and SD of triplicates and have been repeated at least three times.

(E) Site-directed mutagenesis of one of two conserved regions with multiple forkhead-binding motifs in the *ErbB2/HER-2* promoter prevented repression of the *ErbB2* promoter by *Foxp3*. The two binding sites, as illustrated in Figure S2, were deleted individually (deleted DNA sequence, Mut A: AAATCTGGGATCATTTA; Mut B: TTGGAATTTAGATAAA). Mutations of either site prevented *FOXP3*-mediated suppression. The promoter activity was measured and normalized as detailed in (D), except that the amount of promoter DNA was 0.4 μ g/sample. The promoter activities of the vector groups were artificially defined as 1.0. Data shown are means and SD of triplicates. This experiment has been repeated twice with similar results.

(F) *Foxp3*-mediated binding to specific *cis* elements in the *ErbB2* promoter. Nuclear extracts from the *Foxp3-V5*- (F-NE) or vector-transfected control (C-NE) TSA cells were preincubated with ³²P-labeled WT (*W) or mutant probes (*M) in the presence of an unlabeled WT (W) or mutant probe (M). The mixtures were analyzed by PAGE. NS, nonspecific; FP, free probe. The specific *Foxp3*-shifted band is marked by an arrow. Data shown have been repeated three times.

(G) Mutation of forkhead binding motifs (Mut 4) abrogated *FOXP3*-mediated repression, but not basal promoter activity. This is as in (E), except that WT, Mut B, and Mut 4 (mutations that inactivate the *Foxp3* binding as detailed in (F)) of the *ErbB2* promoters were used. This experiment has been repeated twice with similar results. The differences were compared by student t tests with p value provided. Data shown are means and SD of triplicates.

the amounts of the specific *ErbB2* promoter region precipitated by the anti-V5 antibodies in comparison to those that bound to mouse IgG control. As shown in Figure 3C, the anti-V5 antibodies pulled down significantly higher amounts of *ErbB2* promoter DNA than the IgG

control, with the highest signal around 1.6 kb 5' of the transcription starting site.

To test whether the binding correlated with the suppression by *Foxp3*, we produced luciferase reporter using the 1.8, 1.2, and 0.8 Kb upstream of the *ErbB2* TSS and tested

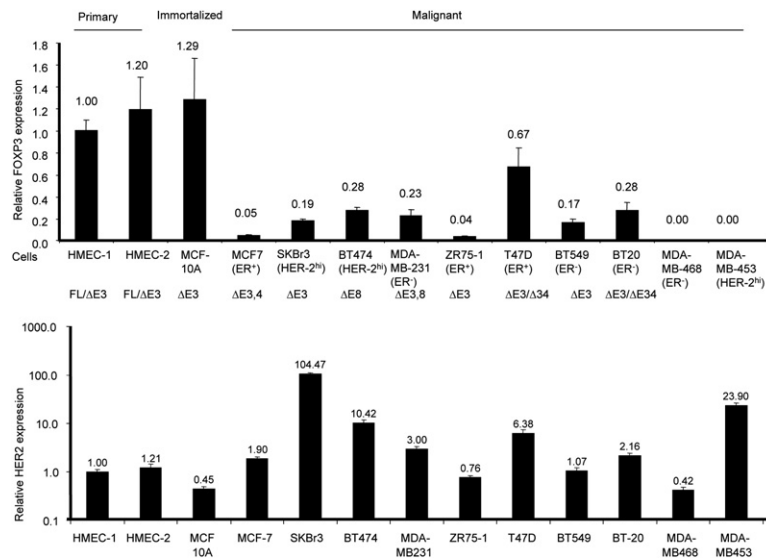


Figure 4. Characterization of *FOXP3* Transcripts in Primary, Immortalized, and Malignant Mammary Epithelial Cells

Relative levels and isoforms of *FOXP3* (the upper panel) and *HER-2* (the lower panel) mRNA. After normalizing against endogenous *GAPDH*, the amounts of transcripts were compared to those found in HMEC-1, which was arbitrarily defined as 1.0. Data shown are means and SD of triplicates. This experiment has been repeated twice with similar results. The reported ER status and the isoforms of the *FOXP3* transcripts detected are indicated. To characterize the isoforms, *FOXP3* mRNA was amplified by two rounds of anchored PCR using primers annealing to exons 1 and 12. The bulk PCR products were sequenced only if one species was found in agarose electrophoresis. When more than one species was observed, the PCR products were cloned and multiple clones were sequenced until all of the species observed in the agarose gel were identified.

the ability of Foxp3 to repress *ErbB2* promoter activity. In three separate cell lines, we observed that the region with the strongest ChIP signal was required for optimal repression by Foxp3 (Figure 3D). Furthermore, we deleted two potential Foxp3 binding sites based on intensity of ChIP signal, abundance of consensus binding sites, and conservation between mouse and human (Figure S2) by site-directed mutagenesis and measured the effect on Foxp3-mediated repression. As shown in Figure 3E, deletion of either binding site substantially increased the *ErbB2* promoter activity in the presence of Foxp3 and thus alleviated Foxp3-mediated repression.

Since the region deleted in Mut B is 100% conserved between mouse and man and since this deletion completely wiped out repression, we used an electrophoretic mobility shift assay (EMSA) to determine whether the forkhead DNA-binding motifs in region B bound to Foxp3. As shown in Figure 3F, the nuclear extracts from the Foxp3-expressing cells specifically retarded migration of the WT but not mutant ³²P-labeled probes compared with control cells. While mutant cold probes did not affect Foxp3-binding activities, WT cold probes significantly diminished them, establishing that the binding of these complexes is specific to forkhead DNA-binding motifs. We therefore carried out site-directed mutagenesis to replace the 12 nucleotides (Mut C) within the *ErbB2* promoter and compared the promoter activity and Foxp3-repression by luciferase assays. While the wild-type promoter was repressed by Foxp3, no repression by Foxp3 was observed when the mutant promoter was used. Moreover, in contrast to the deletional Mut B, the mutations had no impact on the basal activity of the *ErbB2* promoter (Figure 3G). Taken together, our new data make a compelling case that Foxp3 represses the *ErbB2* promoter via specific forkhead-binding motifs.

***FOXP3* Defects in Human Breast Cancer**

We analyzed the levels and isoforms of the *FOXP3* transcripts in a panel of normal human mammary epithelial cells (HMEC), an immortalized but nonmalignant cell line (MCF-10A), and ten malignant breast cancer cell lines differing in ER/PR and HER-2 status. Early passage of HMEC with no methylation in the CpG island of the *P16* promoter (Figure S3) was used to avoid effects associated with *P16* inactivation in postsenescence HMEC cultures (Romanov et al., 2001). As shown in Figure 4A, similar levels of *FOXP3* transcripts were observed in two independent isolates of HMEC and in the immortalized cell line MCF-10A. Each of the ten tumor cell lines had a different degree of reduction in *FOXP3* mRNA levels in comparison to HMEC and MCF-10A. Among them, two were completely devoid of *FOXP3* mRNA, while the others had a 1.5- to 20-fold reduction. We then used anchored primers spanning exons 1–12 to amplify the *FOXP3* transcripts, and then we sequenced the PCR products. As shown in Figure 4, none of the tumor cell lines expressed full-length *FOXP3* transcripts. The HMEC expressed the same two isoforms as observed in the T cells, while MCF-10A expressed the exon 3-lacking isoforms. The same isoform was also found in four tumor cell lines at much lower levels. In addition, three tumor cell lines expressed an isoform lacking both exons 3 and 4. The alternative splicing resulted in a frameshift beginning at codon 70 and an early termination at codon 172. Furthermore, two tumor cell lines expressed a *FOXP3* isoform lacking exons 3 and/or 8. Exon 8 encodes the leucine-zipper domain that is frequently mutated in IPEX patients (Ziegler, 2006). Thus, *FOXP3* is abnormal in breast cancer cell lines. Consistent with a role for *FOXP3* in repressing *HER-2* expression, the majority of the breast cancer cell lines had higher levels of *HER-2* in comparison to normal HMEC (Figure 4, lower panel). However, additional changes are also likely

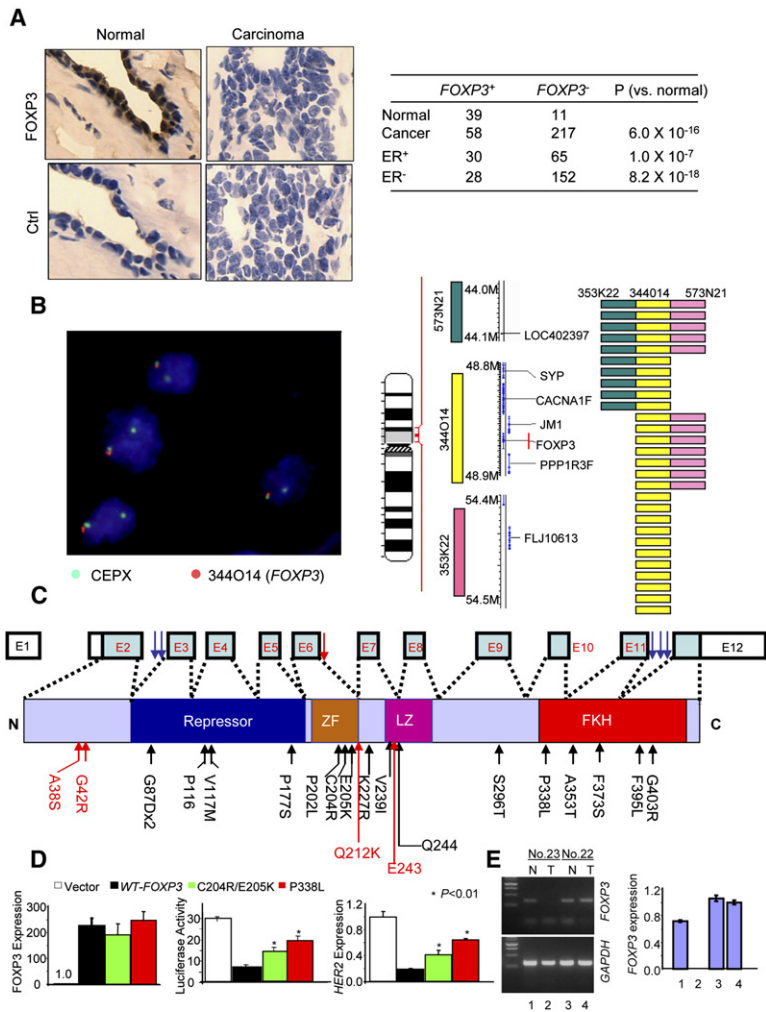


Figure 5. FOXP3 Defects in Human Breast Cancer

(A) Downregulation of the FOXP3 protein among human breast cancer cells. Photographs in the top panels show anti-FOXP3 staining of normal and carcinoma tissues from the same patient, with specificity control shown at the bottom. The number and percentage of FOXP3 positive tissues are shown in the right panel. Samples with nuclear staining by the anti-Foxp3 antibody were scored as positive.

(B) Deletion of the FOXP3 locus in breast cancer cells. Breast cancer tissue microarray samples were analyzed by FISH using three BAC clone probes surrounding a 10 MB region in Xp11.2. A typical FISH for the CEPX (green) and FOXP3 (orange) probes is shown on the left, while the genomic structure of the X chromosome and probe positions are illustrated in the middle panel. A total of 238 samples were analyzed for all probes, with 223 samples providing definitive FISH data. Twenty-eight of the two hundred and twenty-three samples showed deletions as detected by at least one of the three probes. The positions of the deletions in the 28 samples are summarized in the right panel.

(C) Somatic mutation of the FOXP3 gene in breast cancer samples: summary of sequencing data from 65 cases, including 50 formalin-fixed samples and 15 frozen samples. Genomic DNA was isolated from matched normal and cancerous tissues from the same patients and amplified with primers for individual exons and intron-exon boundary regions. Somatic mutations were identified by comparing sequences from normal and cancerous samples from the same patients. The data are from either bulk sequencing of PCR products or from the sequencing of 5–10 clones from PCR products. Only those mutations that

were observed in multiple clones were scored. Mutations identified from 50 cases of formalin-fixed samples are marked in black, while those identified from 15 cases of frozen tissue samples are marked in red.

(D) FOXP3 mutations reduced its repressor activity for the HER-2 promoter in the SKBr-3 cell line. The left panel shows expression of mutant cDNA. The middle panel shows luciferase activity, while the right panel shows the levels of HER-2 transcripts. The difference between WT and 318 P > L and that between WT and 204C > R205E > K are highly significant (p < 0.01). Data shown are means and SD of triplicates and representative of at least two to three independent experiments.

(E) A breast cancer sample with a somatic mutation in intron 6 (case 23) had an inactivated FOXP3 locus. Normal mammary epithelial (N) and tumor (T) cells were isolated by LCM. The FOXP3 transcripts were determined either by PCR using primers spanning exons 5–8 to detect alternatively spliced products or by real-time PCR using primers spanning exons 10–12. The upper and middle panels show photographs of PCR products of FOXP3 or GAPDH loci, while the right panel shows the relative level of FOXP3 transcripts as determined by real-time PCR. Neither assay detected any FOXP3 transcripts in the tumor of case no. 23. Substantial amounts of FOXP3 transcripts were detected in normal samples and tumors in case no. 22 (with a synonymous mutation in exon 7), which was artificially defined as 1.0. Data shown are means and SD of triplicates. This experiment has been repeated twice with similar results.

required for HER-2 overexpression, as three cell lines did not overexpress HER-2 even though the FOXP3 transcripts were greatly reduced.

We took three approaches to determine whether the findings in the mutant mice and human breast cancer cell lines are relevant to the pathogenesis of human breast cancer. First, we used immunohistochemistry to determine expression of FOXP3 in normal versus cancerous tissue. As shown in Figure 5A, while about 80% of the normal breast samples expressed FOXP3 in the nuclei of

the epithelial cells, only about 20% of the cancerous tissue showed nuclear staining. Second, we used fluorescence in situ hybridization (FISH) to determine whether the FOXP3 gene was deleted in the breast cancer samples. The minimal common region of deletion was identified using flanking p-telomeric and centromeric clones. Out of 223 informative samples, we observed 28 cases (12.6%) with deletions in any of the three loci. Interestingly, deletion of the FOXP3 locus was found in all of the 28 cases (Figure 5B and Table S2). These data suggest

that *FOXP3* is likely within the minimal region of deletion in the Xp11 region studied. Although all deletions were heterozygous, the *FOXP3* protein was undetectable in 26 out of 28 cases. Thus, it appears that for the majority of the breast cancer samples, LOH alone was sufficient to inactivate the locus, perhaps due to X-chromosomal inactivation. The two cases with both deletion and *FOXP3* expression had X polysomy with three and four X chromosomes, respectively (Table S2). Thirdly, we isolated DNA from matched normal and cancerous tissues (50 cases with formalin-fixed samples and 15 cases of frozen samples) from patients with invasive ductal carcinoma and amplified all 11 coding exons and intron-exon boundary regions by PCR. Two independent PCR products were sequenced in order to confirm the mutations. Unless the bulk sequencing data were unambiguous (Figures S4A and S4C), the PCR products were cloned, and five to ten independent clones from each reaction were sequenced (Figure S4B). Among the formalin fixed samples, we only used the cases in which the normal tissue samples gave unambiguous sequencing data that matched the wild-type *FOXP3* sequence. When the cancerous tissues were compared with normal tissues from the same patient, 36% (18 out of 50 formalin-fixed samples and 5 out of 15 frozen samples) showed somatic mutations (Table S3). Loss of the wild-type allele was found in 6 out of 23 cases (38%) of cancer samples with somatic *FOXP3* mutations (see Figure S4C for an example). The other cases had heterozygous mutations (Figure S4A). Eighteen mutations resulted in the replacement of amino acids. Most are likely to be critical for *FOXP3* function, as judged from the pattern of mutation in IPEX patients (Ziegler, 2006) or in the conserved zinc finger domain that has so far not been implicated (Figure 5C).

Although most samples had a single mutation of the *FOXP3* gene, we did observe two cases with multiple mutations. In the first sample (Figure S4B; case 3 in Table S3), the two mutations occurred in consecutive codons, resulting in two nonconservative replacements of amino acid residues. Clonal analysis revealed that both mutations occurred in the same clone (Figure S4B). In the second sample (Table S3; case 16), three mutations occurred in intron 11. Since this case lacked a WT allele (Figure S4D), it is likely that all of the mutations occurred in the same allele. The possibility of a mismatch in the cancer and normal samples was ruled out by comparing the normal and cancer samples for polymorphism of two unrelated genes (data not shown).

To directly test whether *FOXP3* mutations affect the repressor activity for the *HER-2* gene, we chose two representative somatic *FOXP3* mutants isolated in the cancer cells and tested their repressor activity for the *HER-2* promoter. One mutation (338P > L) resided in the signature forkhead domain, which is often mutated in the IPEX patient, while the other double mutation (204C > R205E > K) was from the zinc finger domain that has not been implicated in IPEX patients. As shown in Figure 5E, both mutations significantly reduced the repressor activity of

FOXP3. The reduced repression of the *HER-2* promoter correlates with a significantly reduced inhibition of *HER-2* mRNA (Figure 5D).

Four cases had mutations in introns that may potentially affect RNA splicing. We used laser-guided microdissection to isolate normal and cancerous epithelial cells from one case with a mutation in intron 6 (case 23; Table S3). RNA was isolated and tested for the potential effects of the mutation on RNA splicing (using primers on exons 5 and 8) and total *FOXP3* transcript, as quantitated by real-time PCR using primers spanning exons 10–12. Tissues from another patient with a mutation in exon 7 were used as control. As shown in Figure 5E's left panel, primers spanning exons 5 and 8 failed to detect *FOXP3* mRNA from the cancerous tissue of case no. 23. Furthermore, primers spanning exons 10–12 also failed to detect any *FOXP3* transcripts. Substantial levels were detected in the normal epithelial cells of the same patients as well as in normal and cancerous tissues from case no. 22. Since the wild-type allele had been lost in the cancer cells of case no. 23, it is likely that the mutation in intron 6 inactivated *FOXP3*. With an intron of 944 nucleotides, a mutation that prevented splicing of intron 6 would cause premature-termination codon-mediated RNA decay, which is operative in the *FOXP3* gene (Chatila et al., 2000).

FOXP3 Defects and HER-2 Overexpression

To demonstrate a role for *FOXP3* defect in *HER-2* overexpression, we first silenced the *FOXP3* gene in early passage of primary HMEC (Supplemental Fig. S3) using a lentiviral vector expressing *FOXP3* siRNA. As shown in Figure 6A, the *FOXP3* siRNA reduced *FOXP3* expression by more than 100-fold while increasing *HER-2* mRNA by 7-fold. A corresponding increase in cell surface *HER-2* was also observed (Figure 6B). These results implicate *FOXP3* as a repressor of *HER-2* in human breast epithelial cells.

Second, since a major mechanism for *HER-2* upregulation in breast cancer is gene amplification (Kallioniemi et al., 1992), an intriguing issue is whether *FOXP3* is capable of repressing *HER-2* in cancer cells with an amplified *HER-2* gene. We produced a Tet-off line of BT474, a breast cancer cell line known to have *HER-2* gene amplification (Kallioniemi et al., 1992), and transiently transfected it with a *pBI-EGFP-FOXP3*- vector. After drug selection, the cells were cultured either in the presence or absence of doxycycline. While the cells cultured with doxycycline did not express *FOXP3* (data not shown), removal of doxycycline resulted in induction of *FOXP3* in a significant fraction of the cancer cells, which allowed us to compare *HER-2* levels in the *FOXP3*⁺ and *FOXP3*⁻ cells in the same culture by flow cytometry. As shown in Figure 6C, *FOXP3*⁻ cells had about a 5- to 10-fold higher level of the *HER-2* protein on the cell surface in comparison to the *FOXP3*⁺ cells.

Thirdly, we compared the expression of *FOXP3* with *HER-2* expression in breast cancer tissues. As shown in

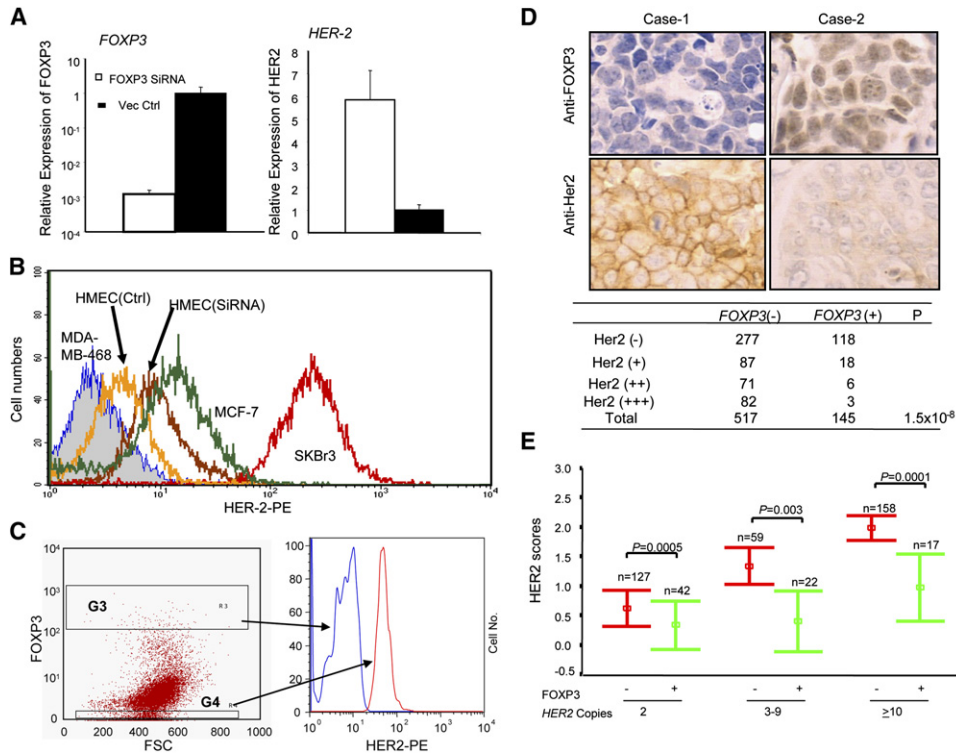


Figure 6. FOXP3 Is an Important HER-2 Repressor

(A) Silencing of FOXP3 resulted in the upregulation of HER-2 in primary human mammary epithelial cells (HMEC). Early passage of HMEC were transduced with lentiviral vector for either control sequence or FOXP3 siRNA. The untransfected cells were removed by selection with blasticidin. At 1 week after transduction, the levels of the FOXP3 and HER-2 transcripts were quantitated by real-time PCR. Data shown are mean and standard error of the mean of relative levels of transcripts (with that in the vector-transduced cells defined as 1.0) and represent those of three independent experiments.

(B) Flow cytometry data showing the effect of FOXP3 silencing on HMEC surface HER-2 levels. HER-2-negative MDA-MB468, HER-2^{lo} MCF-7 and HER-2^{hi} SKBr3 cell lines were included for comparison.

(C) In the Tet-off inducible FOXP3-expressing BT474, FOXP3 repressed HER-2. BT474 cells were first transfected with pTet-Off vector. The transfectants were selected by both blasticidin and G418 in doxycycline-containing medium. The drug-resistant cells were cultured in the absence of doxycycline for 5 days to induce FOXP3. The cells were stained for FOXP3 and HER-2 proteins by flow cytometry. Data shown are histograms depicting HER-2 levels among the gated FOXP3^{hi} and FOXP3⁻ cells based on reactivity to the anti-Foxp3 antibody and are representative of those from two independent experiments.

(D) Inverse correlation between FOXP3 expression (the top panel) and that of the HER-2 (middle panel) among the human breast cancer samples. Tissue microassay samples were stained with either anti-FOXP3 antibodies or anti-HER-2 antibodies and were scored by two different pathologists in a double-blind fashion. FOXP3 staining was scored by nuclear staining with affinity-purified anti-FOXP3 antibodies. A summary of 517 FOXP3⁺ and 145 FOXP3⁻ samples is shown in the bottom panel.

(E) Inverse correlations between FOXP3 expression and HER-2 scores in cells with or without HER-2 amplification. The HER-2 gene-copy number was determined by FISH, while nuclear expression of FOXP3 was determined by immunohistochemistry. Data shown are mean and SD of HER-2 scores of 425 cases of breast cancers grouped by HER-2 copy number. P values were generated by the Mann-Whitney test.

Figure 6D, downregulation of FOXP3 was strongly associated with the overexpression of HER-2, which supports a role for FOXP3 inactivation in HER-2 overexpression in breast cancer. Nevertheless, since many of the FOXP3⁻ cells remained HER-2⁻, it is likely that dysregulation of FOXP3 is insufficient for HER-2 upregulation. On the other hand, since only 3 of 82 FOXP3⁺ cancer cells expressed high levels of HER-2, FOXP3 inactivation is likely important for HER-2 upregulation under most circumstances.

Fourth, we divided breast cancer samples based on their HER-2 gene copy numbers and compared the FOXP3⁺ and FOXP3⁻ cancer samples for the relative

amounts of cell surface HER-2 expression. As shown in Figure 6E, in each of the gene-dose categories, FOXP3⁺ samples had reduced HER-2 scores in comparison to the FOXP3⁻ samples. These results strongly suggest a critical role for FOXP3 in repressing HER-2 expression even in the cases of HER-2 gene amplification.

Fifth, of the 223 informative samples among the 238 that we screened for Xp11.2 deletions, those with deletions encompassing the FOXP3 locus had significantly higher HER-2 scores compared to those without deletions (p = 0.03) (Table S4). Likewise, we compared the relative HER-2 scores among the 50 samples in which we had sequenced all FOXP3 exons. As shown in Table S5, the

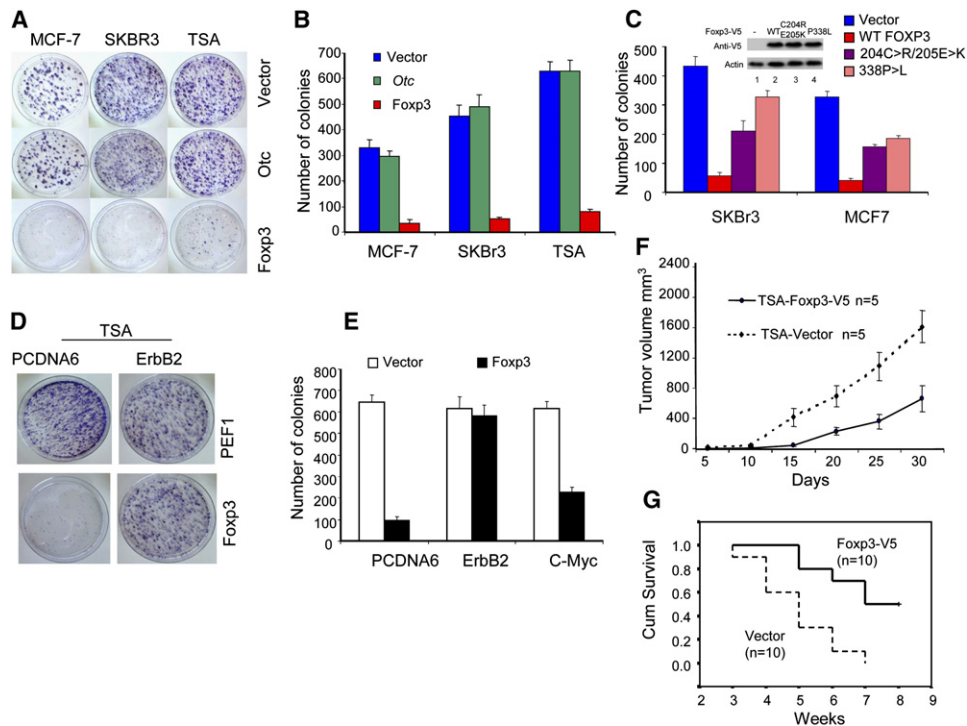


Figure 7. Foxp3 Inhibits the Growth and Tumorigenicity of Multiple Breast Cancer Cell Lines

(A) Breast cancer cell lines MCF-7, SKBr3, and TSA were transfected with equal concentrations of vector alone (Vector), *Foxp3*, or *Otc* cDNA. After 3 weeks of G-418 selection, the drug-resistant clones were visualized by crystal violet dye.

(B) Summary of the colony numbers in three independent experiments as described in (A). Data shown are means and SD.

(C) Somatic mutations identified from breast cancer samples attenuated the growth suppression of the FOXP3. This is as in (A) and (B), except that two somatic mutants were compared with WT FOXP3 cDNA using the two human breast cancer cell lines. Data shown are means and SD of triplicates and are representative of two independent experiments. Expression of WT and mutant proteins at 1 week after transfection is presented in the insert.

(D and E) Ectopic expression of the *ErbB2* but not the *c-Myc* cDNA abrogated *Foxp3*-mediated repression. TSA cells were transfected with either pcDNA6-blasticidin vector or *ErbB2* cDNA and selected with blasticidin for 2 weeks. Pools of blasticidin-resistant cells were supertransfected with the pEF1-G418 vector or *Foxp3* cDNA. The cells were then plated and selected with blasticidin and G418 for 3 weeks. The viable colonies were visualized after staining with the crystal violet dye. Shown in (D) are photographs of a representative plate showing abrogation of *Foxp3*-mediated suppression by *ErbB2*. Shown in (E) are the mean and SD of the colony numbers. This experiment has been repeated twice with essentially identical results.

(F) Expression of *Foxp3* reduced growth rate of tumors. Syngeneic BALB/c mice were injected with 5×10^5 /mouse *Foxp3* or vector-transfected TSA cells in the flank, and the sizes of the local tumor mass were measured using a caliper. Data shown are means and SD and have been repeated once. (G) The survival of tumor-bearing mice was monitored over a 7-week period ($p = 0.0015$, log-rank test). As in (F), except that 10^6 tumor cells/mouse were injected, and the mice were euthanized when they became moribund.

mutations in the FOXP3 gene correlated with higher levels of HER-2 ($p = 0.0083$).

Foxp3/FOXP3 Inhibits Tumorigenicity of Breast Cancer Cells

To test whether the *Foxp3* gene can suppress the growth of breast cancer cells, we transfected the empty vector or the vectors carrying either *Foxp3* (mouse or human origin) or *Otc* cDNA into three breast cancer cell lines, including mouse mammary tumor cell line TSA or human breast cancer cell lines MCF7 (ER⁺HER-2^{low}, no HER-2 amplification) and SKBr3 (ER⁻HER-2^{high} with HER-2 amplification). The untransfected cells were removed by a selection with G418. While the vector-transfected cells grew rapidly, the *Foxp3*-transfected cell lines seldom grew into large colonies. The *Foxp3*-transfected culture had

a drastic reduction in both the size and the number of the drug-resistant colonies. No effect was observed when the *Otc* cDNA was used (Figures 7A and 7B).

To test whether the somatic mutations uncovered from cancerous tissues ablated their growth inhibition, we transfected WT and two mutant *Foxp3* cDNA into SKBr3 and MCF7 cell lines. As shown in Figure 7C, in both cell lines, the mutants had a greatly reduced ability to suppress tumor growth.

To test whether repression of *ErbB2* explains the tumor suppressor activity of the *Foxp3* gene in the ErbB2⁺ cancer cell line, we transfected TSA cells with mouse CMV promoter-driven *ErbB2* cDNA cloned into the pcDNA6 vector and evaluated their susceptibility to *Foxp3*-mediated growth suppression. In this setting, the expression of *ErbB2* was resistant to *Foxp3*-mediated repression

(data not shown). If repression of endogenous *ErbB2* is critical for *Foxp3*-mediated tumor suppression, ectopic expression of *ErbB2* should alleviate the growth inhibition by *Foxp3*. As shown in Figures 7D and 7E, while the pcDNA6-vector-transfected TSA cells remained susceptible to *Foxp3*-mediated repression, the *ErbB2*-transfected TSA cells were completely resistant. In contrast, transfection of *c-Myc* barely alleviated the growth inhibition by *FOXP3* (Figure 7E). These results suggest that *Foxp3* suppresses TSA growth by repressing transcription of *ErbB2*.

We transfected TSA cells with either empty vector or V5-tagged *Foxp3* cDNA. The stable transfectant cell lines were selected by G-418. The vector and *Foxp3*-V5-transfected cell lines were injected into syngeneic BALB/c mice, which were then observed for tumor growth and mouse survival. As shown in Figure 7F, *Foxp3*-transfectants showed reduced growth *in vivo*. The mice that received TSA-vector cells became moribund earlier with higher incidence, while about 50% of the mice that received the *Foxp3*-V5-transfected cells survived more than 7 weeks (Figure 7G). Similarly, *Foxp3*-transfected 4T1, a mouse mammary cancer cell line with *ErbB2* overexpression, also showed reduced tumorigenicity *in vivo* (data not shown).

DISCUSSION

Foxp3 Is an X-Linked Mammary Tumor Suppressor Gene

Serendipitously, we observed that mice heterozygous for the *Foxp3* mutation spontaneously developed mammary cancer at a high rate. Since two independently maintained lines sharing the *Foxp3* mutation have a comparably higher incidence of mammary cancer, the *Foxp3* mutation is likely responsible for the increased rate of breast cancer. Unlike essentially all cancer suppressor genes identified to date, *Foxp3* is X-linked and inactive in cells in which the WT allele was silenced by X inactivation. This is indeed the case, as the low levels of *Foxp3* transcripts in the cancer cells were derived exclusively from the mutant alleles.

Our analysis of human breast cancer samples provides strong support for an important role for the *FOXP3* gene in the development of breast cancer. First, we searched X-chromosomal deletion using three markers encompassing more than 10 MB of Xp11 and found that *FOXP3* is likely the minimal region of deletion. Second, we revealed a high proportion of somatic mutations in the *FOXP3* gene (23 of 65 cases over about 2000 bp exon and intron sequence scanned). The significance of our finding can be discerned indirectly based on the fact that the mutations tended to cluster around important domains, such as the forkhead and the zinc finger domains. In addition, most of the mutations resulted in the nonconservative replacement of amino acids, and cancers with mutations identified had higher levels of HER-2 than those without mutations. The rate of missense to synonymous mutation was 18/3, which greatly exceeds what would be predicted if the mutations were not relevant to tumor

development. More importantly, we demonstrated that two tested mutations in the FKH and zinc finger domains inactivated the repressor activity and tumor growth inhibition and that cancer tissues bearing an intronic mutation had an inactive *FOXP3* locus. Moreover, mutations and deletions of the *FOXP3* locus corresponded to increased HER-2 levels. Third, we have documented extensive downregulation of *FOXP3* among more than 600 cases of breast cancer tissues.

Foxp3 Is a Major Transcriptional Repressor for *ErbB2*

The molecular lesions leading to HER-2 overexpression remain poorly understood. Here we showed that the *Foxp3* mutation resulted in overexpression of *ErbB2*, the murine homolog of *HER-2*. In addition, transfection of *Foxp3* repressed *ErbB2* transcription. More importantly, chromatin immunoprecipitation and EMSA analyses revealed that *Foxp3* binds specifically to its consensus sequence in the 5' of the *ErbB2* gene. Since specific mutations in the promoter abrogate its susceptibility to repression by *Foxp3*, such binding is likely responsible for it.

Importantly, we have demonstrated that for TSA cell line, which has *ErbB2* overexpression, repressing the *ErbB2* locus is responsible for *Foxp3*'s tumor suppressor activity. The requirement for continuous expression of *ErbB2* is best explained by the concept of oncogene addiction (Weinstein, 2002). However, *FOXP3* can also suppress the growth of tumor cell lines that do not grossly overexpress *HER-2/ErbB2*, such as MCF-7. In an effort to identify other potential *FOXP3* targets, we have produced a *FOXP3*-Tet-off MCF-7 cell line that expresses *FOXP3* upon removal of tetracycline (Figure S5A). Using the most current version of Entrez gene-based CDFs for a more accurate GeneChip analysis (Dai et al., 2005), we uncovered widespread changes in the expression of genes that are involved in several pathways critical for cancer cell growth (Figure S5B). Interestingly, ten genes involved in *ErbB2* signaling pathway were repressed by *FOXP3* (Figure S5C). Thus, multiple oncogenes can potentially be upregulated by *FOXP3* inactivation. Taken together, we have demonstrated that *FOXP3* is the first X-linked breast cancer suppressor that represses the *HER-2/ErbB2* oncogene. Given the significant role of HER-2 in the pathogenesis of human breast cancer and the widespread defects of the *FOXP3* locus, it is likely that *FOXP3* is an important suppressor for human breast cancer.

EXPERIMENTAL PROCEDURES

Quantitative Real-Time PCR

Relative quantities of mRNA expression were analyzed using real-time PCR (Applied Biosystems ABI Prism 7700 Sequence Detection System, Applied Biosystems). The SYBR (Qiagen) green fluorescence dye was used in this study. The primer sequences (5'-3') are listed in Table S6.

Chromatin Immunoprecipitation

Chromatin Immunoprecipitation was carried out according to published procedure (Im et al., 2004). Briefly, the Foxp3-V5-transfected TSA cells were sonicated and fixed with 1% paraformaldehyde. The anti-V5 antibodies or control mouse IgG were used to pull down chromatin associated with Foxp3-V5. The amounts of the specific DNA fragment were quantitated by real-time PCR and normalized against the genomic DNA preparation from the same cells.

FOXP3-Silencing Lentiviral Vector

The lentivirus-based siRNA expressing vectors were created by introducing the murine U6 RNA polymerase III promoter and a murine phosphoglycerate kinase promoter (pGK)-driven EGFP expression cassette into a vector of pLenti6/V5-D-TOPO backbone without CMV promoter. A hairpin siRNA sequence of *FOXP3* (target sequence at the region of 1256–1274 nucleotides; 5'-GCAGCGGACACTCAATGAG-3') was cloned into the lentiviral siRNA expressing vectors by restriction sites of *Apal* and *EcoRI*.

Immunohistochemistry and Fluorescence

In Situ Hybridization (FISH)

HER-2 expression was performed using Pathway HER-2 (Clone CB11) (Ventana Medical Systems, Inc., Tucson, AZ) on the BenchMark XT automated system per the manufacturer's recommended protocol. The HER-2 levels were scored by commonly used criteria (Yaziji et al., 2004).

FISH for *FOXP3* deletion was done using BAC clone RP11-344014 (ntLocus X: 48,817,975–48,968,223), which was verified by PCR to contain the *FOXP3* gene. The minimal common region of deletion was done using flanking p-telomeric and centromeric clones, RP11-573N21 (ntLocus X: 43,910,391–44,078,600) and RP11-353K22 (ntLocus X: 54,416,890–54,545,788), respectively.

EMSA

Nuclear extracts were prepared as described previously (Wang et al., 1999). The sequence for the WT probe (W) was AGTTCAATTTG AATTCAGATAAACG. Mutant probe (M) (AGTTCAGCGGAGCGC CAGAGCGCCG) with mutations of all three potential forkhead binding sites was used as specificity control.

Supplemental Data

Supplemental Data include six tables, five figures, Supplemental Experimental Procedures, and Supplemental References and can be found with this article online at <http://www.cell.com/cgi/content/full/129/7/1275/DC1>.

ACKNOWLEDGMENTS

We thank Dr. Fan Meng for assistance in bioinformatics, Drs. Eric Fearon, Albert de la Chapelle, Zhaohui Qin, Michael Caligiuri, and Charis Eng for their valuable discussions and/or critical reading of the manuscript, and Lynde Shaw for secretarial assistance. This study is supported by grants from the National Institutes of Health and the Department of Defense.

Received: July 6, 2006

Revised: September 12, 2006

Accepted: April 10, 2007

Published online: June 14, 2007

REFERENCES

Bennett, C.L., Christie, J., Ramsdell, F., Brunkow, M.E., Ferguson, P.J., Whitesell, L., Kelly, T.E., Saulsbury, F.T., Chance, P.F., and Ochs, H.D. (2001). The immune dysregulation, polyendocrinopathy, enteropathy, X-linked syndrome (IPEX) is caused by mutations of *FOXP3*. *Nat. Genet.* 27, 20–21.

Bofin, A.M., Ytterhus, B., Martin, C., O'Leary, J.J., and Hagmar, B.M. (2004). Detection and quantitation of HER-2 gene amplification and protein expression in breast carcinoma. *Am. J. Clin. Pathol.* 122, 110–119.

Brunkow, M.E., Jeffery, E.W., Hjerrild, K.A., Paepfer, B., Clark, L.B., Yasayko, S.A., Wilkinson, J.E., Galas, D., Ziegler, S.F., and Ramsdell, F. (2001). Disruption of a new forkhead/winged-helix protein, scurfy, results in the fatal lymphoproliferative disorder of the scurfy mouse. *Nat. Genet.* 27, 68–73.

Chang, X., Gao, J.X., Jiang, Q., Wen, J., Seifers, N., Su, L., Godfrey, V.L., Zuo, T., Zheng, P., and Liu, Y. (2005). The Scurfy mutation of FoxP3 in the thymus stroma leads to defective thymopoiesis. *J. Exp. Med.* 202, 1141–1151.

Chatila, T.A., Blaeser, F., Ho, N., Lederman, H.M., Voulgaropoulos, C., Helms, C., and Bowcock, A.M. (2000). JM2, encoding a fork head-related protein, is mutated in X-linked autoimmunity-allergic dysregulation syndrome. *J. Clin. Invest.* 106, R75–R81.

Dai, M., Wang, P., Boyd, A.D., Kostov, G., Athey, B., Jones, E.G., Bunney, W.E., Myers, R.M., Speed, T.P., Akil, H., et al. (2005). Evolving gene/transcript definitions significantly alter the interpretation of GeneChip data. *Nucleic Acids Res.* 33, e175.

Fontenot, J.D., Gavin, M.A., and Rudensky, A.Y. (2003). Foxp3 programs the development and function of CD4+CD25+ regulatory T cells. *Nat. Immunol.* 4, 330–336.

Fontenot, J.D., Rasmussen, J.P., Williams, L.M., Dooley, J.L., Farr, A.G., and Rudensky, A.Y. (2005). Regulatory T cell lineage specification by the forkhead transcription factor foxp3. *Immunity* 22, 329–341.

Garcia de Palazzo, I., Klein-Szanto, A., and Weiner, L.M. (1993). Immunohistochemical detection of c-erbB-2 expression by neoplastic human tissue using monospecific and bispecific monoclonal antibodies. *Int. J. Biol. Markers* 8, 233–239.

Godfrey, V.L., Wilkinson, J.E., Rinchik, E.M., and Russell, L.B. (1991). Fatal lymphoreticular disease in the scurfy (sf) mouse requires T cells that mature in a sf thymic environment: potential model for thymic education. *Proc. Natl. Acad. Sci. USA* 88, 5528–5532.

Godfrey, V.L., Rouse, B.T., and Wilkinson, J.E. (1994). Transplantation of T cell-mediated, lymphoreticular disease from the scurfy (sf) mouse. *Am. J. Pathol.* 145, 281–286.

Im, H., Grass, J.A., Johnson, K.D., Boyer, M.E., Wu, J., and Bresnick, E.H. (2004). Measurement of protein-DNA interactions in vivo by chromatin immunoprecipitation. *Methods Mol. Biol.* 284, 129–146.

Jimenez, R.E., Wallis, T., Tabaszka, P., and Visscher, D.W. (2000). Determination of Her-2/Neu status in breast carcinoma: comparative analysis of immunohistochemistry and fluorescent in situ hybridization. *Mod. Pathol.* 13, 37–45.

Kallioniemi, O.P., Kallioniemi, A., Kurisu, W., Thor, A., Chen, L.C., Smith, H.S., Waldman, F.M., Pinkel, D., and Gray, J.W. (1992). ERBB2 amplification in breast cancer analyzed by fluorescence in situ hybridization. *Proc. Natl. Acad. Sci. USA* 89, 5321–5325.

Knudson, A.G., Jr. (1971). Mutation and cancer: statistical study of retinoblastoma. *Proc. Natl. Acad. Sci. USA* 68, 820–823.

Kristiansen, M., Knudsen, G.P., Maguire, P., Margolin, S., Pedersen, J., Lindblom, A., and Orstavik, K.H. (2005). High incidence of skewed X chromosome inactivation in young patients with familial non-BRCA1/BRCA2 breast cancer. *J. Med. Genet.* 42, 877–880.

Miki, Y., Swensen, J., Shattuck-Eidens, D., Futreal, P.A., Harshman, K., Tavtigian, S., Liu, Q., Cochran, C., Bennett, L.M., Ding, W., et al. (1994). A strong candidate for the breast and ovarian cancer susceptibility gene BRCA1. *Science* 266, 66–71.

Piao, Z., and Malkhosyan, S.R. (2002). Frequent loss Xq25 on the inactive X chromosome in primary breast carcinomas is associated with tumor grade and axillary lymph node metastasis. *Genes Chromosomes Cancer* 33, 262–269.

- Richardson, A.L., Wang, Z.C., De Nicolo, A., Lu, X., Brown, M., Miron, A., Liao, X., Iglehart, J.D., Livingston, D.M., and Ganesan, S. (2006). X chromosomal abnormalities in basal-like human breast cancer. *Cancer Cell* 9, 121–132.
- Romanov, S.R., Kozakiewicz, B.K., Holst, C.R., Stampfer, M.R., Haupt, L.M., and Tlsty, T.D. (2001). Normal human mammary epithelial cells spontaneously escape senescence and acquire genomic changes. *Nature* 409, 633–637.
- Roncuzzi, L., Brognara, I., Cocchi, S., Zoli, W., and Gasperi-Campani, A. (2002). Loss of heterozygosity at pseudoautosomal regions in human breast cancer and association with negative hormonal phenotype. *Cancer Genet. Cytogenet.* 135, 173–176.
- Samuels, Y., Wang, Z., Bardelli, A., Silliman, N., Ptak, J., Szabo, S., Yan, H., Gazdar, A., Powell, S.M., Riggins, G.J., et al. (2004). High frequency of mutations of the PIK3CA gene in human cancers. *Science* 304, 554.
- Schechter, A.L., Stern, D.F., Vaidyanathan, L., Decker, S.J., Drebin, J.A., Greene, M.I., and Weinberg, R.A. (1984). The neu oncogene: an erb-B-related gene encoding a 185,000-Mr tumour antigen. *Nature* 312, 513–516.
- Slamon, D.J., Clark, G.M., Wong, S.G., Levin, W.J., Ullrich, A., and McGuire, W.L. (1987). Human breast cancer: correlation of relapse and survival with amplification of the HER-2/neu oncogene. *Science* 235, 177–182.
- Slamon, D.J., Leyland-Jones, B., Shak, S., Fuchs, H., Paton, V., Bajamonde, A., Fleming, T., Eiermann, W., Wolter, J., Pegram, M., et al. (2001). Use of chemotherapy plus a monoclonal antibody against HER2 for metastatic breast cancer that overexpresses HER2. *N. Engl. J. Med.* 344, 783–792.
- Spatz, A., Borg, C., and Feunteun, J. (2004). X-Chromosome genetics and human cancer. *Nat. Rev. Cancer* 4, 617–629.
- Todorovic-Rakovic, N., Jovanovic, D., Neskovic-Konstantinovic, Z., and Nikolic-Vukosavljevic, D. (2005). Comparison between immunohistochemistry and chromogenic in situ hybridization in assessing HER-2 status in breast cancer. *Pathol. Int.* 55, 318–323.
- Wang, C.Y., Cusack, J.C., Jr., Liu, R., and Baldwin, A.S., Jr. (1999). Control of inducible chemoresistance: enhanced anti-tumor therapy through increased apoptosis by inhibition of NF-kappaB. *Nat. Med.* 5, 412–417.
- Weinstein, I.B. (2002). Cancer. Addiction to oncogenes—the Achilles heel of cancer. *Science* 297, 63–64.
- Wildin, R.S., Ramsdell, F., Peake, J., Faravelli, F., Casanova, J.L., Buist, N., Levy-Lahad, E., Mazzella, M., Goulet, O., Perroni, L., et al. (2001). X-linked neonatal diabetes mellitus, enteropathy and endocrinopathy syndrome is the human equivalent of mouse scurfy. *Nat. Genet.* 27, 18–20.
- Wooster, R., Bignell, G., Lancaster, J., Swift, S., Seal, S., Mangion, J., Collins, N., Gregory, S., Gumbs, C., and Micklem, G. (1995). Identification of the breast cancer susceptibility gene BRCA2. *Nature* 378, 789–792.
- Wooster, R., and Weber, B.L. (2003). Breast and ovarian cancer. *N. Engl. J. Med.* 348, 2339–2347.
- Xing, X., Wang, S.C., Xia, W., Zou, Y., Shao, R., Kwong, K.Y., Yu, Z., Zhang, S., Miller, S., Huang, L., and Hung, M.C. (2000). The ets protein PEA3 suppresses HER-2/neu overexpression and inhibits tumorigenesis. *Nat. Med.* 6, 189–195.
- Yaziji, H., Goldstein, L.C., Barry, T.S., Werling, R., Hwang, H., Ellis, G.K., Gralow, J.R., Livingston, R.B., and Gown, A.M. (2004). HER-2 testing in breast cancer using parallel tissue-based methods. *JAMA* 291, 1972–1977.
- Ziegler, S.F. (2006). FOXP3: Of mice and men. *Annu. Rev. Immunol.* 24, 209–226.

FOXP3 IS AN X-LINK TUMOR SUPPRESSOR GENE IN BREAST CANCER

Weiquan Li, Jennifer Nicodem, Tao Zou, Yang Liu, Pan Zheng

Department Of Surgery, University of Michigan, 1838 BSRB, 109 Zina Pitcher Place, Ann Arbor, MI48109

FoxP3 is among the newest members of the forkhead winged helix family. It was identified during position cloning of *Scurfin*, a gene responsible for X-linked autoimmune diseases in mice and humans (Immune dysregulation, polyendopathy, enteropathy, X-linked). The mutation in mice and those in some human IPEX patients are analogous as they cause frameshift and early termination of translation. Further studies indicated that the gene is responsible for the development of Treg, which explains, at least in part, the autoimmune phenotype of diseases.

In our analysis of the immune functions of mice heterozygous for the FoxP3 mutation, we observed a high rate of spontaneous mammary cancer. The heterozygous female mice are also substantially more susceptible to carcinogen DMBA. These data indicated that Foxp3 may play an important role as a tumor suppressor gene in breast cancer.

Meanwhile, a recent study indicated that mice with a targeted mutation of NFAT4 also developed spontaneous mammary cancers. Since NFAT is an essential partner of FoxP3 in immune regulation, it is of great interest to determine whether a similar interaction is responsible for the observed tumor suppressive activity of FoxP3. So far, what role that FoxP3 and NFAT may play in breast cancer development has not been reported. NFAT family members may be the key partners in the tumor suppressive function of FoxP3 in breast cancer development. Therefore, deciphering the mechanism of how FoxP3 and NFAT function in tumor formation will help understand the cause of the pathogenesis and prevent or treat breast cancer.

In our study, we found the FoxP3 gene was expressed in breast epithelial cells but down-regulated in the mammary cancer tissues. Meantime, over-expression of FoxP3 in a variety of breast cancer cells resulted in a substantial inhibition of their growth. Furthermore, FoxP3 inhibited the transcription of ErbB2, the major oncogene for breast cancer, by targeting and repressing the ErbB2 promoter. Our further analysis demonstrated that the growth inhibition was completely reversed by constitutive expression of the ErbB2 gene. The significance of the genetic defects in human breast cancer has been demonstrated in multiple lines of evidence, including: deletion (12.8% of 232 samples tested); somatic mutation (35% of 65 cases sequenced); and lack of expression (80% of more than 600 cases tested). Our data revealed that FoxP3 is an important breast cancer suppressor gene in mice and humans.

Our analysis of NFAT4 function also provided evidences supporting its role as a tumor suppressor. Our data showed that NFAT4 repressed Erb2 transcription by measuring ErbB2 reporter activity, suggesting NFAT4 may serve as a repressor for ErbB2/Her-2 promoter. NFAT4 was found in a complex with FoxP3, indicating they may functionally play important roles together. Our further analysis also found decrease of NFAT4 expression in some of mice breast cancer samples. In summary, our data suggest FoxP3 and NFAT are important breast cancer suppressor genes in the mouse.